Color vision in polychromatic animals

Christian Garbers
München, 2016

Diese Dissertation wurde angefertigt unter der Leitung von
PD Dr. Thomas Wachtler im Bereich Neurobiologie an der
Ludwig-Maximilians-Universität München.

Erstgutachter: PD Dr. Thomas Wachtler
Zweitgutachter: Prof. Dr. Christian Leibold

Tag der Abgabe: 11 August 2016
Tag der mündlichen Prüfung: 28 November 2016

ERKLÄRUNG

Ich versichere hiermit an Eides statt, dass meine Dissertation selbständig
und ohne unerlaubte Hilfsmittel anggefertigt worden ist. Die vorliegende
Dissertation wurde weder ganz, noch teilweise bei einer anderen
Prüfungskommission vorgelegt. Ich habe noch zu keinem früheren
Zeitpunkt versucht, eine Dissertation einzureichen oder an einer
Doktorprüfung teilzunehmen.

München, den 11 August 2016   _____

(Christian Garbers)

Contents

List of Figures

Schon seit meinen frühsten Zeiten fühlte ich einen Untersuchungstrieb gegen natürliche Dinge. Man legt es manchmal als eine Anlage zur Grausamkeit aus, daß Kinder solche Gegenstände, mit denen sie eine Zeitlang gespielt, die sie bald so, bald so gehandhabt, endlich zerstücken, zerreißen und zerfetzen. Doch pflegt sich auch die Neugierde, das Verlangen, zu erfahren, wie solche Dinge zusammenhängen, wie sie inwendig aussehen, auf diese Weise an den Tag zu legen. Ich erinnere mich, daß ich als Kind Blumen zerpflückt, um zu sehen, wie die Blätter in den Kelch, oder auch Vögel berupft, um zu beobachten, wie die Federn in die Flügel eingefügt waren. Ist doch Kindern dieses nicht zu verdenken, da ja selbst Naturforscher öfter durch Trennen und Sondern als durch Vereinigen und Verknüpfen, mehr durch Töten als durch Beleben sich zu unterrichten glauben.

Johann Wolfgang von Goethe: Dichtung und Wahrheit

1

Overview

The ability for color vision has been demonstrated in many animals. In the fruit fly, it was assumed that the physiological basis for their color vision is mediated by four different opsins called Rhodopsin 3 (rh3), Rhodopsin 4 (rh4), Rhodopsin 5 (rh5), and Rhodopsin 6 (rh6). A fifth opsin the so-called Rhodopsin 1 (rh1) was thought to mediate motion vision but not color vision. I constructed a computational model to predict wavelength discrimination in flies and compared different models to published behavioral data. I found that the published data cannot be explained without taking the signals from rh1 into account.

In collaboration, I tested this prediction experimentally by studying the behavior of flies genetically engineered to only have functional rh1 in combination with one of the other opsins. I found that flies having only rh1 and rh4 were indeed able to discriminate stimuli based on color, which supported the initial findings. In a third step, I analyzed the statistics of natural reflectance spectra with respect to the opsins of Drosophila. I found that including signals from a fifth opsin is useful considering an optimal sampling of the frequency content. I quantified the effect of adding signals from a fifth opsin using mutual information and concluded that the resulting gain in mutual information was higher than that expected. Together with results from the modeling, which indicated that best fits are achieved by including only three opsins, this could mean that Drosophila is not using all of its opsins for color vision. However, rh1 is certainly among

those used.

Vision in humans is color constant, i.e., the color of an object does not change when the illumination, and thereby the light that an object reflects, changes. For an animal, color constancy is essential when identifying objects, yet there is very little behavioural evidence supporting color constancy in the animal kingdom. In a set of experiments, I demonstrated that gerbils can successfully be trained to learn a local contrast task. Furthermore, I devised a two alternative forced choice stimulation protocol, where gerbils are presented with stimuli from a rodent color space such that they learn to discriminate stimuli by their relative local color contrast. The animals successfully learned the task, demonstrating that gerbils have color constant color vision.

2

Introduction

To help to gain a comprehensive understanding of this thesis, and furthermore to properly motivate it, some cornerstones of the scientific history which heavily influenced this work need to be established. Alongside, I also hope to introduce the reader to some interesting background information and historical anecdotes which might help to gain some insights into how the opinions in the field evolved.

2.1   The dawn of color ethology

In 1912, after ten years as a director of the eye clinic in Würzburg, Carl von Hess, who had just accepted a position as "Ordinarius" at the university eye clinic in Munich, published the culmination of his works on comparative color vision. In this monograph, Geheimrat [1] von Hess, who already was a highly distinguished and well-established color vision expert, concluded that while most vertebrates have color vision, fish and all invertebrates are color blind (Hess, 1912).

Von Hess had comparatively studied the ability to see color among different animals. His primary method was to estimate the spectral sen-

---

[1] Von Hess, who had been a student of Ewald Hering and Hubert Sattler, had received the title "königlich Geheimer Hofrat" from the Bavarian king as a reward for staying in Würzburg (i.e., in Bavaria) after receiving calls from Straßburg, Wien, Heidelberg, and Berlin (Fischer, 1971; Trincker, 1972). Being a Geheimer Rat, however, is not uncommon among color experts.

589   527   486
wavelength [nm]
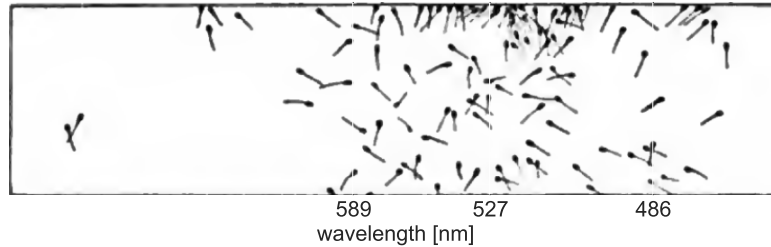
Figure 2.1: Example of an experiment where sand smelts were exposed to light that had been split with a prism. Most of the animals preferred the yellow-greenish area and completely avoided the long wavelength part of the spectrum. Modified from Hess (1912, p.47,Fig.2).

sitivity, which is how sensitive animals are for certain parts of the spectrum, by looking at the animals innate preference for different wavelengths. He then compared those to the spectral sensitivities of color normal and completely color blind (achromatic) humans. He found that, while all terrestrial vertebrates tested showed preferences comparable to the spectral sensitivities of color normal humans, fish (see Fig. 2.1 for an example from his work) and invertebrates showed preferences which were in agreement with the spectral sensitivity of totally color-blind humans. This led him to the conclusion that fish and invertebrates do not see colors.

The impact of these claims can only be evaluated properly when considering the seminal works on plant pollination by Sprengel (1793) and Kölreuter (1761), which had recently been made more popular by Darwin (1876, 1862). These works, which are arguably the foundations of modern pollination ecology, had established that many plants are pollinated by insects. This observation inspired the theory that flowers were colored specifically to attract pollinators[2] which directly implied that insects were

---

[2]And not such that they appear beautiful to humans.

able to see colors.

For Hess, the theory that floral coloring could be a signal specifically tuned towards insects seemed unlikely. First of all his findings explicitly argued against it. But more drastically and with a reasoning that closely followed a line of thought that Johann Wolfgang von Goethe had presented before, [3] Hess accused such ideas of being anthropocentric [sic.].

In the same year in which Hess had published the culmination of his works on comparative color vision, a young scientist by the name of Karl von Frisch started to work in Munich[4]. Frisch had recently discovered that some fish were able to change their body color depending on the color of the background (Frisch, 1912). As Frisch interpreted his findings as evidence supporting color perception in these fish, his observation sparked both his interest in color vision as well as an intense yet fruitful conflict with Carl von Hess.

Frisch was not alone, however, and several previously published studies had reported pieces of evidence supporting color vision in insects and fish before (Müller, 1882; Forel, 1910; Lubbock, 1883, 1889; Nagel, 1902). For example Zolotnitsky (1901) had observed that, after being fed with red larvae, paradise fish tended to bite the red breast fins of telescope-fish. Subsequently, Zolotnitsky (1901) had tested those fish with bits of differently colored yarn and found that more fish jumped for the red yarn than for any other color. In another study, using a food reward, Washburn and Bentley (1906) had successfully trained fish to swim towards a colored wooden square.

All these works had one central shortcoming. In all cases[5] , the results

---

[3]Goethe, who rushed his book on plant development when he was alerted that Sprengler would publish something in the same field, also reproached Sprenglers seminal work because he thought them to be anthropocentric (Meyer, 1967).

[4]Interestingly, even before von Frisch had moved to Bavaria, both had done experiments at famous Stazione Zoologica in Naples which had been founded in 1872 by Anton Dohrn. The Stazione was one of the first scientific institutes that actively fostered international collaboration and hosted many great scientists. Among them famous biologists like August Weissman, Otto Warburg and, of course, the two color scientists Carl von Hess and Karl von Frisch.

[5]Some reviewers (Kelber and Osorio, 2010) exclude the works from Bauer (1910, 1911) from that critique.

could theoretically be explained by the animals using brightness cues instead of color. That is, it could not be excluded that the objects the animals were preferring or imitating, which to the human are easiest to identify because of their color, might have just been identified by the animals, because of their particular brightness. For example, the blue card in Figure 2.2 can easily be recognized by the human observer because it is colored. The same might not be the case for bees. Even if they can be trained to associate this card with a sugar reward, they might just identify the card because of its particular brightness in the same way a human observer might learn to recognize one of the achromatic cards because of its lightness. It is this methodological shortcoming that Hess (1910, 1913) vigorously criticized, albeit maybe in a somewhat overly polemic tone.
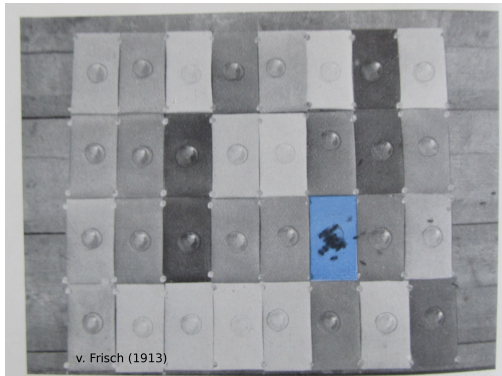
Figure 2.2: Testing for color vision in bees: Example test case, where bees had been rewarded with sucrose solution on a blue colored card. In a situation where they are presented with various gray cards they still go for the blue card (Frisch, 1913b).

Hess's criticism, however, did not deter Frisch (Frisch, 1973) and rather helped him to come up with an operational definition of his topic: **Color Vision - the ability to discriminate two stimuli irrespective of their relative intensities (i.e., only by their spectral composition** (Wyszecki and Stiles, 1982)**).**

Overcoming the methodological shortcomings mentioned above, Frisch performed another set of experiments. He rewarded free-flying honeybees when visiting cards of a particular color (and not when visiting cards colored differently). In the critical test, the colored cards were placed amongst a variety of gray cards and even then the bees still flew directly to the colored cards. If the bees had only learned to choose the colored card because of its particular brightness, they should have also chosen one of the gray cards (see. Fig 2.2 for an example). Thus, Frisch successfully demonstrated that honey bees (and later also fish) could differentiate colors (Frisch, 1913b,a). **What made**

this experiments so convincing is the idea to mix stimuli of varying intensity, thereby discarding intensity as a possible source of information.

For reasons that remain in the dark (Autrum, 1963, 2008), these experiments did not convince von Hess, and he strongly objected to Frisch's findings. As a response, Frisch did a "live" demonstration of his experiments at the 1914 Zoologentagung in Freiburg (Frisch, 1914), which to the frustration of von Hess (Hess, 1918), who was not a participant, convinced many contemporaries and subsequently the bees' ability to see colors was broadly accepted.

Von Frisch's experiments inspired the next generation of researchers and continues to influence color ethology till today (Kühn, 1927; Menzel, 1967; Helversen, 1972; Hernandez de Salomon and Spatz, 1983; Troje, 1993).

2.2 Physiological mechanisms supporting color vision

Since Palmer (1777); Young (1802); Helmholtz (1860) had observed that **three spectraly different stimuli, combined together at different intensities, are enough to produce a perception of practically "all colors" (see Fig 2.3a)**, it had been argued that human color vision is driven by three spectraly different receptive mechanisms: i.e., that humans are trichromatic.

Competing theories, most prominently presented by Hering (1875), however, argued strongly against a "three color theory". He had noted that red and green, as well as blue and yellow, do not appear simultaneously, i.e., **red and green, as well as blue and yellow, are mutually exclusive colors. This observation lead to a color theory based on two opponent systems. One red-green mechanism and one mechanism for blue and yellow.**

For both ideas, psychophysical support could be found (Hurvich and

Jameson, 1957; Guild, 1932; Wright, 1952, 1929, 1941) over the years. Nevertheless, nearly 100 years more needed to pass until Brown and Wald (1963) could show with electrophysiological recordings that, indeed, human color vision is supported by three different classes of photoreceptor cells, the so called l, m, and s cones (see Figure 2.5a). This, however, did not mean that Hering had been wrong. He had been correct in his analysis, but his proposal that opponency between colors was due to the photoreceptors was wrong.

Both, the Palmer-Young-Helmholtz as well as the Hering color theory, can be combined into one model as had already been envisioned by Kries (1902) [6] and more successfully put forward in a complete scheme by Göthlin (1944) (see Fig.2.3b for an illustration).

The idea is to combine the signals from three (trichromacy) receptors into two opponent mechanism in a second stage. This combines the observation that "three spectrally different stimuli are enough" with the finding that red and green as well as blue and yellow are opponent (see Fig. 2.3b for an early illustration), and such a combination of receptor signals into opponent mechanism is the backbone of all modern models of color vision (Guth, Donley, and Marrocco, 1969; Ingling and Huong Peng Tsou, 1977; De Valois and De Valois, 1993; Ingling, Barley, and Ghani, 1996; Hassenstein, 1968; Guth, Massof, and Benzschawel, 1980).

While the debate over the number of receptive mechanisms in humans was waging, scientists also tried to address this question in insects. In Munich, Daumer (1956) had devised experiments, with which he could provide first conclusive arguments that supported a three receptor-based color vision also in bees. Daumer's results, which had been obtained under the supervision of Frisch, were later confirmed by electrophysiological record-

---

[6]Von Kries contributions to color vision - up to this day - have been largely ignored; most probably because they are only available as a "Festschrift" at the Albert-Ludwigs-University of Freiburg. Von Kries, who has been credited as Helmholtz's "greatest German disciple"(Cahan, 1993), was also among those that introduced the duplex theory of vision (rod cells, which will be introduced in Chapter 4.2.5 are used at low light levels and the cone cells at higher light levels).
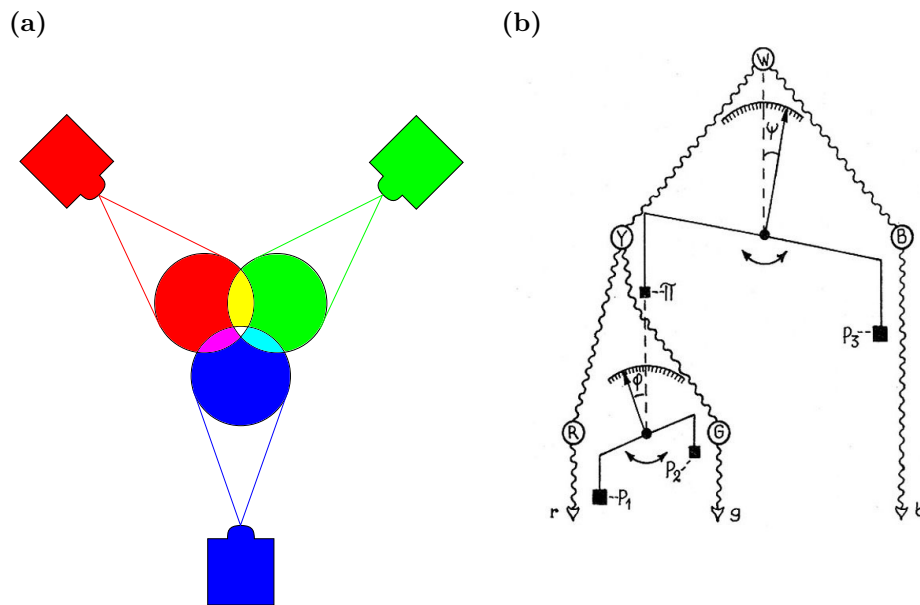
Figure 2.3: Trichromacy: (a) Three light sources mixed with varying intensity create all colors. (b) A two stage color model. Signals from receptors (P1-P3) are combined into two opponent pairs. P1+P2 against P3 decide whether yellow or blue is produced. P1 against P2 decides between red and green. All three combined decide about brightness. Modified from Göthlin (1944).

ing in individual photoreceptors done by Frisch's successor Hansjochen Autrum (Autrum and Zwehl, 1964). In this work the authors established that bees have three photoreceptor types with their respective maximum at 340 nm, 460 nm, and 540 nm (see Fig.2.5a). Not only was the first UV receptor found, furthermore, it seemed to be the case, at least for the next few years, that being trichromatic, i.e., having three receptor types, was generalizable (Autrum, 2008) in the animal kingdom.

2.3   Quantifying color discrimination in animals

The studies just introduced paved the way for the next step towards understanding how color vision is distributed in the animal kingdom. In a seminal work in color ethology, Helversen (1972) presented quantitative data on wavelength discrimination in bees, and 1970 received one of the first (personal communication with Prof. Rainer Hertel) doctoral degrees awarded by the newly founded Faculty of Biology at the Albert-Ludwigs-University in Freiburg. Under the supervision of Bernhard Hassenstein, Helversen, who had studied both Mathematics and Biology, **established a protocol on how to measure a Delta-Lambda ($\delta\lambda$) function, which is a function that quantifies wavelength discrimination over the spectrum (see Fig. 2.4 for an example), in animals.**

He had conditioned bees to choose a particular wavelength over another by using sugar reward. In a subsequent test, he measured their performance by determining how often an animal selected the stimulus with the conditioned wavelength over a stimulus of another. The value derived in this way was termed a "conditioning index" (Helversen, 1972). The procedure above was repeated for several wavelength pairs and presented in several conditioning index functions (see Figure 2.4 for an illustration of a conditioning index function).

For each wavelength used, these functions report the conditioning indexes determined when this reference wavelength was tested against stimuli

of another wavelength. The steepness of such a conditioning curve around the reference wavelength λ_0, that is, the wavelength for which the particular function was derived, was interpreted as a measure of wavelength discriminability at that reference wavelength (Helversen, 1972). To obtain a quantitative $\delta\lambda$ estimate from these curves, an arbitrary learning threshold T was set (e.g., 20% as in Figure 2.4). The amount of wavelength change needed to reach this threshold was then defined as the discriminability at that reference wavelength. By analyzing several conditioning index curves in this way, an estimate of the $\delta\lambda$ function was derived by determining, the value of $\delta\lambda$ for which the discrimination conditioning function $L_{\lambda_0}(\delta\lambda)$ reached the threshold. However, this lead to two different values, one for longer ($\delta\lambda_l$) and one for shorter ($\delta\lambda_s$) wavelengths.

To derive a unique discrimination value per reference wavelength, Helversen could have simply collapsed the values into one by taking the mean (mean transformation), yet, for very different values this would have lead to rather unreliable estimates. **Instead, he derived virtual reference wavelength, for which the discrimination would have been symmetric and determined $\delta\lambda$ values for those. He achieved this, by taking the midpoint of the intervals $[\lambda_0, \ \lambda_0 + \delta\lambda_l]$ and $[\lambda_0 - \delta\lambda_s, \lambda_0]$ as new reference wavelength (see Figure 2.4 for an illustration), denoting $\delta\lambda_l$ or $\delta\lambda_s$ respectively as the wavelength (split-reference transform).**

The $\delta\lambda$ function derived by Helversen nicely fit the expectations from the studies by Daumer (1956) and Autrum and Zwehl (1964) which had established that bees, as well as humans, where trichromatic. Therefore, it was expected that their wavelength discrimination would have two ranges with good discrimination, separated by intermediate ranges where its was supposed to be rather poor. **Good wavelength discrimination should be found in ranges where the absolute slopes of the photoreceptors are high**. With high slopes, changes in the signal are bigger per wavelength step than at ranges where the slope is shallow. With human and bee photoreceptor curves (see Fig. 2.5a), two ranges with higher slopes can be found and therefore, two maxima are expected in the $\delta\lambda$ function.
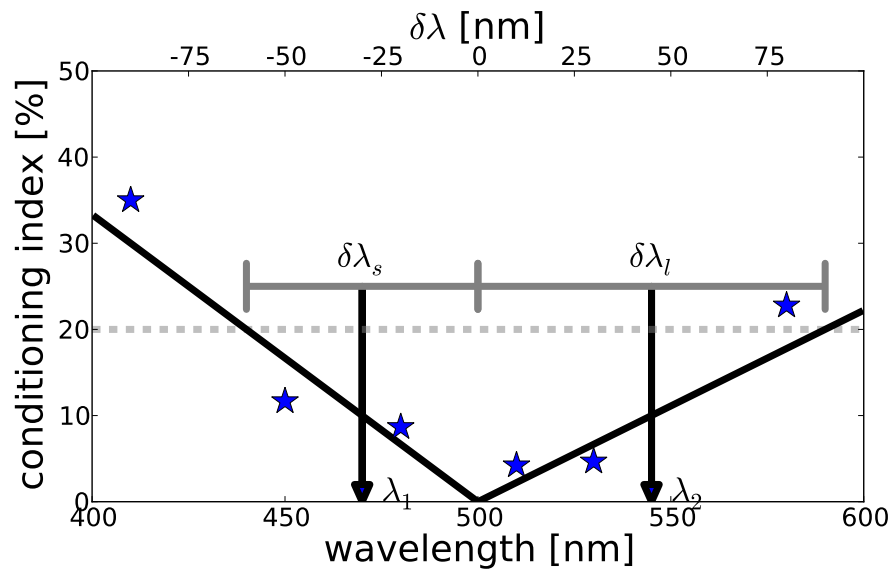
Figure 2.4: Conditioning Index and $\delta\lambda$: An example plot of a conditioning index experiment. Animals have been trained to discriminate a reference stimulus of 500 nm from stimuli of another wavelength as indicated on the x-axes. The y-axis shows for each pair how many animals, above chance, have been able to learn the discrimination. Each star is the result of an experiment. The solid black line is an interpolation for the data points. The dashed line indicates an arbitrarily chosen threshold of 20%. $\delta\lambda$ are the ranges between the reference wavelength and the intersection between the threshold and the interpolation of the data, as indicated by the gray ranges. The midpoints of these ranges, λ_1 and λ_2, are the virtual reference wavelength as used to derive the wavelength discrimination.

As bees have a UV receptor, instead of a human long wavelength receptor, it was furthermore anticipated that their wavelength discrimination function should be shifted to the UV range. Both expectations were fully satisfied as can be seen in Figure 2.5b.

2.4 Color vison in the fly
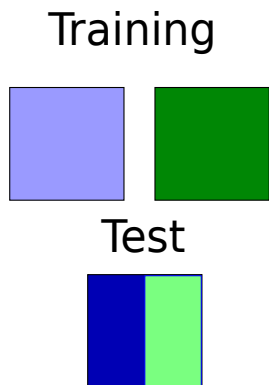
Training

Test

Figure 2.6: Intensities of the stimuli are flipped between training and test.

Not much later, the next animal that joined the color vision club was *Drosophila melanogaster*. Around the same time as Helversen and also at the Albert-Ludwigs Universität Freiburg, albeit at another institute, Menne and Spatz (1977) demonstrated, with an automated procedure which used shaking as an aversive stimulus to condition the animals, that the small fruit flies could be trained to associate color with the shaking. **In a training period, the shaking was paired with a light of a particular wavelength. In the critical test (see above Chapter 2.1) the intensities of the stimuli were exchanged (see Fig. 2.6)**.

As the majority of the flies still avoided the area that was illuminated with light of the conditioned wavelength, the ability for color vision had been demonstrated in flies.

In a subsequent study Hernandez de Salomon and Spatz (1983) used the technique developed by Helversen (1972) to derive a **wavelength discrimination function for Drosophila (see. Fig. 2.7b)**.

As as result of these studies, the question of the physiological basis of fly color vision arose.

The arthropod eye, which is nowadays called compound eye (Heldmaier, Neuweiler, and Rössler, 2012), had originally been named "Ommateum", which literally describes it: An eye out of many (smaller) eyes [7]. In

---

[7]"Ommateum", which is no longer used, is a combination of the Greek eye (Omma) and the Latin -eum, literally meaning many-eyes. The diminutive of Omma "Omma-

(a)
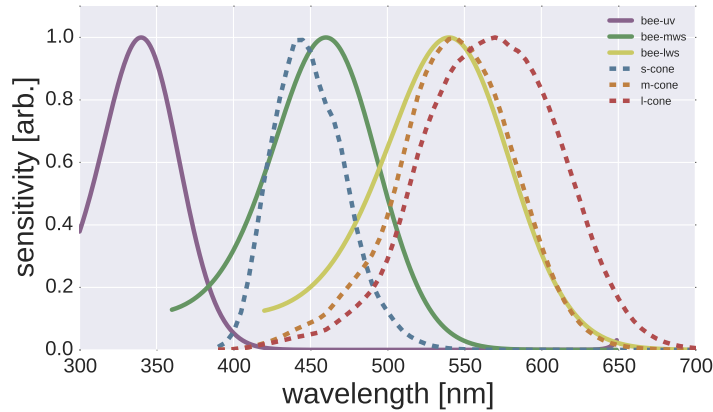
(b)
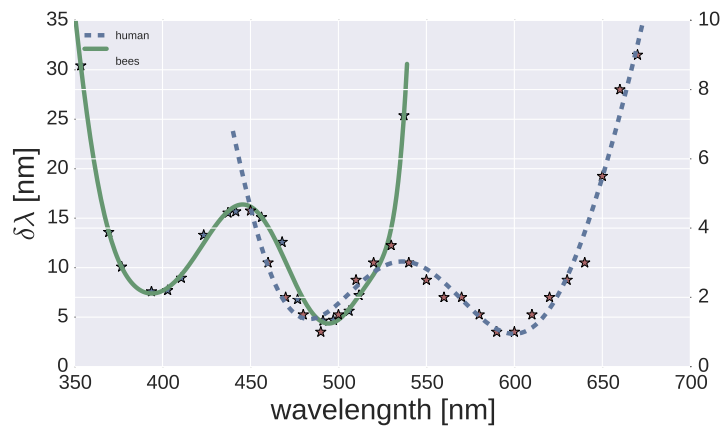
Figure 2.5: Photoreceptors and Spectral Discrimination: (a) Photoreceptor spectral sensitivities in humans (dashed lines) (Stockman and Sharpe, 2000; Stockman, Sharpe, and Fach, 1999) and bees (solid lines) (Daumer, 1956). Ordinate shows wavelength in nanometer and abscissa the spectral sensitivity normalized to peak at one. (b) Wavelength discrimination ($\delta\lambda$) function in humans (Pokorny and Smith, 1970) and bees (Helversen, 1972). Ordinate indicates wavelength discrimination in nanometer. The labels on the left are for the bees, the labels on the right for the humans. Abscissa indicates wavelength in nanometer. Both functions exhibit two ranges of good wavelength discrimination. The bees curve is shifted toward the UV range when compared to the one from humans. Furthermore, wavelength discrimination is good in ranges where two photoreceptors overlap and have a high absolute slope.

(a)

(b)
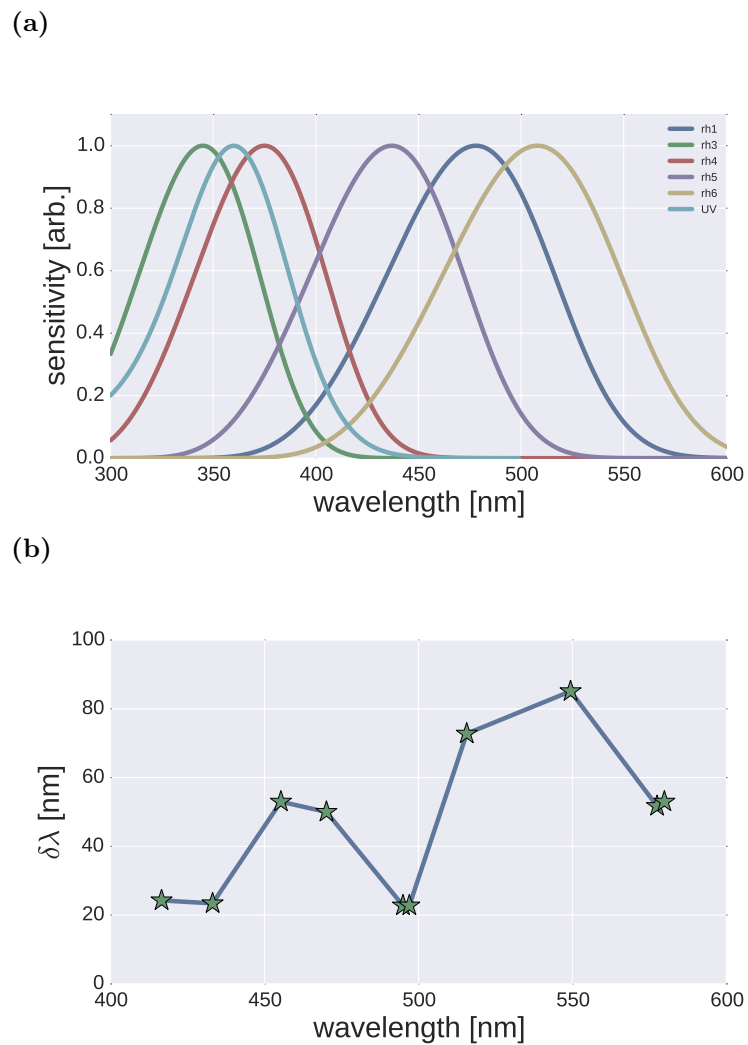
Figure 2.7: (a) Photoreceptor spectral sensitivities in drosophila (Salcedo et al., 2003). Ordinate shows wavelength in nanometer and abscissa shows the spectral sensitivity normalized to peak at one. (b) Wavelength discrimination ($\delta\lambda$) function in drosophila (Hernandez de Salomon and Spatz, 1983). Ordinate indicates wavelength discrimination in nanometer. Abscissa indicates wavelength in nanometer.

drosophila, each of these little eyes (Carrière, 1884) (Ommatidia) has eight photo-receptive cells which can be split into two groups. The first group, the so-called outer photoreceptors, are concentrically arranged around the so-called inner photoreceptors which sit-on-top of each other in between (see Fig. 2.8a). The **outer photoreceptors** of Drosophila, of which there are six in each ommatidium (cells R1-R6 see Figure 2.8b), **are all equipped with the same visually sensitive photopigment**, the so-called Rhodopsin 1 (rh1).

The **inner photoreceptors, however, come in two types**. When the upper one (cell R7 Figure 2.8b) is filled with Rhodopsin 3 (rh3), the lower one (cell R8 Figure 2.8b) is filled with Rhodopsin 5 (rh5). An ommatidium with this configuration is called a "pale ommatidium". In the other configuration, called the yellow ommatidium, the R7 cell is filled with Rhodopsin 4 (rh4) and the R8 cell with Rhodopsin 6 (rh6) (Trujillo-Cenóz, 1972; Braitenberg, 1967). Nowadays, precise recordings of the spectral sensitivity of all receptor types are available (Salcedo et al., 1999, 2003) (see Fig.2.7a) and it is clear that **rh3 and rh4 are sensitive for wavelength in the UV range, rh5 for wavelengths around 450 nm and rh6 around 500 nm** (see Figure 2.1). Furthermore, the **outer receptors are equipped with an accessory pigment that is sensitive in the UV range** and practically gives them a two peaked spectral sensitivity. The same pigment is also present in the yellow ommatidia (Vogt, 1984) of larger flies, yet, the influence on their spectral sensitivity is thought to be less pronounced or absent in Drosophila (Salcedo et al., 1999).

It was noted early, that this anatomical separation into inner and outer receptors might be due to functional differences and it was proposed that the rather large outer receptors are responsible for motion vision, whereas the rather small inner receptors are responsible for color vision (Kirschfeld and Franceschini, 1968). This proposal, which has been compared (see below chapter 4.1.7) to the functional separation found in vertebrate photoreceptors (rods vs. cones), became the de-facto "textbook" model (see Figure 2.8b), yet without being backed up by sound behavioral or physio-

---

tidium" (small eye) however, has survived.
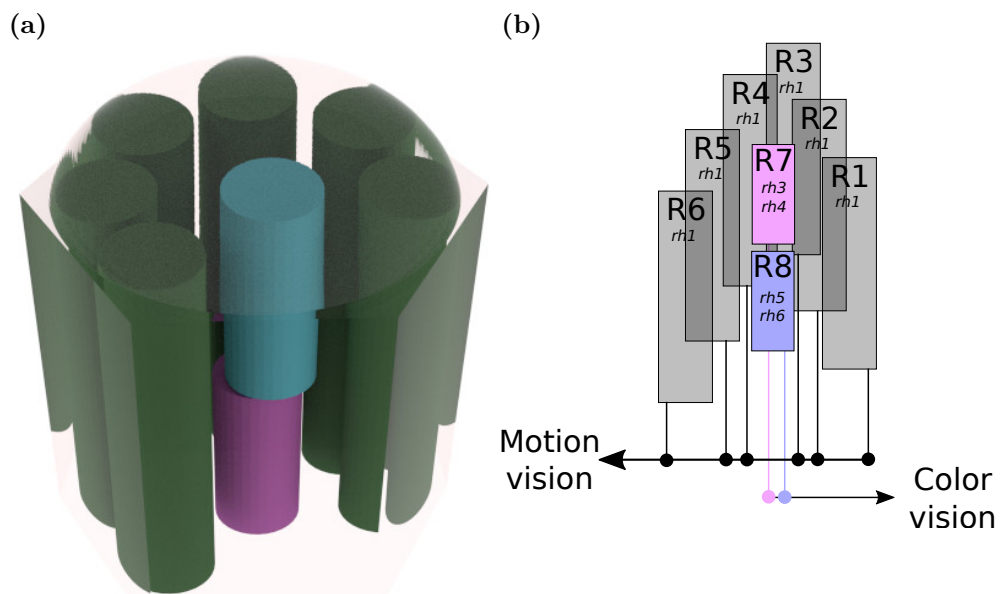
Figure 2.8: Compound eye of drosophila:(a) shows a examplary 3D rendering of an ommatidium. The outer photoreceptor cells R1-R6 (green) are concentrically arranged around the two inner receptors R7 and R8 which sit on top of each other. All outer cells express the photoreceptive opsin rh1. R7 does either express rh3 or rh4 and R8 does express rh5 or rh6. (b) illustrates the "text book" model of the functional separation for the receptor types (adapted from Morante and Desplan (2004)). Outer receptor signals are used for motion vision whereas inner receptor signals are used for color vision (Kirschfeld and Franceschini, 1968).

logical experiments (Troje, 1994).

Motivated by this lack of evidence Troje (1993), under the supervision of Klaus Vogt, trained individual Goldflies (Lucilla) to associate colored stimuli with a sugar reward. He measured conditioning index functions (see Chapter 2.3) with individual flies and provided a mathematical model for these. Based on spectral sensitivities measured in Musca (data for Goldflies were not available) he found that [8] **he could explain the behavioral data with a model that only included two computations: A comparison between rh3 and rh5 as well as a comparison between rh4 and rh6.** This perfectly fits the expectations introduced earlier by Kirschfeld and Franceschini (1968), and since then, has often been interpreted as proof for the idea that **the visual system in flies consists of two parts. A system with high light sensitivity based on the outer receptors and a system, also supporting color vision, based on the inner receptors** (Kirschfeld and Franceschini, 1968).

2.5   Modeling spectral sensitivity and wavelength discrimination

Troje had used a model by which he was able to relate the spectral profiles of the photoreceptors to behavioral data. As other models before and after (Stiles, 1959; Sperling and Harwerth, 1971; Sankeralli and Mullen, 1996; Cole, Hine, and McIlhagga, 1993), the model was based on the assumption of an opponent combination of photoreceptor signals (see above chapter 2.2) and implicitly assumed that the visual performance is ultimately limited by some post-receptoral factors that are statistically independent (Vorobyev and Osorio, 1998).

---

[8]Just a short excerpt from Trojes doctoral thesis illustrates that he was very conservative with the interpretation of his modeling results: "Mit einer theoretischen Überlegung konnte außerdem gezeigt werden, dass die Rezeptorklasse R1-6, die sicherlich den größten Beitrag zur absoluten Empfindlichkeit des Auges leistet, zum Farbensehen nur sehr wenig beitragen könnten".

Figure 2.9: Sketch of the modeling approach: The signal in an opponent channel, i.e., the difference in signaling for two receptors, is calculated for two different stimuli S1 and S2. The higher the distance of this two opponent signals(and for more than one channels the Euclidean distance) the easier it is to discriminate the two stimuli. This can easily be adapted to include more than two receptors.

If, however, the limiting factor is the noise in the receptors and if a receptor contributes to more than one post-receptoral mechanism, then the assumption of independence is not valid. Under such conditions, Vorobyev and Osorio (1998) showed that the spectral sensitivity of many animals can be modeled by calculating a noise weighted distance in an n-dimensional space with a basis set formed by the excitations of the possible opponent mechanisms.

By using this approach, it was possible to predict spectral sensitivity with a model that had as few parameters as the number of photoreceptors present (Vorobyev and Osorio, 1998). With the same assumptions it is also possible to predict wavelength discrimination (Koshitaka et al., 2008) and this type of modeling has since been established as the de-facto standard in the field (Koshitaka et al., 2008; Osorio et al., 2004; Osorio and Vorobyev, 1996; Vorobyev et al., 1998; Vorobyev and Osorio, 1998; Vorobyev et al., 2001; Vorobyev and Ibarra, 2012).

2.6 How many photoreceptors does an animal need

After it had been established that bees and humans are trichromatic, more diversity in the number of receptor types had soon been found. For example, Kretz (1979) showed that the ant *Cataglyphis bicolor* has three regions of good discrimination, separated by areas of poor discrimination. As this ant also has a spectral sensitivity with four maxima, it was concluded that they have four receptor types.

Many birds have four types of cone photoreceptors while, with the notable exception of the old world monkeys, being dichromatic, i.e., having

two cone receptors, is normal for most terrestrial mammals (Osorio and Vorobyev, 2008).

In insects, there is a huge variability in the number and tuning of receptors. The trichromatic bees have already been introduced earlier and I have discussed above how dipterans are thought to have a tetrachromatic color vision, whereas they, nevertheless, have five different receptor types. To illustrate this diversity some more, it is worth mentioning that the swallowtail butterfly *Papilio xuthus* has eight different types of receptors, yet, has only tetrachromatic color vision (Koshitaka et al., 2008).

The most extreme case, concerning the number of different photoreceptors types, can be found in the mantis shrimp (Stomatopoda), with some species having up to sixteen receptors (Kelber and Osorio, 2010).

In the light of this variability, **studies have been dedicated to determining how many different photoreceptor types are actually useful with respect to natural reflectances.** While optimal sampling of the spectral frequencies in natural images would require about 6-12 receptors (Maloney, 1986), considerations with respect to color constancy under changing illumination led to the conclusion that at least for the visual range of humans, trichromacy is quite optimal (Maloney, 1986). This was further supported by the finding that the first three principal components, calculated for natural images, already accounted for roughly 98% of the variability. Vorobyev (1997) analyzed the accuracy of reconstruction of fruit and flower reflectance under realistic levels of receptor noise and found **that trichromacy was optimal in the human visible range (400–700 nm). While a reduction in the number of receptors significantly reduced the reconstruction, adding a fourth receptor did not improve the reconstruction quality. In the same way, tetrachromacy was found to be optimal for the visual range seen by birds (300-700 nm). Why some animals have nevertheless evolved visual systems with way more receptor types intrigues scientists till today (Thoen et al., 2014)**

2.7 Seeing in the ultraviolet - why rodents are not color blind

The bees ability to see in the UV range was established early on (Daumer, 1956; Autrum and Zwehl, 1964). That, in general, many invertebrates, fish, and birds have the same ability became clear over the years. Interestingly, this ability seemed to be absent in mammals (Jacobs, Neitz, and Deegan, 1991). At the end of the eighties Benshoff et al. (1987) analyzed the effect of late-night light exposure on the melatonin concentration in pineal glands of the rodent *Peromyscus leucopus*. They found that, as expected, the concentration dropped as a result of exposure to light of the visual range. To their surprise, however, wavelength as low as 320 nm also reduced the melatonin concentration. Alerted by this Jacobs, Neitz, and Deegan (1991) **demonstrated with ERG recordings in *Mus musculus* that indeed rodents have a UV-sensitive cone pigment in addition to the already discovered pigment that is maximally sensitive at around 500 nm.**

Before this study, rodents had been thought to be cone-monochromats (i.e., they had only one cone type) and, therefore, color blind. Now, that a second cone mechanism had been identified, **it was demonstrated in gerbils that they could be trained to discriminate stimuli based on color** (Jacobs and Deegan II, 1994). Furthermore, it became evident that rodents do not have two different cone classes but rather that **the UV sensitive photopigment is co-expressed with the other opsin but differentially over the retina in a dorsoventral gradient** (Govardovskii et al., 1992). Therefore, different parts of the retina have different spectral sensitivities and cells that compare these regions have only recently been found (Breuninger et al., 2011; Chang, Breuninger, and Euler, 2013).

2.8   Color constancy

Figure 2.10:   Snow Effect (1891) by Claude Monet, National Gallery of Scotland, Oil on canvas, 65.00 x 92.00 cm. The image is in the public domain.

One of the greatest challenges in vision is the question posed when we ask how our visual system achieves the surprising constancy in the coloring of objects in the world. Practically no matter what the illumination, whether bright morning light or the long wavelength dominated dusk, a tomato stays red. In other words, how can the shadow of a haystack (see Figure 2.10) as perceived by Monet, be blue? After all, isn't a shadow just less light?

In his Farbenlehre, Johann Wolfgang von Goethe described experiments where he observed the color of shadows cast by objects illuminated simultaneously by two spectrally different light sources (e.g., moonlight and the light from a candle). To his surprise, he found the shadows vividly colored in hues not apparent when he looked at the illuminating lights (Goethe, 1810).

This effect, however, surprising to Goethe, was not exactly new. According to Monge (1789) Pierre Augustin Boissier de Sauvages, had described the effect earlier, but it is fair to say that it became famous through the writings of Goethe and Count Buffon (Kuehni, 1997).

Additionally Monge (1789) had observed that red objects, when looked at through red transparent filters, non-intuitively appeared not red but as white as the "white" objects in the same scene. Other works contributed more such observations, and it became apparent that **the color of an object is not determined solely by the light that hits the eye.**

It was 1958 when Dr. Edwin H. Land [9] entered the world of color sci-

---

[9]Lands biography is certainly a colorful one. He was the founder and principal stockholder of Polaroid, invented the first instant camera, was an adviser to Dwight D. Eisenhower, part of several early cold war intelligence projects (Lockheed U-2, Corona, Samos, Manned Orbiting Laboratory), and recipient of the Presidential Medal of Freedom.

(a)

(b)
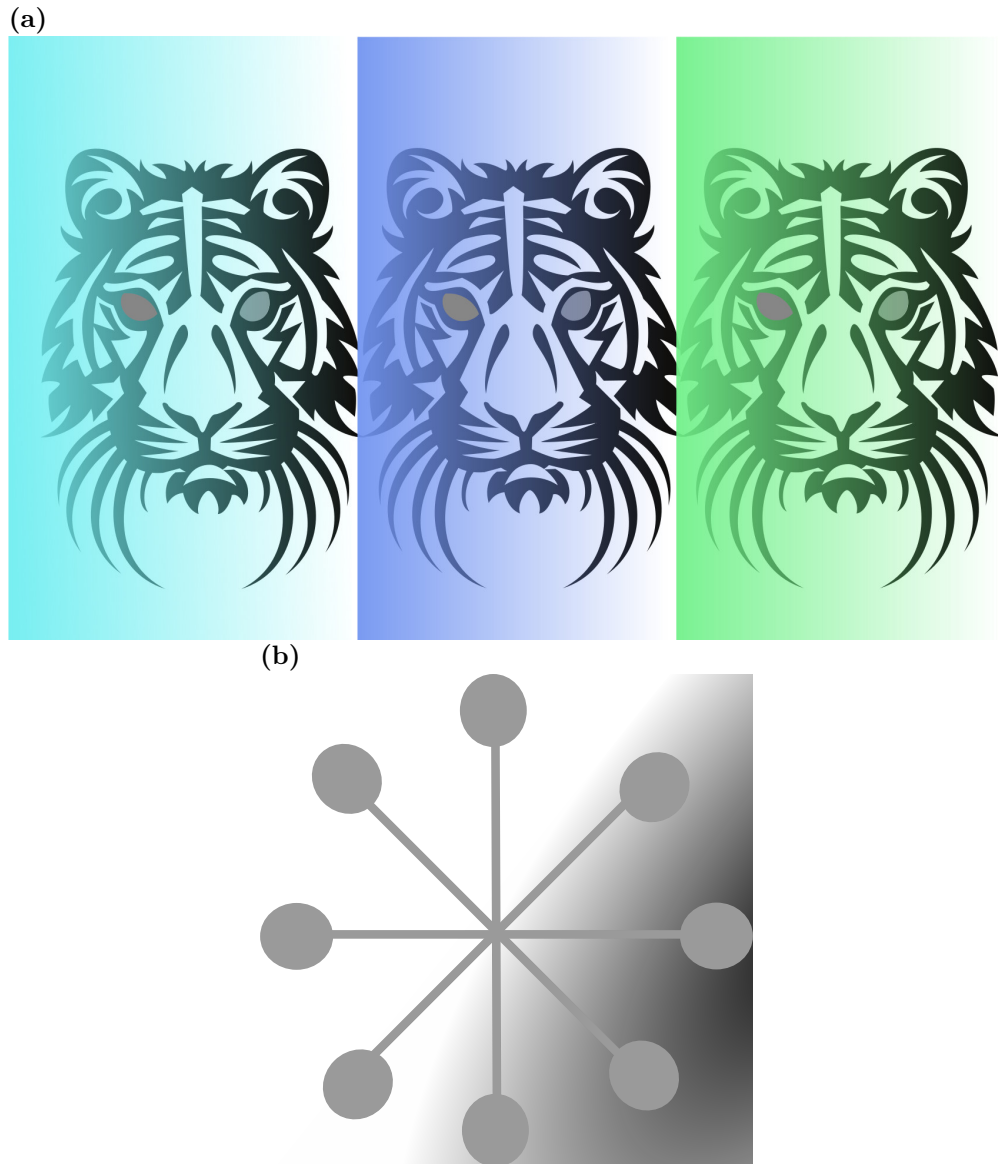
Figure 2.11: Context Effects: (a) The eyeballs of all three tigers have the exact same rgb values. Yet, the right eyes (perspective tiger) are perceived as of having different colors. (Tiger vectors courtesy of http://www.vectorportal.com) (b) All circles and the lines connecting them have the same rgb value. The circles in a darker context, however, appear to be lighter than those in a lighter context.

ence. In a paper that infuriated color scientists of the time (Walls, 1960),
he had argued that the established cornerstones of color science were prac-
tically of insignificant importance (Land, 1959). Among other things, but
most importantly, Dr. Land had found that spectrally identical stimuli,
depending on the context, can be perceived as of having different colors (a
simple example can be seen in Fig. 2.11a). This implied that simple color
mixing models (see Figure 2.3b) are enough to explain which stimuli com-
binations would look alike when isolated. Yet, they could not predict what
colors an object would have in normal situations. Furthermore, during the
development of new color photography techniques, he experimented with
dichromatic light mixtures and found that, with only two lights of different
spectral compositions, he could mix colors that, according to the dominant
trichromatic theory (see Chapter 2.2), should not appear.
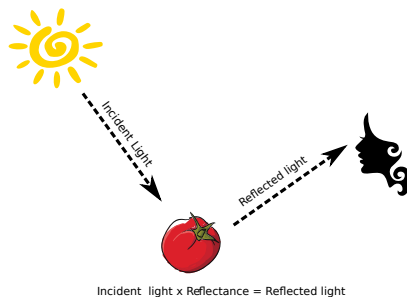
Figure 2.12: Color constancy: The inci-
dent light is reflected from an object and
the reflected light is what hits our eye.
The color of the object is determined by
the reflectance of the object, which can
be reconstructed from the reflected light
if the incident light is known.

Land demonstrated his findings mainly
in public audience based demonstrations,
that were naturally missing the rigor-
ous scientific controls many scientists ex-
pected. This, accompanied by his pre-
tentious personality, made it for many re-
searchers easy to believe that his findings
were mere artifacts. In fact, some even
claimed them to be results of clever manip-
ulations akin to petty magic tricks. How-
ever, over time, it became apparent that
there was a huge piece of information miss-
ing in the understanding of color vision.

**Nowadays we know that the color of an object is not solely de-
termined by the wavelengths it reflects, but also by those (wave-
lengths) it does not, i.e., by its reflectance** (see Figure 2.12).

That was why Goethe's shadows had been so vividly colored. The
illumination had been a mixture of long and short wavelength light. In
this context, the absence of short wavelength light (moonlight shadow)
indicates a reflectance that reflects weakly in the short wavelength range

and subsequently appears "yellow". The same explanation can be used to understand why the eyes of the tiger in Figure 2.11a or the circles in Figure 2.11b appear to have different colors or brightness.

To identify the reflectance of an object, a visual system needs information about the light that was reflected and, additionally, it needs to determine the composition of the light that has illuminated the object.

This had not been unknown to color-scientists during Land's time (Locke, 1935; Helson, 1943). Yet, it had not been discussed in great length and was typically blamed on some adaptation while the textbooks remained virtually silent regarding such phenomena (Mausfeld, 2003).

It were again Land and Mc Cann (1971) who presented first approaches towards an integrated theory on how the visual system might solve the problem of identifying reflectances, and it took color science another ten years to embrace the topic.

That the visual system determines "reflectances" is the reason, objects have the same color practically independent of illumination. The visual system determines the reflectance as **reflectances are biologically more relevant than the light that has been reflected. As the reflectance is a property of an object, it can signal important information about the status of the object, for example, fruit ripeness or sexual status.**

To infer reflectances, **it is important to make use of the information from the larger visual context of the object in question. Specifically, relationships between colors in a scene, i.e., contrasts between object surfaces and their surroundings, are more stable under changing illumination than absolute intensities or spectral compositions** (Foster et al., 2006). Global contrasts, thus, are cues that contribute strongly to color constancy (Foster et al., 2006; Hurlbert and Wolf, 2004; Kraft and Brainard, 1999).

Today, the practical importance of color constancy is widely embraced in vision science and it has been argued that a non-color-constant visual system is practically useless concerning color vision (Mausfeld, 2003). Al-

though color constancy has been shown in primates and fish (Locke, 1935; Dörr and Neumeyer, 2000), the distribution of color constancy among animals is not yet well understood.

3

Publications

3.1 Wavelength discrimination in Drosophila suggests a role of Rhodopsin 1 in color vision

Wavelength Discrimination in Drosophila Suggests a Role of Rhodopsin 1 in Color Vision

Christian Garbers, Thomas Wachtler*

Department Biologie II, Ludwig-Maximilians-Universität München, Planegg-Martinsried, Germany and Bernstein Center for Computational Neuroscience Munich, Munich, Germany

* wachtler@biologie.uni-muenchen.de

Abstract

Among the five photoreceptor opsins in the eye of Drosophila, Rhodopsin 1 (Rh1) is expressed in the six outer photoreceptors. In a previous study that combined behavioral genetics with computational modeling, we demonstrated that flies can use the signals from Rh1 for color vision. Here, we provide an in-depth computational analysis of wildtype Drosophila wavelength discrimination specifically considering the consequences of different choices of computations in the preprocessing of the behavioral data. The results support the conclusion that Drosophila wavelength discrimination behavior can best be explained by a contribution of Rh1. These findings are corroborated by results of an information-theoretical analysis that shows that Rh1 provides information for discrimination of natural reflectance spectra.

Introduction

Color vision is widespread across the animal kingdom. It has been demonstrated in many insect species, including the fruit fly *Drosophila melanogaster*[1]. The sensory basis for color vision is the presence of photoreceptor types with different spectral sensitivities. Five different photoreceptor types exist in the ommatidial eye of Drosophila. Their respective photosensitive opsins are called rhodopsin 1 (Rh1), rhodopsin 3 (Rh3), rhodopsin 4 (Rh4), rhodopsin 5 (Rh5), and rhodopsin 6 (Rh6). [2, 3] The ommatidia can be grouped into two types. In the so-called pale ommatidia the inner receptors cell R7 (R7p) expresses Rh3, while the R8 (R8p) cell, positioned below R7, express Rh5. In the so called yellow ommatidia R7 (R7y) expresses Rh4, while R8 (R8y) expresses Rh6 [4–7]. Furthermore, in the ommatidia that span the dorsal third of the retina, Rh3 is co-expressed within the cells that normally express only Rh4 (R7y) [8]. In the dorsal most rows of cells both inner receptors express Rh3 [9, 10]. Until recently the common assumption was that Rh1 does not contribute to color vision [11, 12]. Furthermore, the outer receptor cells are equipped with an sensitizing pigment, which makes them additionally receptive in the UV [13–15].

In a recent study that combined results from computational modeling, electrophysiology, and behavioral genetics, we have shown that fruit flies are able to discriminate stimuli based on chromatic differences even when only signals originating from Rh1 and a single other opsin are present [16]. This implied that Rh1 can be used for color vision in the fruit fly. The modeling results were based on published data on wavelength discrimination derived in behavioral experiments. Because there is some freedom in the derivation of a quantitative estimate of wavelength discriminability, the method of analysis might have an influence on the outcome. Therefore, we performed an in depth computational investigation on the role and impact of Rh1 signals in wildtype Drosophila wavelength discrimination, and we analyzed in detail whether changes in the assumptions underlying the derivation of behavioral wavelength discrimination data would influence the results.

While it has been shown that dichromatic flies were able to discriminate narrow-band stimuli using signals from Rh1 [16], the influence of Rh1 on wildtype Drosophila color vision is still an open question. In general, the usefulness of having five receptors for color vision could be taken into question. For human color vision, based on reflectance data from Munsell chips and the observation that reflectance spectra are band-limited functions, it has been argued that a finite linear model of 6–12 parameters should be sufficient to completely reconstruct reflectance spectra from "color signals" [17, 18]. This can be interpreted as an upper bound for the maximum number of receptor types that would make sense to code for color [17, 18]. However, the number of photoreceptors that would practically be beneficial has been estimated to be lower [18]. In general, Vorobyev [19] analyzed the accuracy of reconstruction of fruit and flower reflectance under realistic levels of receptor noise. He found that for an animal with a visual system extending into the UV, pentachromacy did not provide a significant benefit over tetrachromacy. It is therefore questionable whether the signals from Rh1 would actually be informative.

We therefore analyzed natural reflectance spectra from a large database [20]. We determined the information content across wavelengths and show that indeed in the range around 500 nm, where we have found that Rh1 is necessary to explain wildtype wavelength discrimination, information about spectra identity is available from Rh1. In an additional theoretical analysis of the natural reflectance spectra in the frequency domain we determined the number of receptor types that would suffice to acceptably approximate the data. We analyzed, based on mutual information [21], the amount of information in the signals from Rh1 and analyzed how much of this information is already transmitted by the other opsin.

Methods

Quantifying wavelength discrimination

The ability to discriminate stimuli varying in wavelength has been quantified by deriving so-called $\delta\lambda$ functions [22]. A $\delta\lambda$ function indicates the minimal change in wavelength that is necessary, at a certain reference wavelength, for an animal to discriminate a stimulus from the reference wavelength. In insects and other animals, such quantitative estimates on wavelength discrimination have been derived from discrimination learning experiments [23]. Animals were conditioned to choose a certain wavelength above another wavelength, and the animals' performance was quantified by determining how many animals, or how often an animal, was able to discriminate the stimuli. The corresponding probability is called a conditioning index [23]. The procedure is repeated for several wavelength pairs, resulting in a conditioning index function (see Fig 1).

To derive a quantitative $\delta\lambda$ estimate from conditioning index functions, a threshold T is defined (Fig 1). The amount of wavelength change necessary to reach this threshold is then
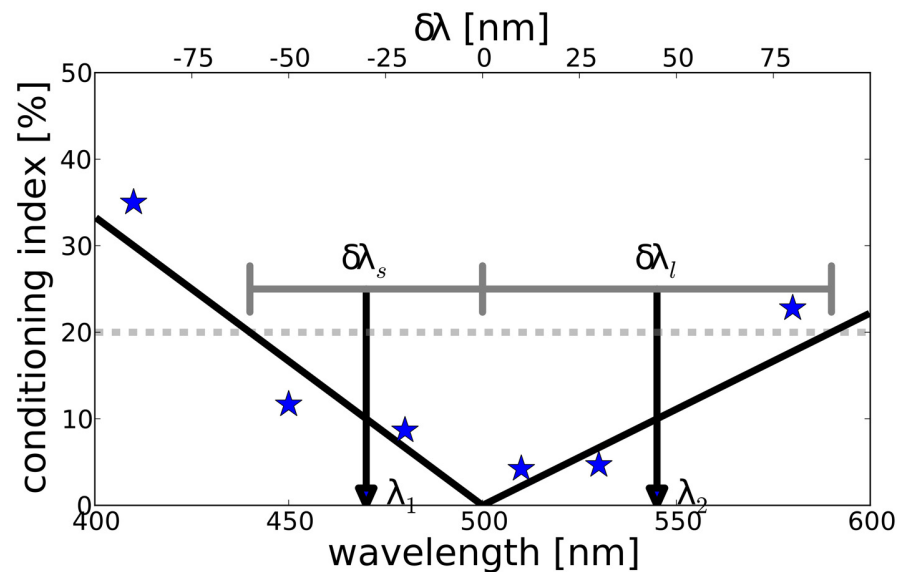
Fig 1. Example plot of conditioning index data. Animals had been trained to discriminate a reference stimulus of 500 nm from stimuli of other wavelengths as indicated on the horizontal axis. The vertical axis shows for each pair how many animals, above chance, gave the correct response. The black solid line shows a linear interpolation of the data points. The dashed line indicates an (arbitrarily chosen) threshold of 20%. $\delta\lambda_i$ are the ranges between the reference wavelength and the intersection between the threshold and the interpolation of the data, as indicated by the gray horizontal lines. The midpoints of these ranges, λ_1 and λ_2, are the virtual reference wavelengths as used to derive the wavelength discrimination function [24].

defined as the discriminability at that reference wavelength. By analyzing several conditioning index curves in this way, an estimate of the $\delta\lambda$ function was derived by determining the $\delta\lambda$ for which the discrimination conditioning function $L_{\lambda_0}(\delta\lambda)$ reached the threshold T,

$$L_{\lambda_0}(\delta\lambda) = T. \tag{1}$$

This threshold is arbitrarily chosen and different values have been used. Therefore the derived estimates constitute only a lower bound of the animal's ability to discriminate light stimuli by wavelength [24].

Eq 1 typically has two solutions, one for longer ($\delta\lambda_l$) and one for shorter ($\delta\lambda_s$) wavelengths. To derive a unique discrimination value per reference wavelength, several strategies have been used. If the two solutions are not too different a method is to take the mean of the two values [25].

$$\frac{\delta\lambda_l + \delta\lambda_s}{2}.$$

If the solutions are very different this results in information loss and a less precise estimate. To preserve more information from the conditioning curves into the $\delta\lambda$ estimates, Von Helversen [23] used a different approach. He kept the two values but derived new virtual reference wavelengths for them by taking the midpoints of the intervals $[\lambda_0, \lambda_0 + \delta\lambda_l]$ and $[\lambda_0 - \delta\lambda_s, \lambda_0]$ (see Fig 1 for an illustration) denoting $\delta\lambda_l$ or $\delta\lambda_s$, respectively, as the wavelength discrimination values for the two virtual reference wavelengths,

$$\lambda_1 = \lambda_0 - \frac{\delta\lambda_l}{2} \tag{2}$$

towards shorter wavelengths, and

$$\lambda_2 = \lambda_0 + \frac{\delta\lambda_s}{2} \tag{3}$$

towards longer wavelengths. We will call this the split-reference transformation.

This approach circumvents the problem of having two discrimination values per reference by creating two virtual references. It therefore results in more data points for the wavelength discrimination function. As both virtual reference wavelengths depend directly on measured $\delta\lambda$s (see Eqs 2 and 3), which have error bars, the positions of the new references are also uncertain. Therefore, these $\delta\lambda$ values have errors in x and y [24].

Modeling wavelength discrimination

To determine wavelength discrimination functions, we used an approach based on the method of Vorobyev and Osorio [26], who modeled spectral sensitivity functions of opponent combinations of receptor responses and calculated the distances between stimuli in the space of such opponent responses, taking into account the estimated noise in the photoreceptors. We did not make any assumptions about the noise and more generally asked whether there is a way, to linearly combine the opponent channels such that the result would fit to the data.

Let $\Delta q_i(\lambda)$ be the signal difference that two stimuli evoke in receptor i at wavelength λ. Then for two receptor types 1 and 2 the signal in a neuronal channel k that combines these two receptor signals opponently is

$$S_k^2(\lambda) = (\Delta q_1(\lambda) - \Delta q_2(\lambda))^2. \tag{4}$$

The Euclidean distance in a space with a basis formed by several of such opponencies can be used to predict spectral sensitivity [26]. In the case of Drosophila with five rhodopsins, there are ten different opponent combinations. From this pool of potential opponent channels we calculated relative spectral sensitivity thresholds for visual systems combining information from several of these channels by summation over the signals from the n respective channels

$$S^2(\lambda) = \sum_{k=1}^{n} w_k S_k^2(\lambda), \tag{5}$$

where w_k is a vector of weights that scales the opponent channels relative to each other.

$\Delta q_i(\lambda)$ corresponds to the slope of the spectral sensitivity of the ith receptor at wavelength λ. From $S^2(\lambda)$ we calculate wavelength discrimination by taking the inverse

$$D(\lambda) = \sqrt{\frac{1}{S^2(\lambda)}}. \tag{6}$$

We fitted wavelength discrimination functions for different visual systems by adapting w_k to minimize the squared distance between model and data from Hernandez de Salomon and Spatz [24]. Fitting was performed with a variant of the Levenberg-Marquart algorithm implemented in the Python programming language [27]. We fitted models for different hypothetical visual systems. We started with models with a single opponent channel, then proceeded to fit all possible combinations of two opponent channels, then three, and so forth. In this way we fitted all possible combination up to eight combined mechanism. Including more channels would have reduced the number of degrees of freedom below 1. However, the systems with large numbers of channels always yielded poor fits with p below 0.05.

Opponent channels were derived from published Drosophila spectral sensitivities and had sensitivity maxima at 478 nm (Rh1), 345 nm (Rh3), 375 nm (Rh4), 437 nm (Rh5) and 508 nm (Rh6), respectively (see Fig 5 in [14]). Spectral sensitivities were scaled to peak at unity.

To quantify goodness of fit between a model and the behavioral data on wavelength discrimination we used the χ^2 statistic

$$\chi^2 = \sum_{i=1}^{n} \frac{(x_i - y_i)^2}{\sigma_i^2}, \tag{7}$$

where x_i are the observed discrimination values and y_i predictions from the model. σ_i is the standard deviation of the data. The error on the wavelength axis (see above) was transformed into a discrimination error by estimating the impact of the wavelength uncertainty with respect to the current model estimate. For a given datapoint we calculated the maximum discrimination uncertainty that the associated wavelength error would have by deriving the maximum discrimination change that the current model estimate had in a range corresponding to the given error around the data point. For the wavelengths λ_i with empirical data on wavelength discrimination

$$E(\eta) = D(\lambda_i) - D(\eta). \tag{8}$$

is the difference in discrimination between the wavelength λ_i and η. By taking the maximum of $E(\eta)$ in a range given by the error in the wavelength Δ_i we derived an upper bound for the discrimination uncertainty due to wavelength uncertainty,

$$\max_{\eta \in [\lambda_i - \Delta_i, \lambda_i + \Delta_i]} \frac{1}{2} |E(\eta)| \tag{9}$$

By adding this additional error to the discrimination error, the χ^2 statistic took uncertainties in both dimension into account. This is a rather liberal strategy which was used to be inclusive towards models without Rh1.

The χ^2 value, which is a weighted sum of squared errors, does not take the number of fitted parameters into account. Under the assumption that the underlying random variable is independent and standard normal, the χ^2 values follow a χ^2 distribution derived for a number of degrees of freedom. From this χ^2 distribution we can directly get the likelihood of a given χ^2 value. We derived likelihoods for all fits. Only fits that could not be excluded under the null hypotheses (p-value > 0.05) that the data had been generated from the model, were analyzed for receptor contributions as described below.

We quantified which receptor types contributed to the discrimination in models for visual systems that fitted the data (p > 0.05) by calculating the weight of a certain receptor in all models relative to the sum of weights for all receptors in all models. In the same way, we quantified the contribution of the ten opponent channels.

To analyze the influence of the chosen transformation from conditioning function to $\delta\lambda$ function, we determined the $\delta\lambda_s$, $\delta\lambda_l$, and λ_0 values used in Hernandez de Salomon and Spatz [24] and re-derived wavelength discrimination functions, using the mean transforms introduced above.

Analysis of natural reflectance spectra

To determine the potential contribution of Rh1 to Drosophila color vision, we quantified the amount of available information as a function of wavelength by calculating the differential entropy of the spectra dataset in 1 nm intervals. Differential entropy extends the idea of Shannon entropy, a measure of average surprise of a random variable, to continuous probability

distributions. In our case, it indicates how informative signal variation at a given wavelength is with respect to spectra identity. The higher the value the more information can be gained by observing the value at that wavelength.

The differential entropy of a random variable x with probability density $f(x)$ is defined as

$$H(x) = -\int_{\mathbb{X}} p(x) \log(p(x))\mathrm{d}x \tag{10}$$

We calculated the differential entropy for each wavelength using Gaussian kernel density estimation as implemented in scipy [27].

To estimate the number of receptors that would theoretically be useful to account for natural color variability, we calculated the power spectral density of the natural reflectance spectra under D65 illumination using discrete Fourier transform. The power spectrum of a reflectance spectrum $x(\lambda)$ describes how the variance of the spectrum is distributed over the frequency components into which it may be decomposed. Note that frequency in this case does not refer to the frequency of the electromagnetic wave but rather to the abscissa of the Fourier transform of the spectral reflectance curve and is therefore measured in cycles per wavelength. If the power spectrum is band limited, i.e. above a certain frequency practically no power is left, then such band limited function can very accurately be approximated by a linear model of a few parameters. The number of parameters is determined by the Whittaker, Kotelnikow and Shannon sampling theorem [28]. In the case of visual systems it determines the number of receptors useful to approximate the spectra in a given visual range (300 nm–550 nm).

The critical question, however, is which receptors are best suited to extract such information and, for the case of Rh1, how much non-redundant information can the fly gain by integrating the information from Rh1. To quantify this, we determined the amount of information about the spectral composition of the environment contained in the photoreceptor signals. We calculated the mutual information between the photoreceptor outputs $\vec{O}$ as determined by the spectral sensitivities and the spectral inputs $\vec{W}$, using the established method of of Lewis and Zhaoping [21]. We did the calculations using the Drosophila spectral sensitivities, normalized to unit area, and one more principal component as well as a a larger set of reflectance spectra. The spectra used were from an online database [20] and were mainly reflectances of various species of flowers. Apart from that, the method was as described by Lewis and Zhaoping [21]. We calculated the information assuming equal noise proportional to the square root of the signal in all receptors. This corresponds to a situation of normal lighting [21].

Mutual information measures how much information about a random variable Y is obtained by observing another variable X. In our case it indicates how much uncertainty about color inputs ($\vec{W}$) is removed by observing the photoreceptor outputs ($\vec{O}$). Formally this is defined as

$$I = \int_{P} p(\vec{O}, \vec{W})\log_2\left[\frac{p(\vec{O}, \vec{W})}{p(\vec{O})p(\vec{W})}\right]\mathrm{d}\vec{W}\mathrm{d}\vec{O}, \tag{11}$$

where $p(\vec{O}, \vec{W})$ are the joint probability distributions of $\vec{O}$ and $\vec{W}$, and $p(\vec{O})$ and $p(\vec{W})$ their respective marginals. We estimated $p(\vec{W})$ from the natural reflectance spectra by means of principal component analysis on the spectra dataset. We represented each spectrum by its power in the first four principal components, which capture 95% of the variance in the data. We then fitted a four-dimensional truncated Gaussian to this dataset and hence derived $p(\vec{W})$. Truncation was done under the constraint that mean and variance were fixed, that is, the variance of the fitted function was the same as the variance of the data. To arrive at $p(\vec{O}, \vec{W})$, we

Table 1. Factors describing the relation between principal component and spectral sensitivity. The values are the inner product between spectral sensitivities and eigenfuctions of the spectra dataset calculated for D65 illumination (see [21] Eq 4).

	Rh1	Rh3	Rh4	Rh5	Rh6
PC 1	5.58	0.944	1.65	4.35	5.92
PC 2	3.38	-3.59	-3.53	1.34	3.24
PC 3	-5.17	-0.654	-2.83	-6.94	-1.84
PC 4	-3.04	-0.67	-0.164	-0.614	-4.70

doi:10.1371/journal.pone.0155728.t001

Table 2. Factors describing the probability density of the spectral sensitivities. First two column give the mean and variance of the first four principal components for the set of reflectances. The third column gives the fraction of the total variance explained by the corresponding principal component. The fourth column gives the associated eigenvalues.

	μ	σ^2	Var. explained	Eigenvalue
PC 1	0	5.05	0.52	3.822e+05
PC 2	0	0.501	0.19	1.386e+05
PC 3	0	1.29	0.17	1.270e+05
PC 4	0	0.75	0.06	4.691e+04

doi:10.1371/journal.pone.0155728.t002

calculated $p(\vec{O}|\vec{W})$ assuming that receptor signals for a given reflectance $\vec{W}$ (calculated with respect to the spectral sensitivity of the receptor and the derived principal components) vary due to Gaussian noise. With $p(\vec{O}|\vec{W})$ known, $p(\vec{O}, \vec{W})$ is simply $p(\vec{O}|\vec{W})p(\vec{W})$ and $p(\vec{O})$ can be calculated as $p(\vec{O}) = \int p(\vec{O}, \vec{W}) d\vec{W}$. Numerical integration was performed on Tesla K80 GPU Accelerators using PyCuda [29] and custom written compute kernels. Detail's on the methods can be found in the original publication [21]. Parameters used to calculate the information can be found in Tables 1 and 2.

Results

Generally, models including Rh1 fitted the data better than models without Rh1 (see Fig 2). Fig 2a shows the distribution of the χ^2 values calculated over all fitted models with and without a contribution of Rh1. Models without Rh1 generally gave poor fits (best fit p-value below 0.001, Fig 2c), while a subset of the models with Rh1 explained the data well (best fit p-value of 0.17, see Fig 2d). Statistics for the best fitting models disregarding one of the opsin types can be found in Table 3.

Contribution of Rh1

The most prominent difference between models with and without Rh1 was the ability of the Rh1 models to fit the steep increase in discriminability between 470 nm and 500 nm that is evident in the data. This increase in discrimination cannot be explained without a contribution of Rh1, as Rh1 is the only opsin with increasing slope in that region (Fig 2b) and such an increase in the slope of the spectral sensitivity is a prerequisite for a better wavelength discrimination.

In the models that fit well (p > 0.05), Rh1 was the opsin that contributed second-most to the fits. Only Rh6 contributed more (Fig 3a). Among the opponent channels, Rh1-Rh6 contributed most to models that gave good fits (Fig 3b). Together, Rh1-Rh6 and Rh4-Rh6 made up more than two thirds of the overall contribution.
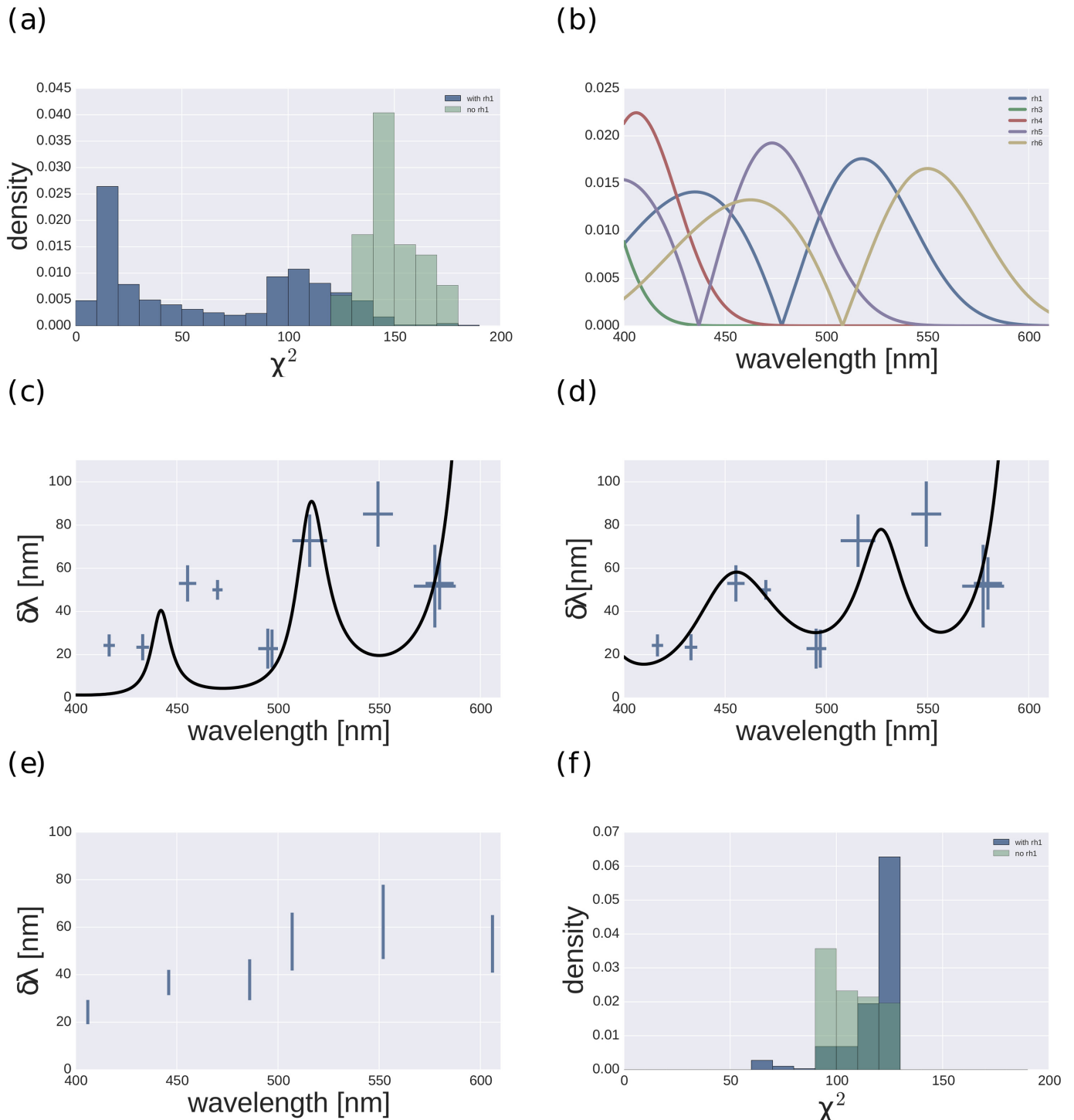
Fig 2. Fit statistic over all possible models and the best fitting models. (a) Histograms of χ^2 values for all fits of models without Rh1 (green) and with Rh1 (blue). (b) Absolute slopes of Drosophila opsins in the visual range. (c),(d) Best fitting models without Rh1 (i.e. Rh4-Rh6, Rh5-Rh3; weights:609.9 177.1) and with Rh1 (Rh1-Rh6, Rh4-Rh6; weights 100.5, 84.4). (e) Mean-transformed data. (f) Histogram of χ^2 values for fits of the mean-transformed data for models without Rh1 (green) and with Rh1 (blue).

doi:10.1371/journal.pone.0155728.g002

Table 3. Best fitting models when one opsin type is removed. The first column indicates the missing opsin type. The second column indicates the mechanism and the third column the associated weights. The fourth column indicate the associated p values.

Missing Opsin	Mechanisms	Weights	p
Rh1	Rh3-Rh5, Rh4-Rh6	610, 177	0.0000
Rh3	Rh1-Rh6, Rh4-Rh6	101, 85	0.17
Rh4	Rh3-Rh6, Rh1-Rh6	125, 219	0.0016
Rh5	Rh1-Rh6, Rh4-Rh6	101, 85	0.17
Rh6	Rh1-Rh3, Rh1-Rh4, Rh3-Rh4, Rh4-Rh5	71, 70, 61, 48	0.0000

Alternate data transformation

While the data from the split-reference tranformation showed multiple wavelength regions of good and poor discrimination, the mean transformation led to data that indicated one wavelength region of good discrimination, for short wavelengths, and one region of less good discrimination, for long wavelengths (Fig 2e). Furthermore, the number of data points was reduced to six (see Methods). While the best fitting model for the data from the alternate transformation was also a model with Rh1, in general all models had to be rejected (p< 0.001) and the clear difference in fit quality, which was apparent for the data from the original transformation, disappeared. This means that no model was able to explain the data from the alternate transformation.

Encoding of natural spectra

Fig 4 shows the statistics of the natural spectra. The average spectrum is maximally reflective in the long wavelength range. Likewise, the differential entropy indicates that the long wavelength range is most informative, with a steep decline in information below 550 nm. In the range between 500 nm-400 nm it reaches a rather stable plateau. This plateau is followed by another

(a)   (b)
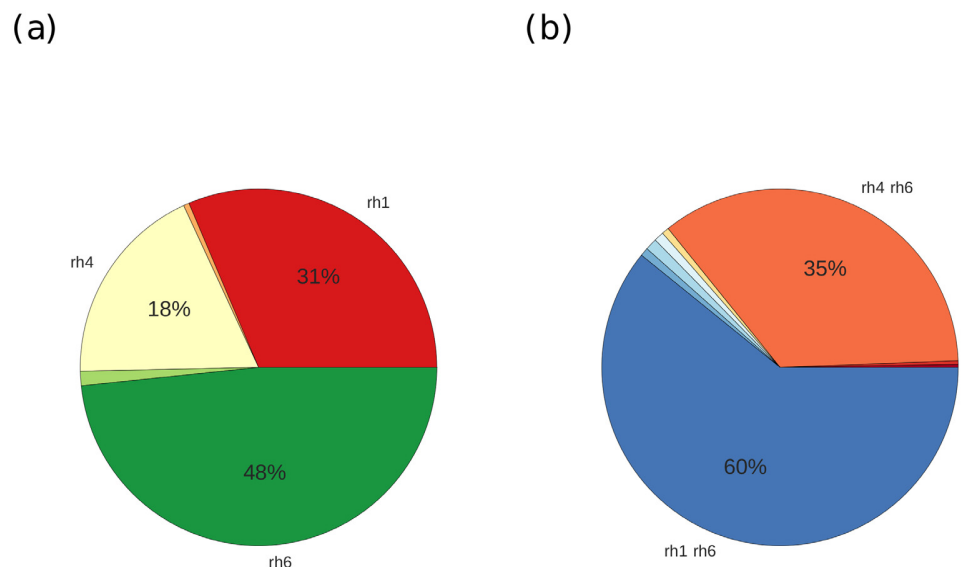
Fig 3. Contributions of receptors and opponent mechanisms to the model fits (p>0.05). (a) Relative contribution of each receptor, measured by the total sum of weights over all fits. (b) Relative contributions of each opponent mechanism; For readability only contributions of 3% or more are labeled.

(a)

(b)

(c)
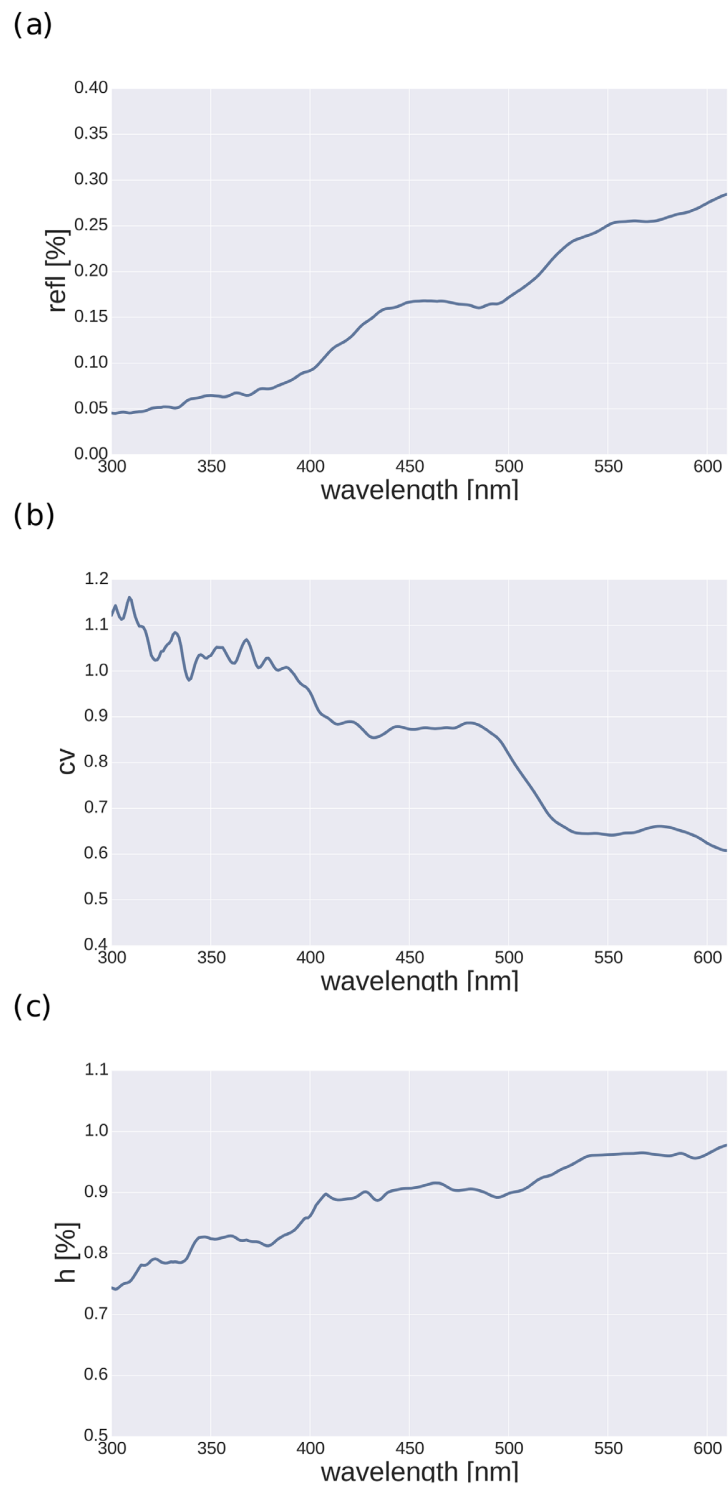
Fig 4. Natural spectra statistics. (a) Average over all spectra in the FRED database. (b) Coefficient of variation as function of wavelength. (c) Differential entropy. All plots show values calculated for each wavelength bin separately.

decline to another plateau below 380 nm. Interestingly, in a range above 490 nm, where Rh1 is the most sensitive opsin (see. Fig 2b), the differential entropy starts to rise, and it is this very area where Drosophila wavelength discrimination is best [24].

The average power spectral density of natural spectra can be seen in Fig 5a. Most power is in the low frequencies, and power spectral density shows a rapid decline with frequency, which becomes slower around 0.01 cy/nm. Fig 5a shows the cumulative distribution of spectra for a given power fraction, calculated for three cut-off frequencies. At a cut-off frequency of 0.011 cy/nm, most of the spectra have already lost 98.5% or more of their power. This is in line with previous findings [18], but here we used a larger set of different reflectance spectra. It confirms that natural reflectance spectra are approximately band limited with a cut-off frequency of 0.01 cy/nm. Thus, it is sufficient to sample changes in reflectance that have a cycle length of 100 nm. Considering the sampling theorem [28] and by assuming a visual range of 300 nm-550 nm, we can conclude that five receptors, evenly spaced 50 nm apart from each other (eg., with peaks at 325 nm, 375 nm, 425 nm, 475 nm, 525 nm) would perfectly sample the natural data variability.

The mutual information in the five receptor types is shown in Fig 6b. The Rh6 opsin is most informative, directly followed by Rh1 and Rh5. The two UV receptor types are only half as informative as their longer wavelength companions. Of the five possible four-receptor combinations, the traditional system without Rh1 is actually most informative, while for the other combinations the informational content is higher when substituting lower wavelength opsins with Rh1. Finally, the addition of the Rh1 opsin to the traditional system, leading to a five receptor system, is only 7% more informative. On average, moving from three to four receptors systems adds 17% of information; from two to three receptors 21% (data not shown).

Discussion

In a previous study we focused on models that, considered as being implied by the retinal architecture, included comparisons between inner ommatidial receptors only (Rh3-Rh5 or Rh4-Rh6). Here we provide a more in-depth analysis on the role of the outer receptors with Rh1. We determined the best fitting opponent models that either included or did not include Rh1. The well fitting models all made use of spectral information from Rh1. Furthermore, the opsin that contributed most to the good fits was Rh6, directly followed by Rh1. Additionally we found that the Rh1-Rh6 opponency together with the Rh6-Rh4 opponency explained most of the data. The reason for this can be found in the spectral profiles of the opponent mechanisms. The only mechanism that had a maximum in the slope near 500 nm, where the data indicate good wavelength discrimination in the fly, was the Rh1-Rh6 opponency. For shorter wavelengths, around 470 nm, the behavioral data suggested a lower discrimination, requiring a lower slope, as exhibited by the Rh1-Rh6 mechanism. Another increase in discrimination at even shorter wavelengths is also supported by the Rh1-Rh6 opponency. Above 500 nm, the data indicated a sharp decline in discriminability. This decline was supported by a decline in the slope of the Rh4-Rh6 opponency, the mechanism which might also well contribute to the increase in discriminability between 470 nm and 400 nm. Thus, a combination of the two opponent mechanisms, Rh4-Rh6 and Rh1-Rh6 already explains the data quite well.

Two aspects of the behavioral data may have led to an overestimation of the role of Rh1. First, there are two data points near 500 nm, which amplifies the requirement of a mechanism that explains the data in this region. However, repeating the analysis with one of these data points excluded did not lead to qualitatively different results. Furthermore, the absence of data in the UV range clearly downplays the role of the two UV opsins (Rh3, Rh4). Nevertheless, while quantitatively the weight of Rh1 in the model fits might overestimate its role, the

(a)
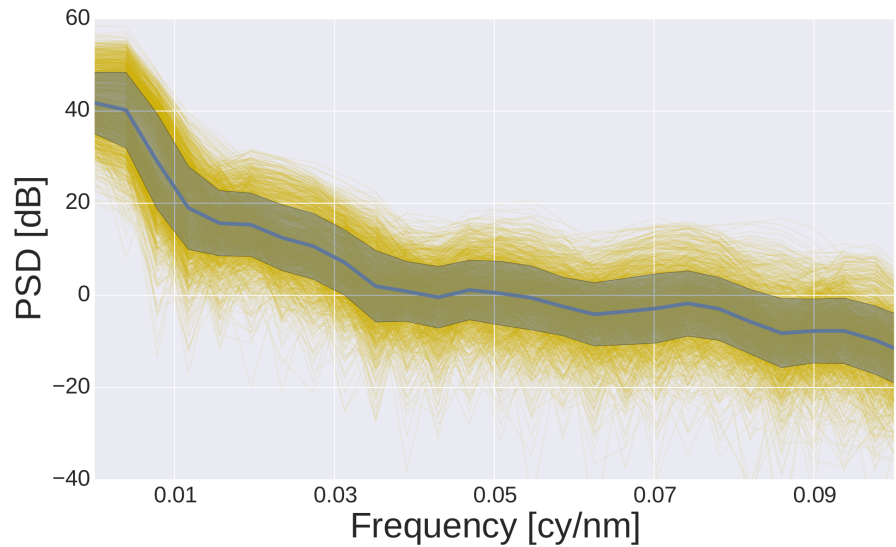
(b)
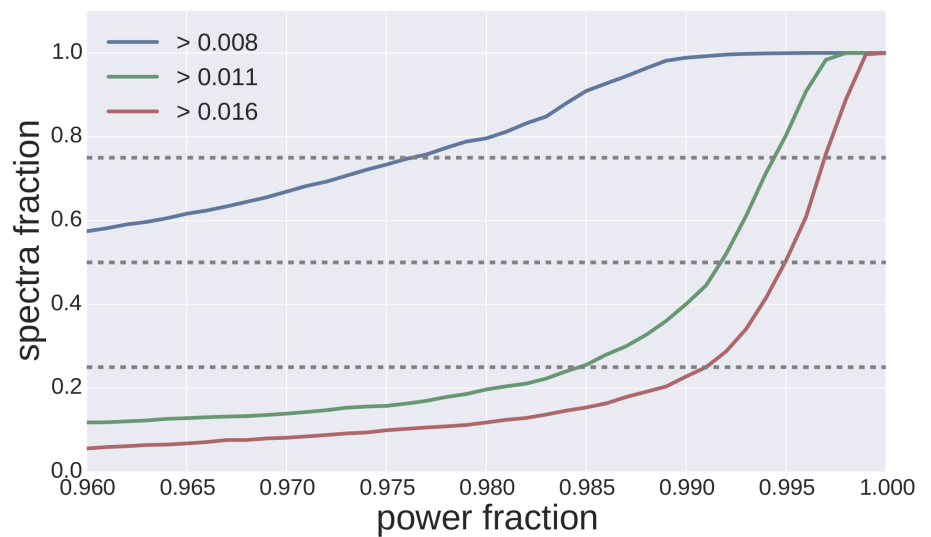
Fig 5. Power spectral density of natural spectra. (a) Average psd calculated over all spectra (blue line, the shaded area indicates standard deviation). Individual psd are plotted as thin yellow lines. The abscissa indicates spectral frequency in cycles per nanometer. The ordinate indicates power measured in dB. (b) Fraction of spectra (ordinate) that have a cumulative power fraction below a certain value (abscissa). Values are plotted for cut-off frequencies of 0.008 (blue), 0.011 (green), and 0.016 (red). Dotted lines indicate quartiles.

doi:10.1371/journal.pone.0155728.g005

qualitative argument holds that the increase in discrimination performance between 470 and 500 nm can only be explained with a contribution of Rh1. Concerning the role of the other opsins it is surprising that Rh5 did not contribute to the best fitting models. Among the models with a p value above 0.05 there were models with significant contribution from Rh5. However,

(a)

(b)

(c)
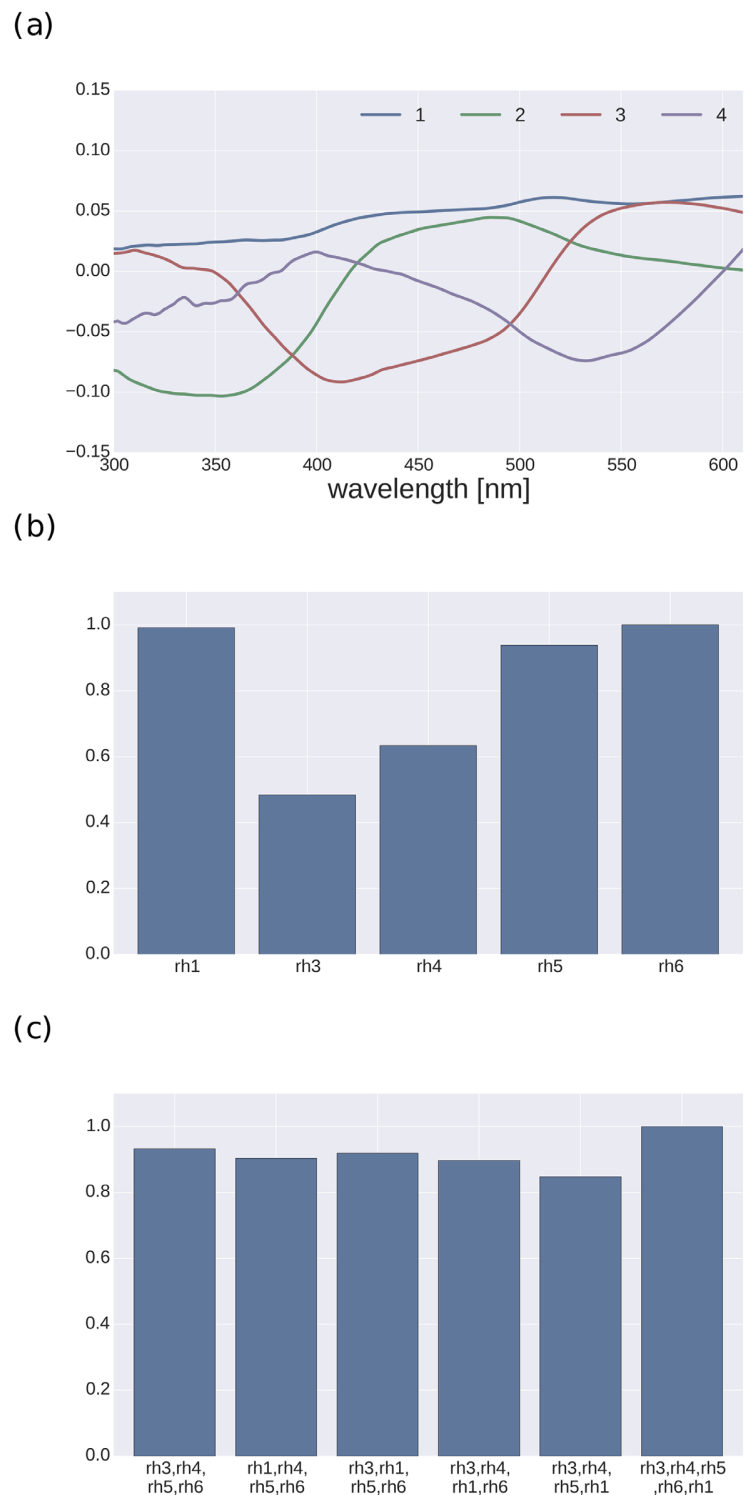
Fig 6. Mutual information. (a) First four principal components calculated over all spectra. Curves indicate unnormalized raw PCA values as a function of wavelength. (b) Mutual information between the individual receptors and the spectra. (c) Mutual information between the five possible systems with four receptors and the system with five receptors. Values are reported as fraction of the maximum [21].

doi:10.1371/journal.pone.0155728.g006

the majority of well fitting models did not include Rh5. Considering the nature and sparsity of the dataset (see also below) as well as the data from dichromatic flies [16], it should not be concluded that Rh5 does not contribute to color discrimination in wildtype Drosophila. Nevertheless, the data used here is best explained by a model that uses only Rh1, Rh4 and Rh6.

Only models using Rh1 yielded fits with p values above 0.05. However, even the best fitting model had a p value of only 0.17. This low value was mainly due to the poor fit to the data point at 550 nm. If this data point is excluded, the fit quality rises to a value of 0.75. It is important to point out that the predicted good wavelength discrimination at 550 nm that can be found in the best fitting models is a direct consequence of the spectral sensitivity of the Rh6 opsin (see Fig 2b). The Rh6 slope peaks at 550 nm and therefore models including Rh6 necessarily predict better discrimination at 550 nm than for longer wavelengths. In their original publication, Hernandez de Salomon and Spatz [24] pointed out that errors in the data increased considerably above 500 nm, and in particular that the value at 578 nm is not significantly different from the value at 550 nm. At wavelengths above 500 nm the overlap between spectral sensitivities, a necessary prerequisite for color discrimination, is low, and moreover, the two curves have slopes of same sign. Together with the low overall sensitivity in this wavelength range [24] it seems feasible that the stimuli were not properly matched for brightness and that therefore values above 500 nm are unreliable. Overall the goodness of fit was not very high for any of the models. Comparable analyses of wavelength discrimination are rare [30], and it is not clear whether better fits could be expected at all.

In our modeling paradigm, opponent channels are insensitive to intensity changes of broadband light, but for monochromatic stimuli, this is not strictly speaking the case. We nevertheless assumed that non-opponent mechanisms do not play a role for wavelength discrimination. This assumption has been shown to be valid in bees [31], but so far not in Drosophila. While the available data for Drosophila are not rich enough to apply the approach used in bees, we tried to fit purely non-opponent models, i.e., models that combine receptor signals additively, including approaches based on the envelope of the spectral sensitivity curves. None of these models yielded fits that were as good as those with opponent models (data not shown). For the more interesting case of a mixture of non-opponent and opponent mechanisms, we introduced all possible non-opponent combinations of two receptors to the mechanisms used for fitting. We performed fits with all possible models combining up to five mechanisms. As was the case for models comprised exclusively of opponent mechanisms, none of the mixed models without Rh1 provided a good fit. Non-opponent mechanisms did not contribute strongly to the best fitting models. For example, the best fitting mixed model had a p value of 0.15 and was a combination of the two chromatic mechanisms that also gave the best fit in the chromatic case (Rh1-Rh6, Rh4-Rh6) and one non-opponent mechanism (Rh4+Rh5). The weights of the three mechanisms were 98, 75 and 6, respectively, indicating a very low contribution of the non-opponent mechanism. In general, non-opponent mechanisms contributed less than 5% of the weight to the models giving good fits, indicating that spectral discrimination in Drosophila is mainly based on opponent signals.

In cases where noise is proportional to the signal, it has been shown that the logarithm of the receptor signals can be a better choice to model spectral data [32]. Several models in the literature also had a nonlinear component [32–34], however linear approaches also have been shown to yield reliable estimates [35]. We therefore performed an analysis assuming logarithmic receptor signals. We found that no model (neither with Rh1 nor without Rh1) gave acceptable fits. The best fit was by a model that combined the two channels Rh1-Rh6 and Rh3-Rh6. However, even with this model, goodness of fit (p< 0.001) was orders of magnitude below the fits of the linear models.

Relating the slope of the spectral sensitivities of the photoreceptors to wavelength discrimination implies that $\delta\lambda$ is small enough so that the slope can be taken as constant. The values reported in [24] can be as high as 80 nm, a value for which it seems unlikely that this assumption is valid. However, there is reason to interpret these values as relative as opposed to absolute. First, it would be inconsistent to have a discrimination threshold of 80 nm at one wavelength, and 50 nm away a threshold of 20 nm, as is the case in this dataset. As explained above, the values derived by the method of Hernandez de Salomon and Spatz depends on an arbitrarily chosen threshold and provides only a lower estimate of the ability of the flies to discriminate wavelength [24]. Furthermore, the data were obtained in experiments where the behavior of a population of flies was measured. In this paradigm, flies that did not learn the task would have decreased the resulting value of wavelength discrimination. Studies of wavelength discrimination in other insects that reported much lower discrimination thresholds [12, 23] had been performed on individual animals. It can be assumed that in those studies, animals that did not learn the task had been excluded

Other studies on wavelength discrimination have specifically included assumptions about background illumination [30]. We therefore tested whether such a modification would improve the fits and tested the model with the assumption of a background illumination with the spectrum of either a Tungsten lamp (see [30]) or the standard daylight D65. However, in both cases the fit quality decreased compared to the model without assumption of a specific background illumination.

It would be of high value to have a larger dataset on Drosophila color discrimination, ideally measured directly at wavelengths where $\delta\lambda$ is comparable for shorter and longer wavelength. With respect to our main finding, a denser sampling of the region between 450 nm and 500 nm could provide a critical test of a contribution of Rh1. It would also be interesting to test animals with stimuli that are metameric with respect to all but one opsin type, as has been done in primates [36] using broadband stimuli. This type of stimulation, however, requires very precise knowledge of the shape of the spectral sensitivities, which is currently not available for Drosophila. Furthermore, it might be hard to achieve high enough contrasts, especially for photoreceptors with similar or broad spectral sensitivities. Testing individual flies [12] in combination with probabilistic choice modeling [37, 38] and the derivation of psychometric functions which account for lapse rates and biases [38–40] might help further to reduce arbitrariness and noise in the estimates.

In general, the mean-data transform results in a discrimination function that is less complex than the function obtained with the split-reference transformation. Besides the reduction in the number of data points, the discrimination function indicates one region of good discrimination in the short wavelength range and one region of poor discrimination in the long wavelength range, with a rather steep transition. While in this case the best fitting model was a model with Rh1 as well, all fits were poor. Thus, the mean-data transformation leads to $\delta\lambda$ estimates that can hardly be explained by a linear combination of the rhodopsin spectral sensitivity slopes. This clearly argues in favor of using the split-reference transformation to derive wavelength discrimination functions at least in cases where the conditioning index functions are rather asymmetric with respect to the reference wavelength.

One caveat of the split-reference transformation is that a change of the criterion level to calculate the $\delta\lambda$ values not only changes the discriminability values. Because the virtual reference wavelengths depend on the derived discriminabilities, both x and y values of the data points change with changing criterion levels. This effect is more severe for datapoints where discrimination is poor than for points with good discrimination. If discrimination is good, the slope of the conditioning index curves is high, implying that a change in the criterion level, defined on the y-axis, leads to small changes in the reference wavelength. Our main finding is mainly due

to two points with good discrimination near 500 nm, and it is therefore rather robust against reasonable changes in the criterion level.

Considering natural reflectance spectra, the conditioned entropy values indicate that, on average, the long wavelength range is most informative, followed by a mid-wavelength region between 400 nm and 500 nm. Interestingly, in a range where spectral information increases (490 nm and above), Rh1 is most sensitive, while the other available receptors are rather insensitive (Fig 2b). Together with the assessment of the power spectral density distribution of natural reflectance spectra, which argue in favor of including a fifth receptor type, this supports our conclusions from the model results.

Analysis of mutual information indicates that that Rh1 is the second most informative Drosophila opsin (see Fig 6b). In general, there is a trend that the more sensitive a receptor type is for the long wavelength the higher its mutual information. The differences of informational value in the four receptor systems are not very large (see Fig 6c), and the addition of Rh1 to the traditional four-receptor system increases the information by only 7%. Compared to the information added when going from three to four receptors, this seems not particularly large. However, it is substantial considering that the fifth principal component accounts for only 3% of the variability.

The important aspect is that Rh1 contributes information, considering that Rh1 is highly correlated with both Rh5 and Rh6.

This does not need to be an optimization and could, as suggested by Kelber and Henze [41], be due to convergence in visual pathways that intersect at higher levels, subserving other functions than optimizing for color vision.

On the other hand, it is possible that not all of the inner receptors contribute to color vision in Drosophila. It is known that the butterfly *Papilio*, with eight different opsins, is only tetrachromatic [30]. Our analysis of the wavelength discrimination data demonstrate that, at least in the visual range, just three receptors are best to model the data. Adding more receptors reduces goodness of fits, not only because of the higher number of parameters, but because discrimination increased where the data suggested poor discrimination.

Potentially, further opsins could contribute in the UV, where currently no wavelength discrimination data for Drosophila are available. However, the reflectance data indicate that among the four opsins there is not much variability in the mutual information, which would speak in favor of a contribution by Rh1 rather than one of the other opsins.

Concerning possible implementations it has been shown that the outer photoreceptors do not terminate in the medulla as the inner photoreceptors but in the lamina neuropil. From there three lamina monopolar cells (L1,L2,L3) connect directly to the medulla, where signals from outer and inner receptors converge [42, 43]. Interestingly, blocking the laminar monopolar cells L1–L3 inhibits blue/green discrimination in Drosophila [16]. Non-columnar projection neurons could mediate interommatidial combination of inner receptor signals [44], however, such combination would not be predicted by our best fitting model. In the calculation of the mutual information we have assumed the same noise level for all opsins. This is certainly an oversimplification, especially considering that there are more outer receptors with Rh1 than inner receptors, and more than twice as many pale than yellow ommatidia [5, 45]. While, in a receptor noise limited regime, this would have an effect on the information for the individual opsins, the values for systems combining several opsins will practically not change. As reported above, for combinations of four opsins there is already very little difference in the mutual information. This is mainly due to the spectral correlation structure between the spectral sensitivities and the smoothness of natural reflectances. Neither the high correlation between the shapes of the spectral sensitivities nor the smoothness of natural spectra, however, is changed by different noise levels when calculating mutual information.

Koshitake et al. [30] modeled wavelength discrimination in the butterfly with an approach that also builds on chromatic comparisons, but assumes that discrimination is limited by the noise in the photoreceptors. We found such a model to work poorly for the Drosophila data used here (data not shown). First, absolute thresholds could not be replicated, and even after introduction of a scaling parameter, fits with noise levels based on receptor count did not provide acceptable errors (p< 0.001).This could be an indication that color discrimination in Drosophila is not limited by receptor noise but by postreceptoral stages.

Troje [12] studied wavelength discrimination in the goldfly and found that it is possible to explain the behavioral data without the incorporation of the signals from Rh1. There are several prominent and also subtle differences between the data used in that study and the data we used. Like the data from Hernandez de Salomon and Spatz [24], the results by Troje [12] indicate good discrimination around 500 nm. Besides the difference that the model by Troje [12] tries to predict the learning curves directly, whereas our models predict the wavelength discrimination function, given the similarities in the data, why do the results differ?

The critical difference lies in the spectral sensitivity functions used. In particular the Rh6 spectral sensitivity function that we used, which was directly measured in Drosophila [14], however expressed in the outer receptors, is broader than the one used by Troje [12], which was measured in Musca [46] and is narrower because of screening by the R7 receptor. This Rh6 function has an absolute slope change in the region between 470 nm and 500 nm, and it is likely that with the Drosophila Rh6 spectral sensitivities used by us the results by Troje [12] would have been different. A different Rh6 spectral sensitivity could be an alternative explanation to a contribution of Rh1 to Drosophila wavelength discrimination, if the Rh6 curve would have a higher slope near 500 nm than near 470 nm. However, for this to occur the point of inflection of the Rh6 spectral sensitivity curve would need to be shifted by almost 50 nm, which seems unlikely with shielding from R7.

In conclusion, we have confirmed that the behavioral data on wavelength discrimination in Drosophila can hardly be understood without incorporating Rh1. This result is mainly due to the good discrimination around 500 nm which directly relates to the spectral sensitivity of the Rh1 opsin. Neither a different weighting scheme nor reasonable modifications in the derivation of the discrimination function alter this conclusion. The contribution of Rh1 to the best fitting models is prominent, and a model comparing signals from Rh1, Rh6 and Rh4 already provides a good explanation of the discrimination behavior of the wild type fly. With respect to the encoding of natural reflectance spectra, the spectral positioning of Rh1 is actually not optimal for discrimination. The power spectral density of natural spectra indicates that five receptor spectral sensitivities would be optimal for the visual range of Drosophila. However, this argument is based on the assumption of an equidistant sampling of the spectrum with rather broad receptoral functions located roughly fifty nanometer apart. It is rather obvious that this is not the case for Rh1, Rh3, and Rh4. Furthermore, the double peaked nature of the sensitivity of the Rh1 containing receptors render them suboptimal for unambiguous spectral discrimination [12]. Whether color vision is important for Drosophila at all is an open question [47], but the behavioral data indicate a role for Rh1 when color discrimination is tested, and our theoretical analysis of natural reflectance data shows that there is information in the signals of a fifth opsin in general, and Rh1 in particular.

Supporting Information

S1 Data. Spectra IDs. S1_Data.csv lists the ids (see http://www.reflectance.co.uk/) of all spectra used in this study.
(CSV)

Acknowledgments

Author Contributions

Conceived and designed the experiments: CG TW. Analyzed the data: CG. Wrote the paper: CG TW.

References

1. Menne D, Spatz HC. Colour vision in Drosophila melanogaster. Journal of Comparative Physiology A: Neuroethology, Sensory, Neural, and Behavioral Physiology. 1977; 114(3):301–312. doi: 10.1007/BF00657325

2. Rister J, Desplan C, Vasiliauskas D. Establishing and maintaining gene expression patterns: insights from sensory receptor patterning. Development. 2013; 140(3):493–503. doi: 10.1242/dev.079095 PMID: 23293281

3. Hardie RC. Functional organization of the fly retina. Springer; 1985.

4. Franceschini N, Kirschfeld K, Minke B. Fluorescence of photoreceptor cells observed in vivo. Science. 1981; 213(4513):1264–1267. doi: 10.1126/science.7268434 PMID: 7268434

5. Chou WH, Hall KJ, Wilson DB, Wideman CL, Townson SM, Chadwell LV, et al. Identification of a novel Drosophila opsin reveals specific patterning of the R7 and R8 photoreceptor cells. Neuron. 1996; 17 (6):1101–1115. doi: 10.1016/S0896-6273(00)80243-3 PMID: 8982159

6. Huber A, Schulz S, Bentrop J, Groell C, Wolfrum U, Paulsen R. Molecular cloning of Drosophila Rh6 rhodopsin: the visual pigment of a subset of R8 photoreceptor cells. FEBS letters. 1997; 406(1):6–10. doi: 10.1016/S0014-5793(97)00210-X PMID: 9109375

7. Papatsenko D, Sheng G, Desplan C. A new rhodopsin in R8 photoreceptors of Drosophila: evidence for coordinate expression with Rh3 in R7 cells. Development. 1997; 124(9):1665–1673. PMID: 9165115

8. Mazzoni EO, Celik A, Wernet MF, Vasiliauskas D, Johnston RJ, Cook TA, et al. Iroquois complex genes induce co-expression of rhodopsins in Drosophila. PLoS Biol. 2008; 6(4):e97. doi: 10.1371/journal.pbio.0060097 PMID: 18433293

9. Fortini ME, Rubin GM. The optic lobe projection pattern of polarization-sensitive photoreceptor cells in Drosophila melanogaster. Cell and tissue research. 1991; 265(1):185–191. doi: 10.1007/BF00318153 PMID: 1913776

10. Wernet MF, Labhart T, Baumann F, Mazzoni EO, Pichaud F, Desplan C. Homothorax switches function of Drosophila photoreceptors from color to polarized light sensors. Cell. 2003; 115(3):267–279. doi: 10.1016/S0092-8674(03)00848-1 PMID: 14636555

11. Kirschfeld DK, Franceschini N. Optische Eigenschaften der Ommatidien im Komplexauge von Musca. Kybernetik. 1968; 5(2):47–52. doi: 10.1007/BF00272694 PMID: 5702780

12. Troje N. Spectral categories in the learning behaviour of blowflies. Z Naturforsch C. 1993; 48:96–104.

13. Kirschfeld K, Feiler R, Hardie R, Vogt K, Franceschini N. The sensitizing pigment in fly photoreceptors. Biophysics of Structure and Mechanism. 1983; 10(1–2):81–92. doi: 10.1007/BF00535544

14. Salcedo E, Huber A, Henrich S, Chadwell LV, Chou WH, Paulsen R, et al. Blue- and Green-Absorbing Visual Pigments of Drosophila: Ectopic Expression and Physiological Characterization of the R8 Photoreceptor Cell-Specific Rh5 and Rh6 Rhodopsins. J Neurosci. 1999; 19(24):10716–10726. PMID: 10594055

15. Salcedo E, Zheng L, Phistry M, Bagg EE, Britt SG. Molecular Basis for Ultraviolet Vision in Invertebrates. The Journal of Neuroscience. 2003; 23(34):10873–10878. PMID: 14645481

16. Schnaitmann C, Garbers C, Wachtler T, Tanimoto H. Color Discrimination with Broadband Photoreceptors. Current Biology. 2013; 23(23):2375–2382. doi: 10.1016/j.cub.2013.10.037 PMID: 24268411

17. Barlow HB. What causes trichromacy? A theoretical analysis using comb-filtered spectra. Vision Research. 1982; 22(6):635–643. doi: 10.1016/0042-6989(82)90099-2 PMID: 6981244

18. Maloney LT. Evaluation of linear models of surface spectral reflectance with small numbers of parameters. Journal of the Optical Society of America A. 1986; 3(10):1673. doi: 10.1364/JOSAA.3.001673

19. Vorobyev M. Costs and benefits of increasing the dimensionality of colour vision system. Biophysics of photoreception: molecular and phototransductive events. 1997; p. 280–289.

20. Arnold SEJ, Faruq S, Savolainen V, McOwan PW, Chittka L. FReD: The Floral Reflectance Database —A Web Portal for Analyses of Flower Colour. PLoS ONE. 2010; 5(12):e14287. doi: 10.1371/journal.pone.0014287 PMID: 21170326

21. Lewis A, Zhaoping L. Are cone sensitivities determined by natural color statistics? Journal of Vision. 2006; 6(3). doi: 10.1167/6.3.8 PMID: 16643096

22. Wright WD, Pitt FHG. Hue-discrimination in normal colour-vision. Proceedings of the Physical Society. 1934; 46(3):459. doi: 10.1088/0959-5309/46/3/317

23. Helversen Ov. Zur spektralen Unterschiedsempfindlichkeit der Honigbiene. Journal of comparative physiology. 1972; 80(4):439–472. doi: 10.1007/BF00696438

24. Hernandez de Salomon C, Spatz HC. Colour vision inDrosophila melanogaster: Wavelength discrimination. Journal of Comparative Physiology A: Neuroethology, Sensory, Neural, and Behavioral Physiology. 1983; 150(1):31–37. doi: 10.1007/BF00605285

25. De Valois RL, Morgan HC. Psychophysical studies of monkey vision—II. Squirrel monkey wavelength and saturation discrimination. Vision Research. 1974; 14(1):69–73. doi: 10.1016/0042-6989(74)90117-5 PMID: 4204838

26. Vorobyev M, Osorio D. Receptor noise as a determinant of colour thresholds. Proceedings of the Royal Society of London Series B: Biological Sciences. 1998; 265(1394):351. doi: 10.1098/rspb.1998.0302 PMID: 9523436

27. Jones E, Oliphant T, Peterson P, et al. SciPy: Open source scientific tools for Python; 2001.

28. Kotel'nikov VA. On the transmission capacity of'ether' and wire in electric communications. Physics-Uspekhi. 2006; 49(7):736. doi: 10.1070/PU2006v049n07ABEH006160

29. Kloeckner A, Pinto N, Lee Y, Catanzaro B, Ivanov P, Fasih A. PyCUDA and PyOpenCL: A scripting-based approach to GPU run-time code generation. Parallel Computing. 2012; 38(3):157–174. doi: 10.1016/j.parco.2011.09.001

30. Koshitaka H, Kinoshita M, Vorobyev M, Arikawa K. Tetrachromacy in a butterfly that has eight varieties of spectral receptors. Proceedings of the Royal Society B: Biological Sciences. 2008; 275(1637):947–954. doi: 10.1098/rspb.2007.1614 PMID: 18230593

31. Brandt R, Vorobyev M. Metric analysis of threshold spectral sensitivity in the honeybee. Vision research. 1997; 37(4):425–439. doi: 10.1016/S0042-6989(96)00195-2 PMID: 9156174

32. Vorobyev M, Brandt R, Peitsch D, Laughlin SB, Menzel R. Colour thresholds and receptor noise: behaviour and physiology compared. Vision Research. 2001; 41(5):639–653. doi: 10.1016/S0042-6989(00)00288-1 PMID: 11226508

33. Stiles WS. A modified Helmholtz line-element in brightness-colour space. Proceedings of the Physical Society. 1946; 58(1):41. doi: 10.1088/0959-5309/58/1/305

34. Backhaus W, Menzel R. Color distance derived from a receptor model of color vision in the honeybee. Biological Cybernetics. 1987; 55(5):321–331. doi: 10.1007/BF02281978

35. Kelber A. Receptor based models for spontaneous colour choices in flies and butterflies. Entomologia Experimentalis et Applicata. 2001; 99(2):231–244. doi: 10.1046/j.1570-7458.2001.00822.x

36. Yeh T, Lee BB, Kremersy J. Temporal response of ganglion cells of the macaque retina to cone-specific modulation. Journal of the Optical Society of America A. 1995; 12(3):456–464. doi: 10.1364/JOSAA.12.000456

37. Busse L, Ayaz A, Dhruv NT, Katzner S, Saleem AB, Schölvinck ML, et al. The Detection of Visual Contrast in the Behaving Mouse. The Journal of Neuroscience. 2011; 31(31):11351–11361. doi: 10.1523/JNEUROSCI.6689-10.2011 PMID: 21813694

38. Garbers C, Henke J, Leibold C, Wachtler T, Thurley K. Contextual processing of brightness and color in Mongolian gerbils. Journal of Vision. 2015; 15(1):13. doi: 10.1167/15.1.13 PMID: 25589297

39. Wichmann FA, Hill NJ. The psychometric function: I. Fitting, sampling, and goodness of fit. Perception & psychophysics. 2001; 63(8):1293–1313. doi: 10.3758/BF03194544

40. Prins N. The psychometric function: The lapse rate revisited. Journal of Vision. 2012; 12(6):25. doi: 10.1167/12.6.25 PMID: 22715196

41. Kelber A, Henze MJ. Colour vision: parallel pathways intersect in Drosophila. Current biology: CB. 2013; 23(23):R1043–1045. doi: 10.1016/j.cub.2013.10.025 PMID: 24309280

42. Fischbach PKF, Dittrich APM. The optic lobe of Drosophila melanogaster. I. A Golgi analysis of wild-type structure. Cell and Tissue Research. 1989; 258(3):441–475. doi: 10.1007/BF00218858

43. Meinertzhagen IA, O'neil SD. Synaptic organization of columnar elements in the lamina of the wild type in Drosophila melanogaster. Journal of comparative neurology. 1991; 305(2):232–263. doi: 10.1002/cne.903050206 PMID: 1902848

44. Morante J, Desplan C. The color-vision circuit in the medulla of Drosophila. Current Biology. 2008; 18(8):553–565. doi: 10.1016/j.cub.2008.02.075 PMID: 18403201

45. Chou WH, Huber A, Bentrop J, Schulz S, Schwab K, Chadwell LV, et al. Patterning of the R7 and R8 photoreceptor cells of Drosophila: evidence for induced and default cell-fate specification. Development. 1999; 126(4):607–616. PMID: 9895309

46. Hardie RC, Kirschfeld K. Ultraviolet sensitivity of fly photoreceptors R7 and R8: Evidence for a sensitising function. Biophysics of Structure and Mechanism. 1983; 9(3):171–180. doi: 10.1007/BF00537814

47. Lunau K. Visual ecology of flies with particular reference to colour vision and colour preferences. Journal of Comparative Physiology A. 2014; 200(6):497–512. doi: 10.1007/s00359-014-0895-1

3.2 Color Discrimination with Broadband Photoreceptors

Article

Color Discrimination
with Broadband Photoreceptors

Christopher Schnaitmann,[1,5,*] Christian Garbers,[2]
Thomas Wachtler,[2,3] and Hiromu Tanimoto[1,4,*]
[1]Max-Planck-Institut für Neurobiologie, 82152 Martinsried,
Germany
[2]Department Biology II, Ludwig-Maximilians-Universität
München, 82152 Martinsried, Germany
[3]Bernstein Center for Computational Neuroscience Munich,
82152 Martinsried, Germany
[4]Tohoku University Graduate School of Life Sciences,
980-8577 Sendai, Japan

Summary

Background: Color vision is commonly assumed to rely on photoreceptors tuned to narrow spectral ranges. In the ommatidium of *Drosophila*, the four types of so-called inner photoreceptors express different narrow-band opsins. In contrast, the outer photoreceptors have a broadband spectral sensitivity and were thought to exclusively mediate achromatic vision.
Results: Using computational models and behavioral experiments, we demonstrate that the broadband outer photoreceptors contribute to color vision in *Drosophila*. The model of opponent processing that includes the opsin of the outer photoreceptors scored the best fit to wavelength discrimination data. To experimentally uncover the contribution of individual photoreceptor types, we restored phototransduction of targeted photoreceptor combinations in a blind mutant. Dichromatic flies with only broadband photoreceptors and one additional receptor type can discriminate different colors, indicating the existence of a specific output comparison of the outer and inner photoreceptors. Furthermore, blocking interneurons postsynaptic to the outer photoreceptors specifically impaired color but not intensity discrimination.
Conclusions: Our findings show that receptors with a complex and broad spectral sensitivity can contribute to color vision and reveal that chromatic and achromatic circuits in the fly share common photoreceptors.

Introduction

Color vision enables animals to visually discriminate objects based on their spectral properties [1]. It facilitates efficient object recognition, such as identification of food sources or choosing mates [2]. This ability relies on a neuronal comparison of signals from photoreceptors that differ in spectral sensitivity [3]. The compound eye of the fruit fly *Drosophila melanogaster* contains five spectrally different types of photoreceptors, each expressing a single opsin [4]. Each ommatidium contains a set of eight photoreceptors (R1–R8; Figure 1A). The outer photoreceptors (R1–R6) of all ommatidia express the same opsin gene, *rh1* (also known as *ninaE*), and

exhibit a two-peaked broadband spectral sensitivity [5, 6] (Figure 1B). These receptors have been considered analogous to vertebrate rod cells [7, 8] and are important for a wide range of achromatic visual behavior, including dim-light vision and motion detection [6–9]. The inner photoreceptors (R7 and R8; Figure 1A) express one of four opsins with different spectral sensitivities [4] (Figure 1B). Opsins Rh3 or Rh4 are expressed in R7, opsins Rh5 or Rh6 in R8, of so-called pale or yellow ommatidia, respectively [4] (Figure 1A). The inner photoreceptors have been shown to function in various visual behaviors, such as phototaxis [10]. Given the single-peaked narrowband spectral sensitivities of inner photoreceptors, it is commonly assumed that these provide the only input to color vision in flies [7, 11]. However, the respective contributions of the five photoreceptor types to color vision have not been conclusively established [11, 12]. Here we asked whether signals from the broadband photoreceptors and their postsynaptic neurons are used in *Drosophila* to obtain information on the wavelength composition of a visual stimulus.

Results

Behavioral Assay for Color Discrimination in *Drosophila*

While innate phototactic choice has been employed to study spectral preference in *Drosophila* [10, 13, 14], it is unknown whether this behavior is related to color vision [15]. We therefore chose visual discrimination learning—a behavioral paradigm that allows us to control intensity invariance [1, 16–18]. We improved a previously reported conditioning assay in which flies learn to discriminate two colored visual stimuli using sugar reward [19] (Figure S1 available online). Conditioned stimuli were generated by high-power light-emitting diodes (LEDs) with peak intensities at 452 nm (blue) and 520 nm (green), respectively (Figure 1C). While flies significantly discriminate high-intensity blue (bright blue) and green (bright green), it is not clear whether discrimination is based on color or intensity (Figure 1D). Conditioning with differential intensities of either blue or green (1:10 ratio) resulted in significant intensity discrimination (Figure 1D), raising a possibility that the blue/green discrimination might be achromatic.

To ensure that discrimination was based on color, we introduced an intensity mismatch between training and test [18]. Flies were trained with low-intensity blue (dark blue; 10% of bright blue) and bright green, but were tested to discriminate bright blue and bright green. Flies consistently exhibited conditioned approach toward the trained color, despite the 10-fold intensity mismatch (Figure 1E). Similarly, discrimination was not impaired when flies were trained with bright blue/dark green and tested with bright blue/bright green (Figure 1E). Finally, to assess response priority on color and intensity cues [16, 17], we trained flies with dark blue/bright green and tested them with bright blue/dark green, and vice versa (intensity inversion). This experimental design allows us to assess whether flies use a conflicting color or intensity cue [16, 17], as conditioned approach to the color or intensity cue will result in a positive or negative learning index, respectively. Both combinations of the intensity inversion revealed choice priority on the color cue, demonstrating that

[5]Present address: Neurobiologie/Tierphysiologie, Institut für Biologie 1, Albert-Ludwigs-Universität Freiburg, 79104 Freiburg, Germany
*Correspondence: christopher.schnaitmann@biologie.uni-freiburg.de (C.S.), hiromut@m.tohoku.ac.jp (H.T.)

CrossMark
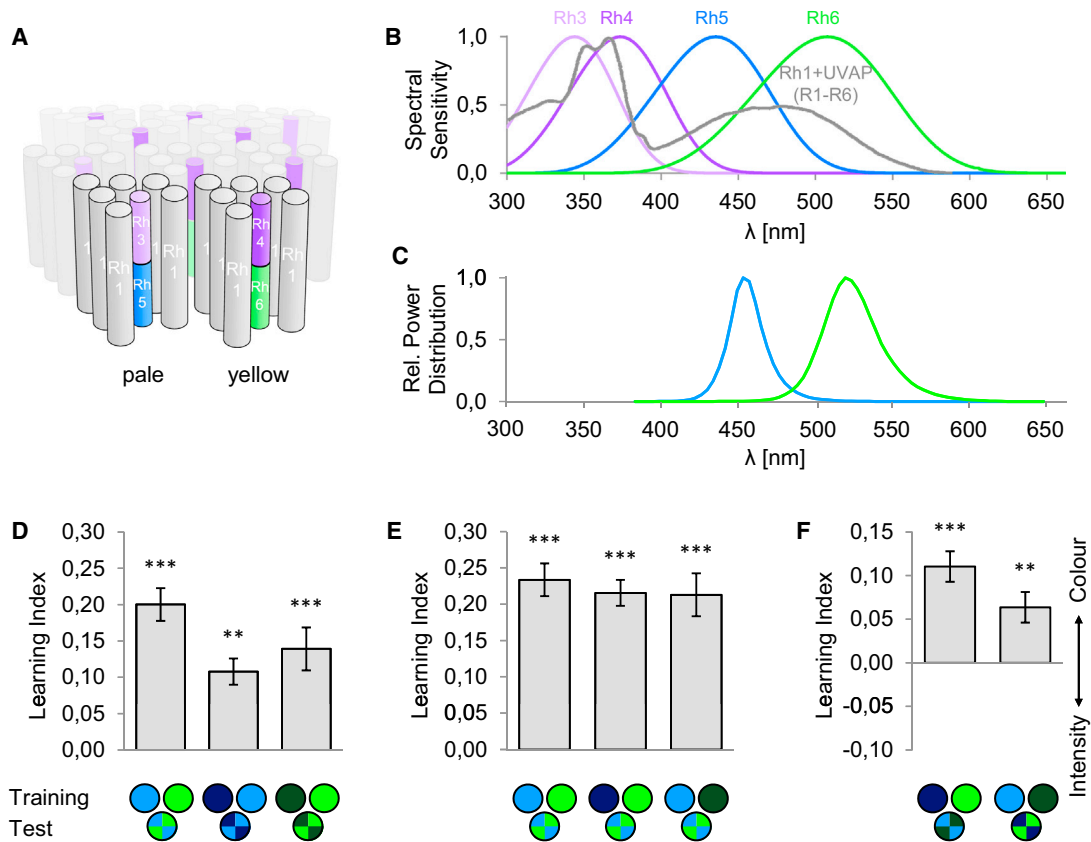
Figure 1. Color Discrimination Learning in *Drosophila*

(A) Composition of opsin types in pale and yellow ommatidia. Six outer photoreceptors (R1–R6; gray) express Rh1. R7 expresses Rh3 or Rh4, and R8 expresses Rh5 or Rh6, depending on the ommatidia class (pale or yellow).

(B) Normalized spectral sensitivities of the different Rhodopsins in the *Drosophila* eye. Rh1 alone is maximally sensitive at 478 nm; an accessory pigment (UVAP) underlies the UV sensitivity of R1–R6 (gray). Data were adapted from [5].

(C) Emission spectra of LEDs used in behavioral experiments.

(D–F) Visual discrimination learning of the fly. Conditioned stimuli, one of which is paired with a sugar reward, and test stimuli are depicted with three circles.

(D) Wild-type flies show significant memory in the bright blue/bright green and in the intensity discrimination tasks (n = 9–18).

(E) Flies choose the color cues despite 10-fold intensity mismatch between training and test (n = 16–20).

(F) Flies show significant color learning despite the conflicting 10-fold intensity inversion between training and test (n = 15–16). Note that intensity learning would result in a negative learning index.

Bars and error bars represent means and SEM, respectively. **p < 0.01; ***p < 0.001; ns, no significance. See also Figure S1.

discrimination was based on spectral composition of conditioned stimuli (Figure 1F).

Broadband Photoreceptors Contribute to Color Discrimination

To determine which photoreceptors feed into color vision, we fitted a model of color opponent processing to experimental results of wavelength discriminability in *Drosophila* [20]. The model predicts discrimination thresholds based on signals in color opponent channels [21]. Variants of the model that included signals from inner receptors gave poor fits to the behavioral data (Figures 2A and 2B), whereas goodness of fit was improved when including the outer photoreceptors (Figure 2C). The superior performance of models including the outer photoreceptors was mainly due to the increasing sensitivity slope of Rh1 in the region around 500 nm, where wavelength discrimination is best (Figure S2). Thus, a contribution of the outer photoreceptors to color vision is necessary to explain the published data on wavelength discrimination in *Drosophila*.

Color Discrimination with Restricted Photoreceptor Sets

To experimentally identify the receptor types responsible for color discrimination, we generated flies with restricted sets of functional photoreceptors. We used blind mutants (*norpA[7]*) that lack Phospholipase C and restored phototransduction by expressing *norpA[+]* with different combinations of *rhodopsin-GAL4* drivers [22, 23]. Specificity of GAL4 expression was verified using confocal microscopy (Figures S3A–S3J). To determine functional rescue of photoreceptors, we measured electroretinogram (ERG) responses of the rescue flies with single *rh-GAL4* lines. We used the same LED stimulation as in the conditioning experiments (or UV LED for *rh3-GAL4*) and found that all *norpA* rescues restored light sensitivity (Figures 3A, S3K, and S3L).

We rescued *norpA* in all types of photoreceptors by combining four *rh-GAL4* drivers in the same fly (i.e., *norpA[7] rh1-GAL4/Y; rh5-GAL4 rh6-GAL4/UAS-norpA; rh3+rh4-GAL4/+*) and examined their color-discrimination behavior. The rescue flies fully discriminated bright blue/bright green at the wild-type level (Figure 3B) and exhibited a positive
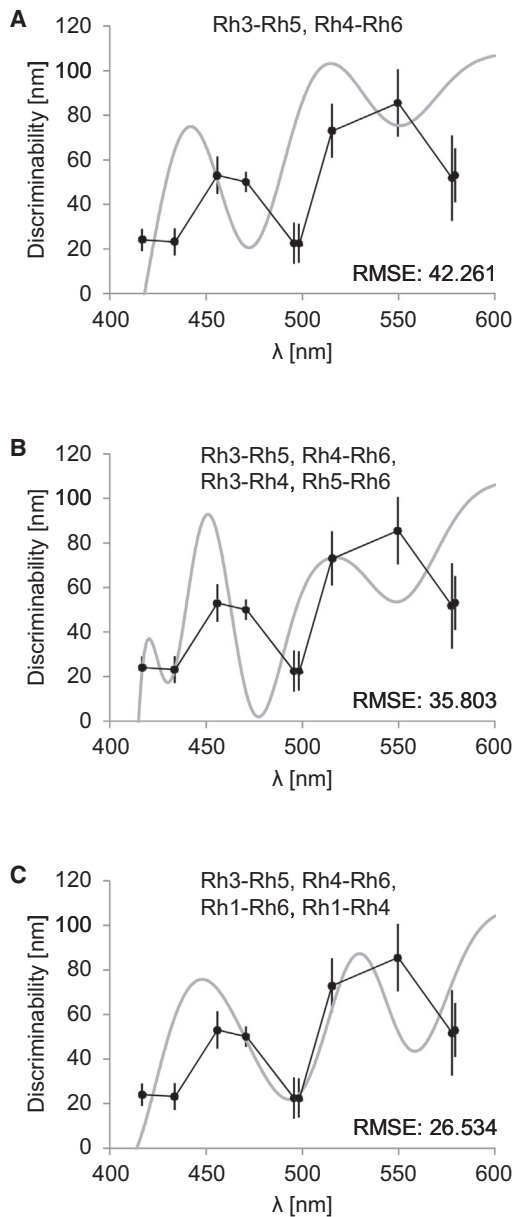
Figure 2. Models of Color Opponent Processing Predict a Contribution of the Outer Photoreceptors to Color Discrimination

Fits of models employing different combinations of color opponent signals (gray curves) to wavelength discrimination in *Drosophila* [20, 21]. Goodness of fit is measured by root-mean-square error corrected for the number of degrees of freedom (RMSE).

(A) Standard model with opponent combinations of inner photoreceptor signals.

(B) The model with the inner photoreceptors including "interommatidial" opponency (i.e., Rh3-Rh4 and Rh5-Rh6) fits slightly better than the standard model.

(C) A model including outer receptor signals achieves a substantially better fit. Note that this model has the same number of parameters as the model in (B). Data points and error bars represent means and SEM, respectively. See also Figure S2.

learning index under intensity inversion, thus demonstrating true color discrimination (Figure 3C). We next generated *norpA* rescue flies in which either all photoreceptors in pale (*rh1-GAL4*, *rh3-GAL4*, and *rh5-GAL4*) or yellow (*rh1-GAL4*,

rh4-GAL4, and *rh6-GAL4*) ommatidia were functional. Interestingly, the yellow, but not pale, rescue was fully sufficient for bright-blue/bright-green discrimination (Figure 4A). As the sugar preference of the pale rescue flies was not impaired (data not shown), we conclude that pale ommatidia alone are not sufficient for the blue/green discrimination task (Figure 4A). They might play a role for discrimination of other spectral stimulus pairs.

To determine the minimal set of photoreceptors for blue/green discrimination, we generated flies with *norpA* rescue in the three pairwise photopigment combinations in yellow ommatidia (Rh1-Rh4, Rh4-Rh6, and Rh1-Rh6). The combinations of Rh1-Rh4 and Rh4-Rh6 were sufficient for discrimination of bright blue/bright green (Figure 4B), whereas Rh1-Rh6 rescue flies were not able (Figure 4B). Rh1-Rh6 rescue flies did not show color but intensity discrimination in the intensity inversion experiment (Figure 4C). Strikingly, the intensity inversion experiment revealed that both dichromatic combinations of Rh1-Rh4 and Rh4-Rh6 allowed spectral discrimination of blue and green stimuli (Figure 4C). Importantly, the ERG experiments showed that the blue/green intensity ratio is within 10-fold in the rescue with *rh1-GAL4* and *rh6-GAL4*, assuring the successful intensity inversion with dark blue and bright green, and vice versa, at the neural level (Figure S3K). Due to the high blue/green sensitivity ratio of Rh4, the dark blue might be brighter than the bright green for the Rh1-Rh4 rescue flies (Figure S3K), potentially confounding the interpretation of the result (Figure 4C). We therefore performed an intensity inversion experiment where the intensities of dark blue and bright green during training were matched for Rh4 according to the ERG measurements (Figure S3L). Rh1-Rh4 rescue flies still used the color cue under this condition (Figure S4A). Rescue with the single *rh4-GAL4* or without driver did not restore significant color discrimination (Figure S4B), confirming that a neuronal comparison of multiple receptor outputs is required for color vision. Altogether, these results demonstrate that both outer and inner photoreceptors contribute to color vision. The qualitative discrimination difference of the dichromatic rescues in Rh1-Rh4 and Rh1-Rh6 suggests differential computation underlying the signal integration of the outer photoreceptors and the different inner photoreceptor types (i.e., R7 and R8).

The Blockade of Lamina Monopolar Cells Selectively Impairs Color Discrimination

The outer photoreceptors, unlike the other four inner photoreceptors, terminate in the lamina neuropil (Figure 5A). The three lamina monopolar cells (LMCs; L1, L2, and L3) convey the outputs of the outer photoreceptors directly to different layers of the medulla, where visual information of inner and outer photoreceptors converge [24, 25] (Figure 5A). To examine the role of L1–L3 in color discrimination, we blocked the output of these LMCs using *ort^C2-GAL4* [14] and *UAS-shi^ts1* [26]. Strikingly, this blockade caused a severe impairment in bright-blue/bright-green discrimination (Figure 5B). Intact intensity discrimination showed that appetitive visual memory and behavioral expression were not defective (Figure 5C). As *ort^C2-GAL4* additionally labels Dm8, amacrine cells in the medulla that receive R7 output [14] (Figure 5A), we examined a split-GAL4 driver *vglut ∩ ort^C2-GAL4* to express *shi^ts1* specifically in Dm8 neurons, as well as in a small number of L1 neurons and glia-like cells [14]. These flies did not show any impairment in the bright-blue/bright-green discrimination (Figure 5D). Furthermore, we blocked LMCs with another GAL4
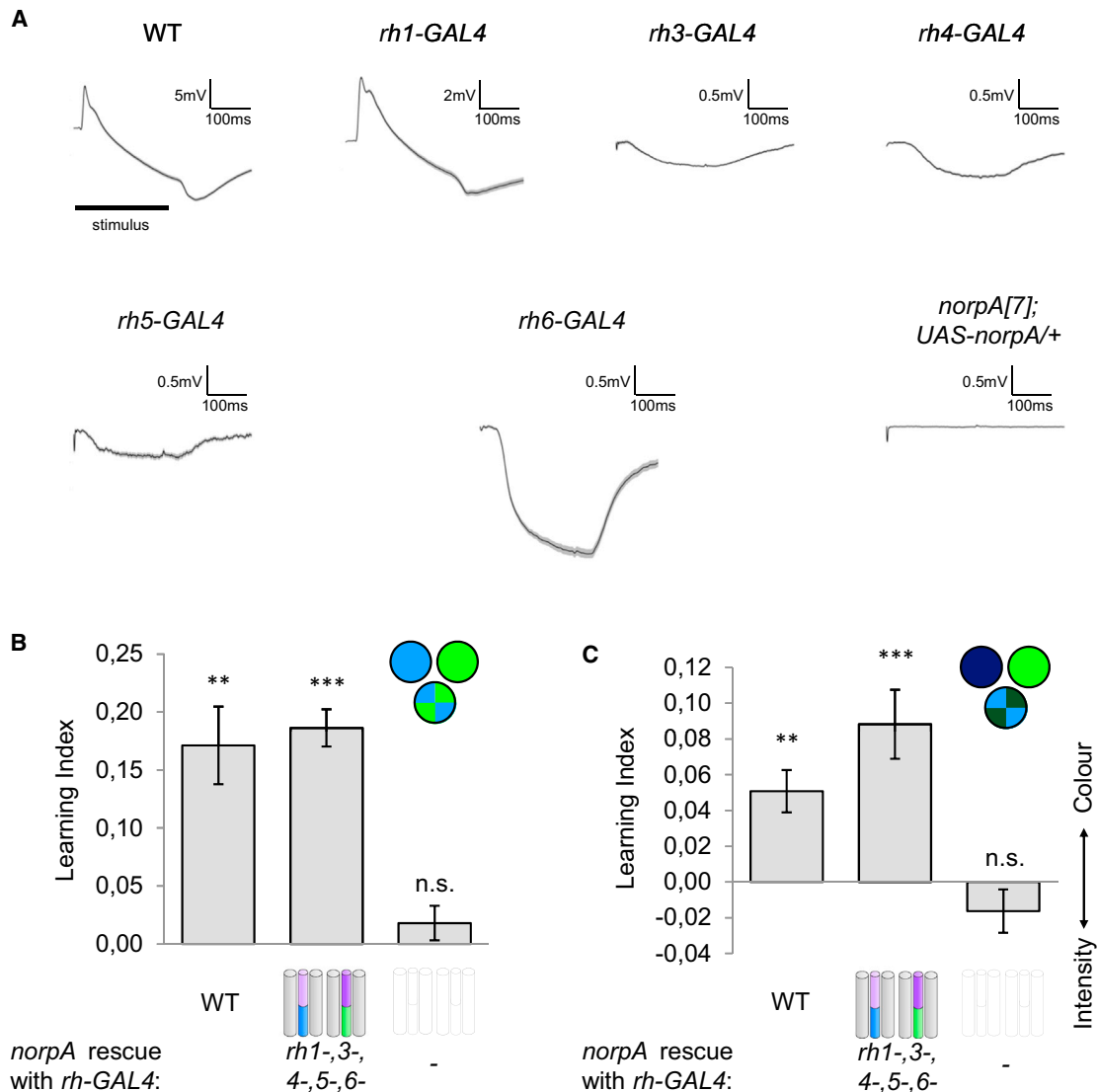
Figure 3. Targeted *norpA* Rescue Restores Photoreceptor Function

(A) ERG traces to dark-blue stimulation of flies with targeted rescues of *norpA* using different *rh-GAL4* drivers (n = 4–8 per genotype). For the rescue with *rh3-GAL4* or without a driver, ERG traces in response to a UV LED (410 nm) or bright blue are plotted, respectively.

(B) The *norpA* rescue in all photoreceptor types fully restores bright-blue/bright-green discrimination learning to the wild-type level, while *norpA* mutant flies containing the rescue construct without driver exhibit no significant discrimination (n = 9–17).

(C) The choice of the rescue flies in all photoreceptors is based on color rather than intensity in the intensity inversion experiment (n = 12–20).

Bars and error bars represent means and SEM, respectively. **p < 0.01; ***p < 0.001; ns, no significance. See also Figure S3.

driver, *R48A08-GAL4*, that strongly labels L1 and L2, as well as two unknown cell types in the medulla [27]. *R48A08-GAL4/ UAS-shi[ts1]* flies were severely impaired in discriminating bright blue and bright green, while their intensity discrimination was intact (Figures 5E and 5F). Thus, we conclude that the LMCs are selectively required for blue/green discrimination.

Discussion

Combining modeling with genetic manipulations and behavioral experiments, we identified the photoreceptor types for blue/green discrimination in *Drosophila* (Figures 4 and S5). Functional color discrimination with the opsin pairs Rh1-Rh4 and Rh4-Rh6 indicates that postreceptoral computations underlying color vision may occur within an optic cartridge

deriving from a single ommatidium [28]. Neuronal comparison of differential receptor outputs may be through color opponent mechanisms [29]. TM5 cells in the medulla neuropil are a candidate for color opponent cells comparing Rh1 and Rh4 signals, since they integrate the outputs of LMCs (especially L3) and R7 [14]. Alternatively, the postreceptoral comparisons might take place further downstream in the optic neuropils [30]. Future physiological studies will be necessary to further elucidate this neuronal computation.

Our findings redress the longstanding assumption that solely narrow-band inner photoreceptors mediate color vision [7, 11]. The sensitivity of Rh1 covers a wide spectral range, but it is not uniform (Figure 1B). While this spectral sensitivity is not optimal to represent colors, it nevertheless provides information about differences in wavelength composition. This is in

A

Learning Index (y-axis: -0,05 to 0,25)

** *** n.s. n.s.

WT

norpA rescue with *rh-GAL4*: — *rh1-,4-,6-* *rh1-,3-,5-* —

B

Learning Index (y-axis: -0,05 to 0,20)

* n.s. **

norpA rescue with *rh-GAL4*: *rh1-,4-* *rh1-,6-* *rh4-,6-*

C

Learning Index (y-axis: -0,08 to 0,12)

** ** ** * ** n.s.

WT

Colour ↑ Intensity ↓

norpA rescue with *rh-GAL4*: — *rh1-,4-,6-* *rh1-,4-* *rh1-,6-* *rh4-,6-* —
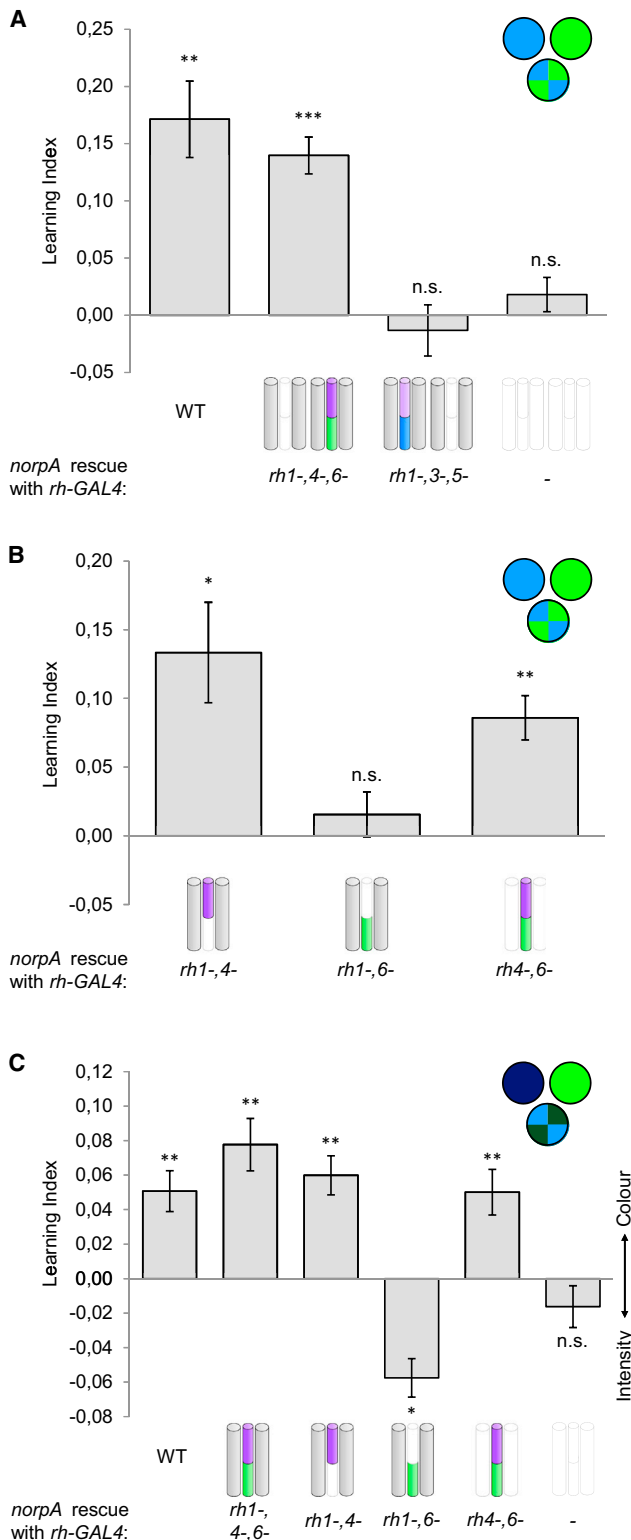
Figure 4. Minimal Sets of Photoreceptors for Color Discrimination

(A) *norpA* rescue flies with functional yellow, but not pale, ommatidia significantly discriminate bright blue and bright green (n = 10–17).

(B) Bright-blue/bright-green discrimination of flies with pairwise *norpA* rescue in yellow ommatidia. Rescue flies with *rh1-GAL4/ rh4-GAL4* or *rh4-GAL4/rh6-GAL4* show significant discrimination, while rescue flies with *rh1-GAL4/rh6-GAL4* cannot discriminate the stimuli (n = 8–17).

line with the rescued color discrimination with the dichromatic opsin pair Rh1-Rh4 (Figure 4C). Considering the sufficiency of inner photoreceptors for blue/green discrimination (Figures 4 and S5), the role of the outer photoreceptors may be to create an additional opponency dimension for enhanced color discrimination in specific wavelength regions.

The outer photoreceptors have predominant functions in achromatic vision, such as motion detection. Exploitation of the outer photoreceptor pathway for multiple visual functions is advantageous for animals with limited neuronal resources. A recently discovered contribution of *Drosophila* R7/R8 to motion detection corroborates our findings of a differential use strategy [31]. Downstream mechanisms for decoding converged color and motion information await future studies.

Experimental Procedures

Fly Strains

All flies were raised in standard cornmeal medium at 25°C and 60% relative humidity under a 14/10 hr light/dark cycle. The X chromosomes of all transgenic strains were replaced with that of wild-type Canton-S (*w*[+]). Flies were tested 2–6 days after eclosion. For *norpA* rescue experiments, correct genotypes (Table S1) of given crosses were selected before experiments. All rhodopsin GAL4 drivers were kindly provided by Claude Desplan [32]. For *norpA* restoration, *UAS-norpA.K(1)* was used (derived from Bloomington stock number 26267). To test requirement of Rh1, we used a null mutant of *ninaE* (*ninaE*[8]) with little photoreceptor degeneration [33]. To block the function of neuronal subsets in the lamina neuropil, we crossed the *UAS-shi*[ts1] [26] line to different driver lines: *+; +; ort*[C2]*-GAL4* [14] (L1–L3, DM8), *+;vGlut-dVP16AD/CyO; ort*[C2]*-GAL4DBD/TM6B* [14] (few L1, most DM8), and *R48A08-GAL4* [27] (L1, L2, unknown medulla tangential cell type, unknown proximal medulla cell type; see http://flweb.janelia.org/ for expression pattern [34]). For anatomical analysis, the above driver lines were crossed to *y w; UAS-mCD8::GFP/CyO*.

Behavioral Assay

Flies were trained and tested using a visual appetitive differential conditioning assay [19] with modifications (Figure S1). For narrow-spectral illumination, we constructed a stimulation module using computer-controlled high-power LEDs with peak wavelengths 452 nm and 520 nm (Seoul Z-Power RGB LED) or 456 nm and 520 nm (H-HP803NB, and H-HP803PG, 3W Hexagon Power LEDs, Roithner Lasertechnik) for blue and green stimulation, respectively. LEDs were housed in a base 144 mm below the arena, which allowed homogeneous illumination of a filter paper as a screen. For separate illumination of each quadrant, the light paths of LEDs were separated by light-tight walls in a cylinder with air ducts. "Bright" and "dark" blue and green stimuli were used as explained throughout the manuscript. The intensities were controlled by current and calibrated using a luminance meter BM-9 (Topcon Technohouse) or a PR-655 SpectraScan Spectroradiometer as follows: 0.483 W sr^{-1} m^{-2} (bright blue), 0.048 W sr^{-1} m^{-2} (dark blue), 0.216 W sr^{-1} m^{-2} (bright green), 0.022 W sr^{-1} m^{-2} (dark green), 0.437 W sr^{-1} m^{-2} (Rh4-adapted bright blue), 0.044 W sr^{-1} m^{-2} (Rh4-adapted dark blue), 0.874 W sr^{-1} m^{-2} (Rh4-adapted bright green), and 0.087 W sr^{-1} m^{-2} (Rh4-adapted dark green).

Before experiments, flies were starved at 25°C to a mortality rate of 20%–30% [19]. Flies received four-cycle differential conditioning. Stimulation of the whole arena with one color/intensity was paired with a sucrose reward (2 M) for 1 min, and after a 12 s break in the dark the other color/intensity was presented without reward. The cylindrical arena consisted of a Petri dish (⌀ 92 mm; Sarstedt) on which flies could freely move, a pipe wall, and a second Petri dish used for a lid (Figure S1). The pipe's smooth inner

---

(C) *norpA* mutants with directed photoreceptor rescues in the intensity inversion task. Pairwise rescues with *rh1-GAL4/rh4-GAL4* or *rh4-GAL4/ rh6-GAL4* show significant color preference rather than intensity preference as the wild-type or "yellow rescue" flies. Rescue flies with *rh1-GAL4/rh6-GAL4* significantly choose the intensity cue (n = 12–30).

For wild-type and *norpA[7];UAS-norpA/+* in (A) and (C), the same data are plotted as in Figure 3. Bars and error bars represent means and SEM, respectively. *p < 0.05; **p < 0.01; ***p < 0.001; ns, no significance. See also Figures S4 and S5.
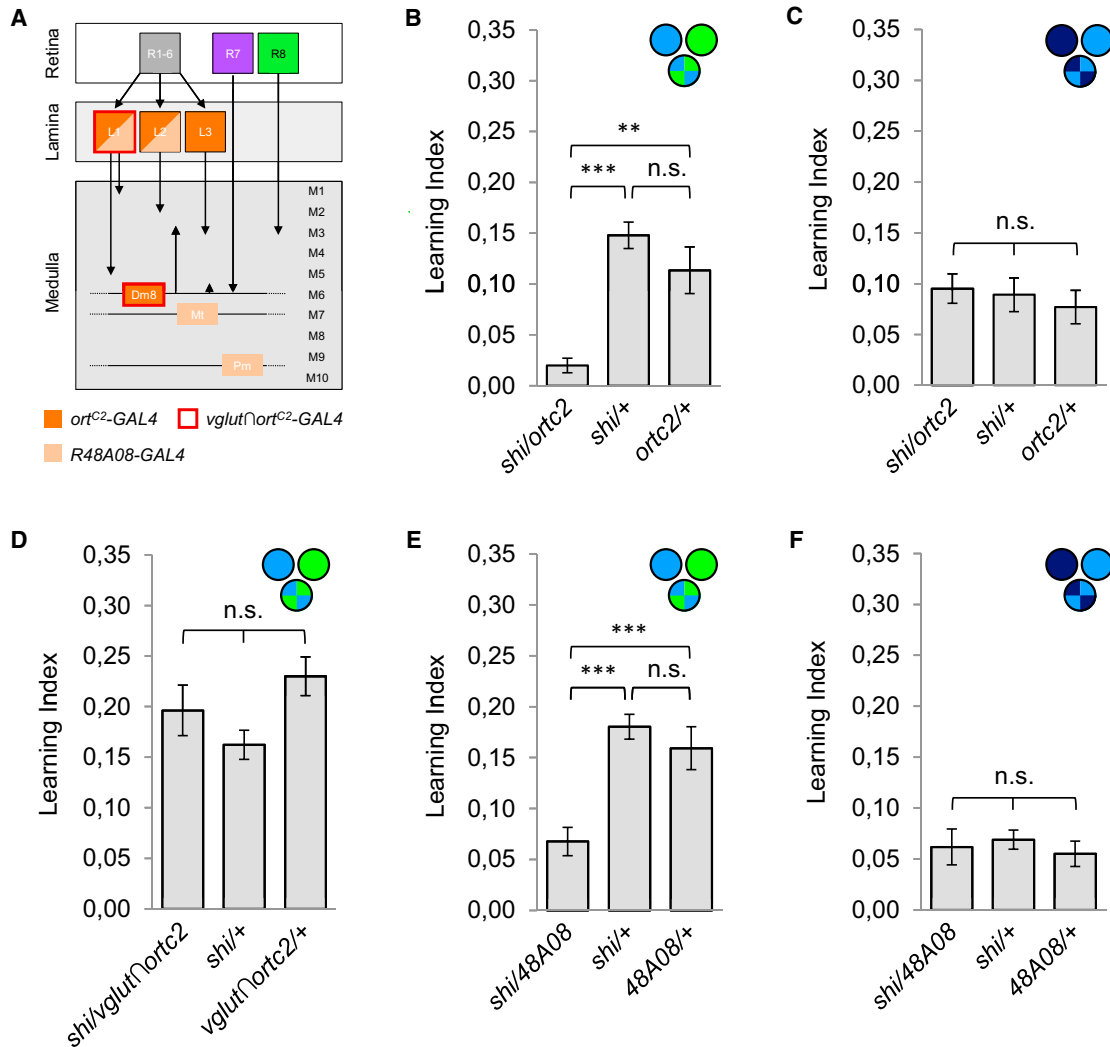
Figure 5. Lamina Monopolar Cells Are Required for Color Discrimination

(A) L1, L2, and L3 receive direct input from the outer photoreceptors R1–R6 and convey their signals to different layers in the medulla. Outputs of inner and outer receptors can converge in the medulla as well as in the downstream lobula complex. Cells labeled by the GAL4 drivers used in the blocking experiments are colored with dark orange or light orange or red outline (Dm8, distal medulla cell type; Mt, medulla tangential cell type; Pm, proximal medulla cell type).

(B) Blocking L1–L3 and Dm8 with Shi[ts1] and ort^{C2}-GAL4 specifically impaired bright-blue/bright-green discrimination (n = 13–18).

(C) Intensity discrimination is not impaired with the same blockade (n = 15–16).

(D) Blocking DM8 and a few L1 cells with splitGAL4 driver $vglut \cap ort^{C2}$-GAL4 does not significantly impair bright-blue/bright-green discrimination (n = 12–19).

(E) Bright-blue/bright-green discrimination is significantly impaired by blocking L1, L2, and two other cell types with R48A08-GAL4 (n = 8–13).

(F) Intensity discrimination is not impaired with the same blockade (n = 17–23).

Bars and error bars represent means and SEM, respectively. **p < 0.01; ***p < 0.001; ns, no significance.

surface and the lid were coated with Fluon (Fluon GP1, Whitford Plastics) to ensure that flies stayed on the filter paper at the bottom of the arena. Reward presentation was switched by inverting the whole arena, tapping the flies gently to detach them from the Petri dish, and exchanging the dishes with sugar or water. In half of the experiments, the reward/no reward sequence was reversed to cancel any effect of order. In the test period, flies were given the choice between two stimuli, presented in two quadrants each.

Conditioned response of the trained flies was recorded with CMOS cameras (FireflyMV, Point Grey Research) for 90 s. The learning index was based on two groups (50–100 flies each), which had been trained reciprocally in terms of the two visual stimuli used. Stimulus preference was determined by the distribution of flies in the arena. A preset macro for ImageJ (W.S. Rasband, US National Institutes of Health) was used to count the number of flies in each quadrant in every frame of our video recordings (90 frames recorded at 1 Hz) [19]. Flies touching a border between two quadrants were excluded.

We calculated a preference index for green (PI_G) for each time point by the difference between the number of flies on the green quadrants and the number on the blue quadrants, divided by the total number of flies counted. PI_G was calculated in both reciprocal experiments (i.e., green rewarded [G+ B−] and blue rewarded [G− B+]):

$$PI_G = \frac{\#Green - \#Blue}{\#Total}$$

A learning index (LI) was calculated by subtraction of PI_G values of the two reciprocally trained groups and by division of the resulting value by 2:

$$LI = \frac{PI_G(G + B-) - PI_G(G - B+)}{2}$$

The LI was calculated for each frame of a recorded video and averaged over the entire test phase (1–90 s), yielding an LI that represented the average performance of the flies. For experiments with *UAS-shi^{ts1}*, flies were trained and tested at 33°C after preincubation at the restrictive temperature for 30 min.

ERG Recordings

ERGs were measured as previously described (C. Garbers et al., 2012, Front. Comput. Neurosci., abstract). In brief, cold-anesthetized flies were attached to a holder with nail polish, which was also used to prevent movement of head and legs. A recording and an indifferent (reference) glass microelectrode filled with 0.1 M KCl were placed just beneath the cornea of the stimulated eye and in the thorax, respectively. The signal recorded at room temperature was amplified using an Intronix 2015f amplifier and digitally acquired using a NI PCI-6025E data acquisition board. Visual stimulation from the behavioral experiments (dark blue or bright green) was reproduced by using the same LEDs, intensities, and filter paper screen. Data acquisition and stimulation were controlled with the Relacs toolbox [35]. Using a modified closed-loop light clamp technique [36], wild-type and *norpA*-rescue flies were analyzed for their spectral sensitivity ratio for blue and green LEDs. As an internal reference of the interleaved ERG (INTER ERG) (C. Garbers et al., 2012, Front. Comput. Neurosci., abstract), we used the response to the blue LEDs set to the "dark" intensity as in the behavioral experiments. Using an iteratively updated linear regression model, the intensity of the green LED was adjusted to the level that evoked the same ERG response as the blue reference LED. The ERG response was defined as the difference in the average signals 10 ms before stimulation onset and 10 ms before offset. The stimulation protocol consisted of a 100 ms green light followed by 500 ms of no stimulation before 100 ms of the blue reference light followed by 500 ms of no stimulation. An average response difference to the blue reference was calculated based on five cycles of the stimulation protocol, and the measurement was repeated until the difference reached less than 4% of the reference amplitude. At least eight measurements in two flies were done per genotype. Blue/green intensity ratios were calculated by normalization of the dark-green stimulus with the green LED intensity producing the same signal amplitude as the reference (dark blue).

Immunohistochemistry and Microscopy

The retina of flies was prepared in agarose sections [37]. In brief, heads were fixed in 4% formaldehyde in PBT (PBS and 0.3% Triton X-100), embedded in 7% agarose (Biomol), and sectioned horizontally at 80 μm with a vibrating microtome (Leica VT 1000S). Agarose sections were bleached in 0.1% NaBH$_4$ for 30 min to reduce autofluorescence of the red eye pigment and were subsequently blocked with 3% normal goat serum for 30 min at room temperature. Preparations were incubated overnight at 4°C with the antibodies against GFP (1:1000) and Rh6 (a gift from Claude Desplan; 1:5,000) in the blocking solution. After washing with PBT, slices were incubated overnight at 4°C with AlexaFluor-568- and AlexaFluor-633-conjugated secondary antibodies in the blocking solution. Preparations were rinsed and mounted in Vectashield (Vector Laboratories). Confocal stacks were collected with Olympus FV-1000 microscope (Olympus). Image processing was performed with ImageJ.

Modeling Wavelength Discrimination

To compare spectral discrimination abilities, we calculated the contrast that two stimuli evoke at a hypothetical postreceptor neuronal stage [21]. For two stimuli, let $\Delta q_i(\lambda)$ be the difference in excitation for receptor i at wavelength λ. Then for two receptor types 1 and 2, the signal contrast in a neuronal channel k that combines these two receptor signals opponently can be written as

$$\Delta S_k^2(\lambda) = (\Delta q_1(\lambda) - \Delta q_2(\lambda))^2. \qquad \text{(Equation 1)}$$

To predict discrimination for a visual system combining information from more than one opponent channel, we sum over the k respective mechanisms:

$$\Delta S^2(\lambda) = \sum_{k=0}^{n} w_k S_k^2(\lambda), \qquad \text{(Equation 2)}$$

where w_k is a vector of weights that scale the channels relative to each other. For the special case of wavelength discrimination, $\Delta q_i(\lambda)$ corresponds to the slope of the receptor spectral sensitivity of receptor i at wavelength λ. Calculation of this relative discrimination at each wavelength λ yields an estimate of the spectral sensitivity function. We fitted this function to the data [21] by adjusting w such that the resulting squared differences between the

estimates and the data were minimized. Goodness of fit was calculated via the chi-square statistic, treating the data [20] as normally distributed.

Statistics

Statistical analyses were performed with the use of Prism (GraphPad Software). If groups did not violate the assumption of normal distribution, one sample t tests were used to test difference from zero. Otherwise, a nonparametric Wilcoxon signed rank test was employed. p values of both tests were Bonferroni corrected. For comparison of groups, none of which violated the assumption of normal distribution or homogeneity of variance, mean performance indices were compared with a one-way ANOVA followed by planned multiple pairwise comparisons (Bonferroni correction). Where comparisons with multiple control groups gave distinct significance levels, only the most conservative result is shown.

Supplemental Information

Supplemental Information includes five figures and one table and can be found with this article online at http://dx.doi.org/10.1016/j.cub.2013.10.037.

References

1. Kelber, A., Vorobyev, M., and Osorio, D. (2003). Animal colour vision—behavioural tests and physiological concepts. Biol. Rev. Camb. Philos. Soc. *78*, 81–118.
2. Osorio, D., and Vorobyev, M. (2008). A review of the evolution of animal colour vision and visual communication signals. Vision Res. *48*, 2042–2051.
3. Rushton, W.A.H. (1972). Pigments and signals in colour vision. J. Physiol. *220*, 1P–31P.
4. Rister, J., Desplan, C., and Vasiliauskas, D. (2013). Establishing and maintaining gene expression patterns: insights from sensory receptor patterning. Development *140*, 493–503.
5. Salcedo, E., Huber, A., Henrich, S., Chadwell, L.V., Chou, W.-H., Paulsen, R., and Britt, S.G. (1999). Blue- and green-absorbing visual pigments of Drosophila: ectopic expression and physiological characterization of the R8 photoreceptor cell-specific Rh5 and Rh6 rhodopsins. J. Neurosci. *19*, 10716–10726.
6. Hardie, R.C. (1985). Functional organization of the fly retina. Prog. Sens. Physiol. *5*, 1–79.
7. Pichaud, F., Briscoe, A., and Desplan, C. (1999). Evolution of color vision. Curr. Opin. Neurobiol. *9*, 622–627.
8. Strausfeld, N.J., and Lee, J.-K. (1991). Neuronal basis for parallel visual processing in the fly. Vis. Neurosci. *7*, 13–33.
9. Yamaguchi, S., Wolf, R., Desplan, C., and Heisenberg, M. (2008). Motion vision is independent of color in Drosophila. Proc. Natl. Acad. Sci. USA *105*, 4910–4915.
10. Yamaguchi, S., Desplan, C., and Heisenberg, M. (2010). Contribution of photoreceptor subtypes to spectral wavelength preference in Drosophila. Proc. Natl. Acad. Sci. USA *107*, 5634–5639.
11. Troje, N. (1993). Spectral categories in the learning behaviour of blowflies. Z. Naturforsch. Teil C Biochem. Biophys. Biol. Virol. *48*, 96.
12. Fukushi, T. (1994). Colour perception of single and mixed monochromatic lights in the blowfly Lucilia cuprina. J. Comp. Physiol. A *175*, 15–22.

13. Fischbach, K.F. (1979). Simultaneous and successive colour contrast expressed in "slow" phototactic behaviour of walking Drosophila melanogaster. J. Comp. Physiol. A *130*, 161–171.

14. Gao, S., Takemura, S.Y., Ting, C.-Y., Huang, S., Lu, Z., Luan, H., Rister, J., Thum, A.S., Yang, M., Hong, S.-T., et al. (2008). The neural substrate of spectral preference in Drosophila. Neuron *60*, 328–342.

15. Menzel, R., and Greggers, U. (1985). Natural phototaxis and its relationship to colour vision in honeybees. J. Comp. Physiol. A *157*, 311–321.

16. Bicker, G., and Reichert, H. (1978). Visual learning in a photoreceptor degeneration mutant of Drosophila melanogaster. J. Comp. Physiol. A *127*, 29–38.

17. Tang, S., and Guo, A. (2001). Choice behavior of Drosophila facing contradictory visual cues. Science *294*, 1543–1547.

18. Menne, D., and Spatz, H.-C. (1977). Colour vision in Drosophila melanogaster. J. Comp. Physiol. A *114*, 301–312.

19. Schnaitmann, C., Vogt, K., Triphan, T., and Tanimoto, H. (2010). Appetitive and aversive visual learning in freely moving Drosophila. Front Behav Neurosci *4*, 10.

20. Hernandez de Salomon, C., and Spatz, H.C. (1983). Colour vision in Drosophila melanogaster: wavelength discrimination. J. Comp. Physiol. A *150*, 31–37.

21. Vorobyev, M., and Osorio, D. (1998). Receptor noise as a determinant of colour thresholds. Proc. Biol. Sci. *265*, 351–358.

22. Inoue, H., Yoshioka, T., and Hotta, Y. (1985). A genetic study of inositol trisphosphate involvement in phototransduction using Drosophila mutants. Biochem. Biophys. Res. Commun. *132*, 513–519.

23. Wernet, M.F., Velez, M.M., Clark, D.A., Baumann-Klausener, F., Brown, J.R., Klovstad, M., Labhart, T., and Clandinin, T.R. (2012). Genetic dissection reveals two separate retinal substrates for polarization vision in Drosophila. Curr. Biol. *22*, 12–20.

24. Fischbach, K., and Dittrich, A. (1989). The optic lobe of Drosophila-melanogaster 0.1. a Golgi analysis of wild-type structure. Cell Tissue Res. *258*, 441–475.

25. Meinertzhagen, I.A., and O'Neil, S.D. (1991). Synaptic organization of columnar elements in the lamina of the wild type in Drosophila melanogaster. J. Comp. Neurol. *305*, 232–263.

26. Kitamoto, T. (2001). Conditional modification of behavior in Drosophila by targeted expression of a temperature-sensitive shibire allele in defined neurons. J. Neurobiol. *47*, 81–92.

27. Tuthill, J.C., Nern, A., Holtz, S.L., Rubin, G.M., and Reiser, M.B. (2013). Contributions of the 12 neuron classes in the fly lamina to motion vision. Neuron *79*, 128–140.

28. Morante, J., and Desplan, C. (2008). The color-vision circuit in the medulla of Drosophila. Curr. Biol. *18*, 553–565.

29. Menzel, R., and Backhaus, W. (1989). Color Vision Honey Bees: Phenomena and Physiological Mechanisms (Berlin: Springer-Verlag).

30. Kien, J., and Menzel, R. (1977). Chromatic properties of interneurons in the optic lobes of the bee. II. Narrow band and colour opponent neurons. J. Comp. Physiol. A *113*, 35–53.

31. Wardill, T.J., List, O., Li, X., Dongre, S., McCulloch, M., Ting, C.-Y., O'Kane, C.J., Tang, S., Lee, C.-H., Hardie, R.C., and Juusola, M. (2012). Multiple spectral inputs improve motion discrimination in the Drosophila visual system. Science *336*, 925–931.

32. Mollereau, B., Wernet, M.F., Beaufils, P., Killian, D., Pichaud, F., Kühnlein, R., and Desplan, C. (2000). A green fluorescent protein enhancer trap screen in Drosophila photoreceptor cells. Mech. Dev. *93*, 151–160.

33. Kumar, J.P., and Ready, D.F. (1995). Rhodopsin plays an essential structural role in Drosophila photoreceptor development. Development *121*, 4359–4370.

34. Jenett, A., Rubin, G.M., Ngo, T.-T.B., Shepherd, D., Murphy, C., Dionne, H., Pfeiffer, B.D., Cavallaro, A., Hall, D., Jeter, J., et al. (2012). A GAL4-driver line resource for Drosophila neurobiology. Cell Rep *2*, 991–1001.

35. Benda, J., Gollisch, T., Machens, C.K., and Herz, A.V. (2007). From response to stimulus: adaptive sampling in sensory physiology. Curr. Opin. Neurobiol. *17*, 430–436.

36. Franceschini, N. (1979). Voltage Clamp by Light - Rapid Measurement of the Spectral and Polarization Sensitivities of Receptor-Cells. Invest. Ophthalmol. Vis. Sci. *18* (*Suppl.*), 5.

37. Gruber, F., Knapek, S., Fujita, M., Matsuo, K., Bräcker, L., Shinzato, N., Siwanowicz, I., Tanimura, T., and Tanimoto, H. (2013). Suppression of conditioned odor approach by feeding is independent of taste and nutritional value in Drosophila. Curr. Biol. *23*, 507–514.

3.3 Contextual processing of brightness and color in Mongolian gerbils

Contextual processing of brightness and color in Mongolian gerbils

Christian Garbers*

Department Biologie II, Ludwig-Maximilians-Universität München, Planegg-Martinsried, Germany

Josephine Henke*

Department Biologie II, Ludwig-Maximilians-Universität München, Planegg-Martinsried, Germany

Christian Leibold

Department Biologie II, Ludwig-Maximilians-Universität München, Planegg-Martinsried, Germany
Bernstein Center for Computational Neuroscience Munich, Munich, Germany

Thomas Wachtler

Department Biologie II, Ludwig-Maximilians-Universität München, Planegg-Martinsried, Germany
Bernstein Center for Computational Neuroscience Munich, Munich, Germany

Kay Thurley

Department Biologie II, Ludwig-Maximilians-Universität München, Planegg-Martinsried, Germany
Bernstein Center for Computational Neuroscience Munich, Munich, Germany

Brightness and color cues are essential for visually guided behavior. However, for rodents, little is known about how well they do use these cues. We used a virtual reality setup that offers a controlled environment for sensory testing to quantitatively investigate visually guided behavior for achromatic and chromatic stimuli in Mongolian gerbils (*Meriones unguiculatus*). In two-alternative forced choice tasks, animals had to select target stimuli based on relative intensity or color with respect to a contextual reference. Behavioral performance was characterized using psychometric analysis and probabilistic choice modeling. The analyses revealed that the gerbils learned to make decisions that required judging stimuli in relation to their visual context. Stimuli were successfully recognized down to Weber contrasts as low as 0.1. These results suggest that Mongolian gerbils have the perceptual capacity for brightness and color constancy.

Introduction

Vision plays an important role for the discrimination and recognition of objects. However, varying illumination conditions can result in drastic changes of intensity and spectral composition of the light reflected from an object. The ability of the visual system to compensate for such influences of illumination, known as brightness and color constancy, is therefore essential for reliable object recognition in varying environments (Figure S1). Humans achieve color constancy by taking into account information from the larger visual context. Specifically, relationships between colors in a scene, i.e., contrasts between object surfaces and their surroundings, are more stable under changing illumination than absolute intensity or spectral composition (Foster, 2011). For example, an object with higher reflectance will always reflect more light compared to a neighboring object with lower reflectance although their absolute intensities will vary with changing illumination. Local and
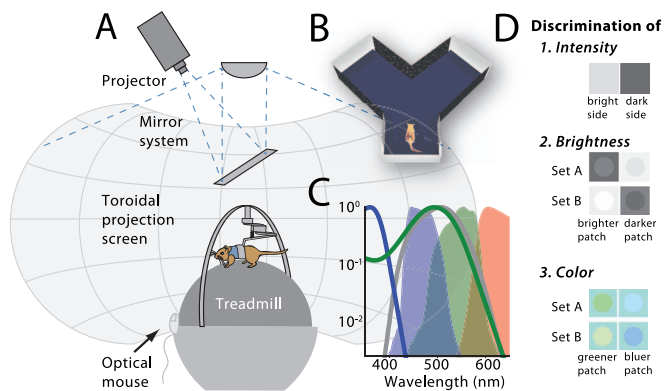
Figure 1. Testing visual discrimination in gerbils. (A) Experimental apparatus. (B) Virtual Y-shaped maze for 2AFC experiments. At trail start, the animal is located in the stem of the Y. Visual stimuli are presented at the end walls of the two arms. The animal responds by walking into the chosen arm. (C) Spectra of gerbil photoreceptors and projector primaries. Blue, green, and gray solid lines show the spectra of gerbil S and M cones and rods, respectively. Colored filled curves represent the spectra of the projection system. (D) Example stimulus sets for the three discrimination tasks. See text for details.

global contrasts thus are cues that contribute strongly to color constancy (Foster, 2011; Hurlbert & Wolf, 2004; Kraft & Brainard, 1999). Studies on the abilities of nonhuman vertebrates to make contextual visual judgments as required for color constancy are rare (Dörr & Neumeyer, 2000; Locke, 1935). In particular, nothing is known so far about whether rodents can use such important second-order visual cues for behavior.

Among rodents, vision is particularly well developed and ecologically important in Mongolian gerbils (*Meriones unguiculatus*), which exhibit a unique receptor configuration (Govardovskii, Röhlich, Szél, & Khokhlova, 1992) and behavior under daylight conditions (Pietrewicz, Hoff, & Higgins, 1982). The Mongolian gerbil's retina is composed of two cone and one rod photoreceptor types (Jacobs & Deegan, 1994; Jacobs & Neitz, 1989). The cones are maximally sensitive at wavelengths around 360 nm (S cones) or around 490 nm (M cones), respectively (Jacobs & Deegan, 1994; Figure 1C). Gerbil M cones show the most prominent short wavelength shift known in mammals with a sensitivity maximum that lies at shorter wavelengths than that of the rods (Jacobs & Neitz, 1989).

Here we introduce an experimental paradigm to investigate visually guided behavior in gerbils. In our experiments, the animals learned to select visual stimuli based on their brightness or color relative to a surrounding background, suggesting that Mongolian gerbils may exhibit brightness and color constancy. In addition, our data reveal principles of the related task learning dynamics.

Methods

Animals

Experiments were performed with four adult female Mongolian gerbils (*Meriones unguiculatus*). Training started at an age of 8 months, at which the animals weighed between 80 and 90 g. The animals received a diet that kept their weight at about 85%–90% of their free feeding weight. All experiments were approved according to national and European guidelines on animal welfare (Reg. von Oberbayern, AZ 55.2-1-54-2532-10-11).

Experimental apparatus

We used a virtual reality (VR) setup (Figure 1A) for rodents in which the animal was placed on a Styrofoam sphere acting as a treadmill. Movements of the animal induced rotations of the sphere that were detected by two infrared sensors connected to a computer. The computer generated and updated a virtual visual scene that was displayed via a video projector and a mirror system on a projection screen surrounding the treadmill. The distance of the screen from the animal was 65 cm. For real-time rendering, we used Vizard Virtual Reality Toolkit (v3.18, WorldViz, http://www.worldviz.com/; for a more detailed description, see Thurley et al., 2014). Calibration of the stimulation apparatus and verification of luminance and chromaticity of individual stimuli was done using a PR-655 SpectraScan® Spectroradiometer (Photo Research, Inc.).

We performed three different visual discrimination experiments (achromatic intensity discrimination, brightness constancy, and chromatic contrast discrimination) using a forced choice paradigm. Visual targets were presented at the ends of the arms of a virtual Y-shaped maze; the other walls of the maze were covered with black-and-white striped and dotted textures (Figure 1B). No other virtual light sources were used to ensure controlled intensity and chromatic contrast of the stimuli. At the beginning of each trial, an animal was located at the end of the virtual Y maze's stem facing its fork (see Figure 1B). The end walls subtended 28° × 28° of visual angle initially and increased in size as the animal approached them in the VR. The animal had to run to the end of the correct arm to receive a food reward (Nutri-plus gel, Virbac, Bad Oldesloe, Germany). In addition, the animal received visual

feedback at the end of each trial. The entire projection screen was either set to black (correct) or to white (wrong) for two seconds (1 and 49 mW·sr^{-1}·m^{-2}, respectively). A new trial was initiated by reintroducing the animal at the virtual Y maze's stem. Stimulus presentation was randomized between left and right arms. Each experimental session lasted until the animal had performed at least 20 decisions or, during training, until 15 min had passed. Animals performed one to two sessions per day.

Behavioral training

The animals were accustomed to the VR for about 2 weeks (Thurley et al., 2014). Afterward, the animals performed the actual visual discrimination experiments. For each type of experiment, the animals were first trained with conditions in which high contrasts were used. The training period lasted until the animals had learned the task, i.e., they made correct decisions above chance for at least 3 days in succession. In each experiment, half of the animals were trained for one stimulus condition (e.g., to choose the brighter stimulus); the others were trained for the other condition.

Stimuli

Stimulus differences were quantified by Weber contrast $I_1/I_2 - 1$, where $I_1 > I_2$ represent the intensities of stimuli that have to be discriminated. In the brightness discrimination task, the animals had to discriminate a high-intensity stimulus from a low-intensity stimulus presented at different arms of the Y maze (Figure 1D). Here contrast was defined as contrast between the bright and the dark arm.

For the brightness contrast experiment, the animals had to discriminate the contrasts of stimuli consisting of a central patch on a uniform background at the end of each maze arm. Stimulus patches were circular with a diameter of two thirds of the height of the stimulus wall. In one of the arms, the center patch was of higher intensity than the background; in the other arm, it was darker. Contrast was the same in both cases (Figure 1D). To exclude that animals could solve the task based on absolute intensity, two stimulus sets were used in which the overall intensities were exchanged but the local intensity relationships remained the same (Figure 1D). Average stimulus radiances were 10 mW·sr^{-1}·m^{-2} for the dark stimuli and 42 mW·sr^{-1}·m^{-2} for the bright stimuli. Chromatic contrasts were produced by either increasing the intensity of the green projector primary and decreasing the intensity of the blue primary in the stimulus patch relative to

the background (+G−B stimulus), or vice versa (−G+B stimulus), illustrated in Figure S2. The amounts of changes in each primary were chosen to achieve equally large but opposite cone contrasts in M and S cones. To minimize the possibility of errors due to uncertainties in the spectral shapes of the cone sensitivities in the long wavelength range, the red display primary was not used for the chromatic stimuli. Cone excitations were calculated as the inner products between the display spectra and the gerbil spectral sensitivity functions (Jacobs & Deegan, 1994; see also Figure 1C). To exclude that achromatic cues could be used to solve the task, two stimulus sets were used, in which overall intensities varied but the local chromatic contrasts remained the same (Figure 1D).

Analysis of behavior

We assessed the performance of the animals in two ways: (a) by evaluating the correctness of a decision and (b) to determine stimulus-unrelated influences on decision making, by analyzing which arm of the Y maze the animals took. Because both parameters are binomially distributed random variables, we used binomial tests for significance testing. Confidence intervals were calculated as Clopper-Pearson intervals based on the beta distribution. For differences between proportions, we tested with a chi-squared test. Data analyses were done with Python 2.7 using the packages Numpy 1.7.1, Scipy 0.12, Statsmodels 0.5.0 (Seabold & Perktold, 2010), and Matplotlib 1.3 (Hunter, 2007).

Psychometric analysis

Contrast values were computed as positive numbers, and the sign of the contrast was used to indicate in which arm of the Y maze the rewarded stimulus was placed. Psychometric functions are thus given as percentage of rightward choices as a function of this signed Weber contrast. A negative contrast value indicates that the target stimulus was presented at the left arm; a positive contrast indicates that the target was on the right. We fitted psychometric data with the function

$$\psi(c) = \lambda_l + (1 - \lambda_l - \lambda_r)F(c; m, w) \qquad (1)$$

where $F(c)$ is a cumulative Gaussian and $F^{-1}(c)$ its inverse. The variables $\lambda_{l \backslash r}$ represent the lapse rates for leftward and rightward choices, respectively. The parameter $m = F^{-1}(50\%)$ is the mean of the cumulative Gaussian $F(x)$ and determines the left-right bias. The width $w = F^{-1}(1-\alpha) - F^{-1}(\alpha)$ represents the interval over which the psychometric function is growing, i.e.,

a way to parameterize its slope. We set $\alpha = 25\%$ such that w corresponds to the interval [25%, 75%]. Thus, ω can be regarded as a discriminability threshold or as "just noticeable difference." Because two stimuli were present in the brightness contrast and chromatic contrast experiments, the threshold contrasts reported here slightly underestimate the values that would be obtained for single stimuli. For fitting Equation 1 to the data, we used a Bayesian inference approach that relies on a Markov chain Monte Carlo method (Kuss, Jäkel, & Wichmann, 2005) implemented in the Psignifit 3.0 package (Fründ, Haenel, & Wichmann, 2011).

Probabilistic choice modeling

As an alternative way to describe the behavioral data, we made use of a probabilistic choice model (Busse et al., 2011). The model assumes influences from three different sources on the decision in the current trial: (a) a sensory component $v\,[c(t)]$ that describes the impact of the contrast stimulus c in trial t, (b) history terms describing the influence of a previous correct $s(t-1)$ or false choice $f(t-1)$, and (c) a general bias b_0 into which all other influences are collapsed, such as a general preference for one arm of the Y maze or a tendency to lapse. The history sequences are mutually exclusive, i.e., for correct trials, $f(t) = 0$ and $s(t) = \pm 1$ if the chosen arm is right or left. Correspondingly, if the decision was wrong, we set $s(t) = 0$ and $f(t) \pm 1$. In a reduced version of the model, we left out the history terms. All model components were linearly combined into a decision variable

$$z(t) = v[c(t)] + b_s\, s(t-1) + b_f\, f(t-1) + b_0, \qquad (2)$$

which itself was assumed to determine the probability

$$p = \frac{1}{1 + \exp(-z)} \qquad (3)$$

of choosing the right arm by sampling from a Bernoulli distribution.

To derive the parameters $v(c)$, b_s, b_f, and b_0 of the model, we fitted a generalized linear model using Statsmodels 0.5.0 (Seabold & Perktold, 2010) and assumed a binomial distribution family with a logit link function. To assist fit convergence at reasonable values, we restricted the z values to remain within ± 3 via a quadratic penalty term $(|z| - 3)^2$ for $|z| > 3$. We simulated the model by applying the same sequence of presented contrasts as in the experiments and taking the history according to the outcome of the last simulated trial. The probability p from Equation 3 for the simulated z values was then used for binary random sampling. To determine the intervals that contained

95% of the simulation runs in the figures below, we performed 25 to 50 runs.

For better visualization, we fitted the contrast responses inferred from behavior $v(c)$ with a hyperbolic ratio function of contrast (Albrecht & Hamilton, 1982)

$$f(c) = R_0 + R_{\max} \frac{c^n}{c_{50} + c^n} \qquad (4)$$

where R_0 is the baseline, $R_{\max}$ the overall responsiveness, c_{50} the semisaturation contrast, and n determines the steepness.

Results

We performed three different visual experiments with Mongolian gerbils (Figure 1D) using a two-alternative forced choice (2AFC) paradigm. For precise control of stimulus presentation and behavioral measurement, we implemented the tasks in VR (Harvey, Collman, Dombeck, & Tank, 2009; Hölscher, Schnee, Dahmen, Setia, & Mallot, 2005; Thurley et al., 2014; Figure 1A, B and Methods).

Training for intensity discrimination

In the first series of experiments, animals had to discriminate stimuli of different intensities (see Figure 1D) that were presented on opposing arms of a virtual Y maze. Half of the animals were rewarded for choosing the arm with the brighter stimulus; the other half were rewarded for the darker stimulus. The intensity difference between the training stimuli corresponded to a Weber contrast of 2. In all gerbils, performance increased gradually over sessions and became significantly different from chance level after about nine sessions, corresponding to between 200 and 300 trials. At this point, performance was at 75% correct or higher (binomial test, $p \leq 0.05$; Figure 2).

To understand choice behavior during task learning, we analyzed the data with respect to which arm of the Y maze the animals chose (Figure S3A). All animals initially showed a strong preference for choosing the Y's left arm. These leftward biases largely disappeared with ongoing training (binomial test, $p > 0.05$ for all animals in the final sessions).

As a more systematic account of choice behavior, we described the learning dynamics using a probabilistic choice model (Busse et al., 2011, and Methods). For the training data, we used a reduced model with only two components: (a) the influence $v(c)$ of the stimulus contrast c and (b) an overall bias b_0. Choosing the two-parameter variant allowed for fitting the model to each session separately despite the rather low number of
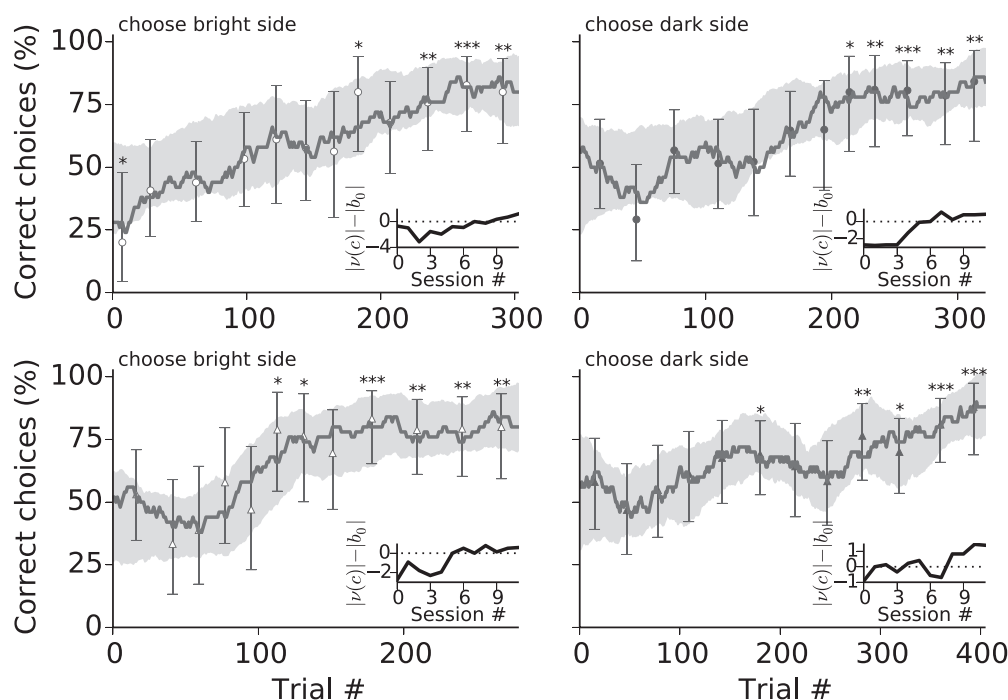
Figure 2. Learning intensity discrimination. Individual learning curves are given for each of the four gerbils. The dark solid lines depict the performance over trials. The curves were calculated with a moving average of 50-trial window size. Markers represent session averages, corresponding error bars are 95% binomial confidence intervals, and stars designate significant difference from chance level according to a binomial test (* $p \leq 0.05$, ** $p \leq 0.01$, *** $p \leq 0.001$). The animals on the left panels (open symbols) had to choose the brighter stimulus, the animals on the right panels (filled symbols) the darker stimulus. Gray shaded areas delimit intervals that contain 95% of simulation runs with the probabilistic choice model. Insets: Difference between the magnitudes of the two model parameters, the sensory term $v(c)$ and the bias b_0 for consecutive sessions. Layout of the panels and symbols identify data from the same animal throughout the paper.

available data points (on average, an animal performed 27 ± 6 trials per session). The model fits were in good agreement with the data, and the development of the model's parameters over sessions confirmed the above conclusions (Figure 2 insets): Initially the bias term b_0 was large in comparison to the influence of the stimuli $v(c)$, corresponding to strong preferences for one of the maze's arms. During training, the contribution of $v(c)$ increased, and behavior became less and less influenced by the bias b_0. Finally, choice behavior depended more strongly on the stimulus $v(c)$ than on the side.

From these results, we conclude that gerbils can learn to do intensity discrimination in a virtual 2AFC paradigm. The animals' initial preferences for choosing one of the maze arms was overcome by training, leading to consistent stimulus-dependent choice behavior.

Intensity task

With the trained animals, intensity discrimination was tested for 16 sessions using stimuli with smaller intensity differences. Performance was largely stable for most contrasts from the beginning (Figure S3B). Figure

3 shows the psychometric data such that it takes into account the side at which the target stimulus was presented. The percentage of rightward choices is plotted as a function of contrast with positive contrast values corresponding to target stimuli presented on the right arm and negative contrast values corresponding to target stimuli presented on the left arm.

By fitting psychometric functions to the data, we analyzed choice behavior with regard to (a) stimulus discriminability and (b) influences of side preferences. Accordingly, we derived the following characteristic parameters: (a) a discriminability threshold w that quantifies the contrast interval in which behavioral performance changes over 50% and (b) a side bias m together with the leftward/rightward lapse rates $\lambda_{l/r}$ (see Methods for details).

Sensory thresholds w were 0.5 for one animal and between 0.1 and 0.2 for the other three animals. Overall, the animals' performances displayed considerable idiosyncrasies. Two of the animals showed strong left biases, resulting in almost perfect performance when target stimuli were presented on the left (i.e., negative values on the abscissae in Figure 3) but remaining barely above chance for targets on the right. Both animals had lost their left arm preference at the
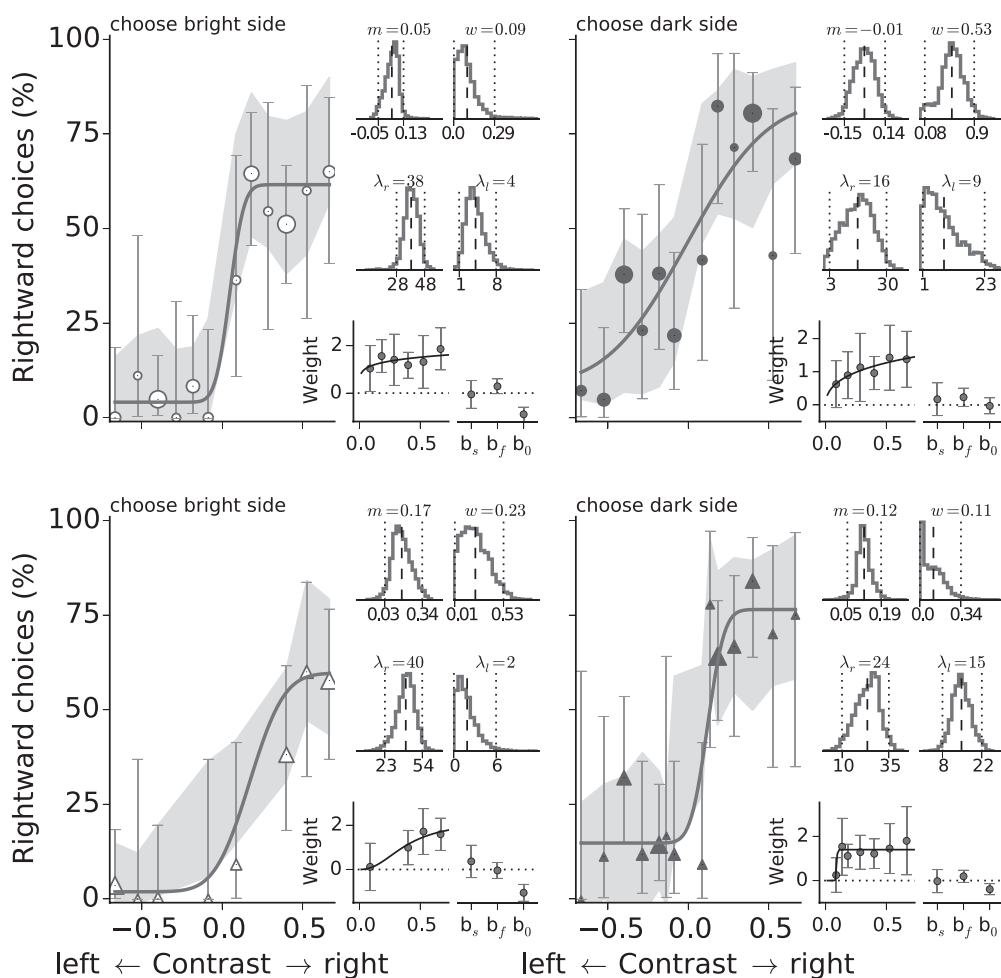
Figure 3. Psychometric results for intensity discrimination. The figure is organized similarly to Figure 2. Psychometric functions for the individual animals are given as the percentage of rightward choices as a function of the contrast between the brighter and the darker stimulus. The size of the symbols is proportional to the number of trials included in the data point. Error bars are binomial confidence intervals. Solid lines are fitted psychometric functions. The gray shaded areas are intervals that contain 95% of single simulation runs with the probabilistic choice model. The four upper small panels to the right of each plot give distributions of parameters of the psychometric functions derived from the Bayesian inference approach. For notation, see main text and Methods. Above each of those panels, the average parameter values are given and indicated with dashed lines. These averages are the estimates used for the fits given in the main panels. Dotted lines give the 95% confidence intervals of the respective parameter. Lower small panels show model parameters with 95% confidence intervals. Solid lines are fits with a hyperbolic ratio function.

end of the training phase with larger stimulus differences (cf. Figure S3A, bottom left). This behavior is in line with a strategy mix that lets the animal choose right only if it is confident that the target is on the right side but suggests going left otherwise. For the other two animals, left arm preferences were less pronounced. Both animals displayed more similar lapse rates for leftward and rightward choices.

The bias m showed a less heterogenous picture across animals but was in line with a general left preference (Figure 3). In contrast to the lapse rates, the parameter m captures side biases at low absolute contrast.

We also fitted the probabilistic choice model to the psychometric data. The model's stimulus-dependent parameters $v(c)$ were monotonously increasing with contrast, and the overall biases b_0 were in agreement with the psychometric analyses above (Figure 3, bottom inset panels). Arm preferences have different signs in the model's b_0 and the psychometric function's m parameters (i.e., a left bias is represented by $b_0 < 0$ but $m > 0$). Because history parameters describing past successes b_s or failures b_f have been reported to be important for explaining choice behavior (Busse et al., 2011), we included them in the analysis. However, their influence turned out to be negligible given that both

parameters did not differ significantly from zero (bottom-most small panels in Figure 3).

Our VR intensity discrimination paradigm thus allowed for determining psychometric discriminability thresholds. The quantification of choice behavior and performance was consistent between classical psychophysical analysis and probabilistic choice modeling.

Brightness task

We next investigated whether gerbils are able to select stimuli based on their intensity relative to the immediate surround. In this experiment, the animals had to compare stimuli consisting of a central uniform stimulus patch on a background (see Figure 1D). Two of the animals had to choose the side on which the test patch was of higher intensity than its background (brighter stimulus), and the other two animals had to choose the side on which the test patch was of lower intensity than its background (darker stimulus). To exclude that animals could use absolute intensity as a cue, two sets of stimulus pairs with different absolute intensity levels were used (see Figure 1D and Methods) and selected randomly from trial to trial. During training, we used stimuli with Weber contrasts of 0.225.

The task is illustrated in more detail in Figure 4A, in which we provide stimuli and choices of one animal from the last trials of the training for the brightness task. The animal was trained to choose the stimulus that was darker than its immediate surround independent of the stimulus' overall intensity. In the 16 trials given, the animal identified the target stimulus 13 times, and it did not use a strategy based on overall intensity. Similar results were obtained for all of our animals during the training of the brightness task.

During training, the animals' decisions were at chance level for the first 100 to 150 trials (about five sessions). Afterward, performance rather abruptly became significant and saturated at about 75% correct choices (Figure S4A). Again choice behavior initially showed left arm preferences (Figure S4B). At the end of training, performance was similar for both stimulus sets (chi-squared test, $p > 0.2$ for all animals). Because the animals had been trained in the previous experiment to compare the intensities of the stimuli presented at the left and right arms, we reasoned that in the beginning they might try to apply those learned strategies. However, this was not the case. With respect to absolute intensities, the choices were close to chance level and remained like this throughout (Figure S4A). As in the intensity discrimination task, the results were also reflected in the parameters of the reduced probabilistic choice model (Figure S4A, insets).

After training, test stimuli with lower contrasts were interspersed with the training stimuli. To keep the animals motivated, we began with a test/training stimulus ratio of 0.75. This ratio was subsequently reduced until none of the training stimuli remained. In total, we undertook 19 test sessions with each animal. The psychometric data are shown in Figure 4. Again performance was similar for both associated stimulus sets (chi-squared test, $p > 0.07$ for all animals and contrasts). From the beginning, animals performed at a stable level for each contrast, indicating that they immediately generalized the task from the training stimuli to stimuli with contrasts and intensity levels they had never encountered before (Figure S4C). Biases m as determined from the psychometric functions were relatively low. Similarly, the probabilistic choice model indicated only small biases and history contributions but a substantial contribution of the sensory terms.

All four animals were able to discriminate stimuli down to a contrast of 0.1 or below. These results demonstrate that gerbils are able to select visual stimuli based on relative brightness cues.

Color task

In a final series of experiments, we tested the gerbils' ability to select color stimuli based on color contrast relative to the background. Two of the animals had to choose the side on which the test patch color was shifted toward the green projector primary relative to the background (+G−B stimulus); the other two animals had to choose the side on which the test patch color was shifted toward the blue primary (−G+B stimulus). Again two sets of stimuli with different absolute intensity levels were used to exclude that animals could use intensity, achromatic contrast, or absolute cone excitation as cues. Furthermore, we assigned the +G−B and −G+B tasks to the animals such that the two animals with the darker target in the achromatic contrast experiment were assigned different chromatic targets, and likewise the two animals with the brighter target in the achromatic contrast experiment were assigned different chromatic targets.

For training, we used stimuli with chromatic contrasts of 0.5. Again performance was at chance level initially and gradually increased with training (left panel of Figure S5A). After about 200 trials (five sessions), all animals achieved close to 75% correct choices. Performance was not different for the different stimulus sets (chi-squared test, $p > 0.17$ for all animals). A strategy based on achromatic cues was not adopted by the animals (Figure S5A). Choice behavior was influenced by maze arm preferences early in training, similarly as in the previous experiments, and to some extent remained throughout the training in two animals (Figure S5B).
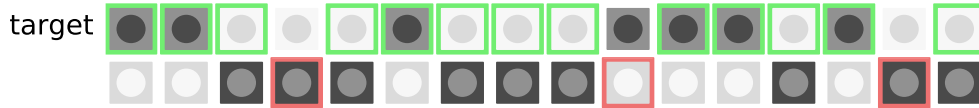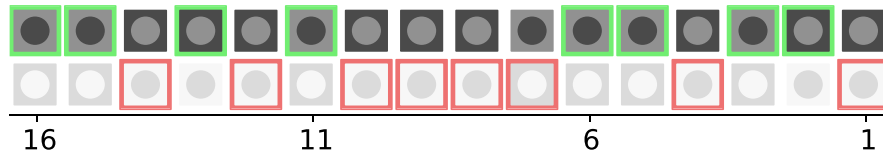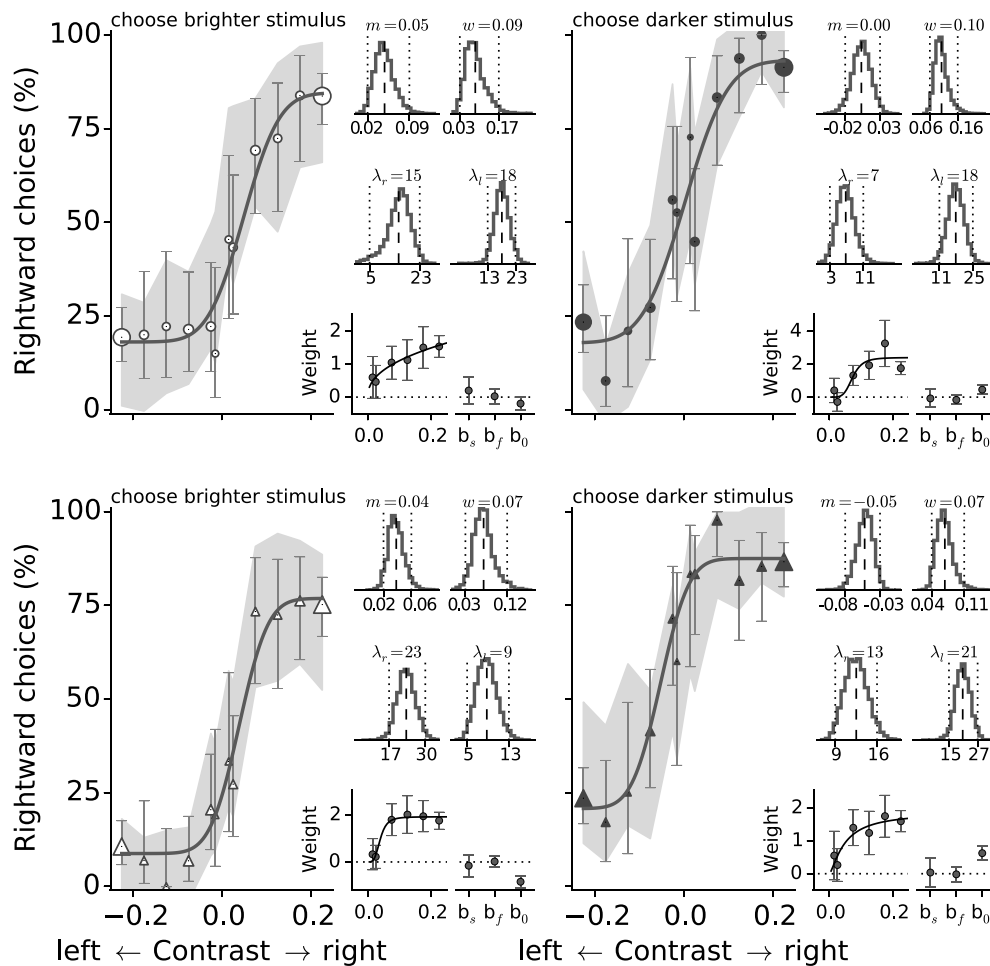
Figure 4. Psychometric results for the brightness task. (A) Final trials in the training phase of the brightness task for an example animal (bottom right in B). Upper panel: Stimulus pairs are given for each trial with targets in the upper and distractors in the lower row. The animal's choices are indicated with green (correct) and red (false) frames around the stimulus in the trial. Note that, in the experiments, target and distractors were presented on left and right arms of the maze at random. Lower panel: Same data as above but plotted corresponding to what would be expected if the animal had used a strategy based on overall intensity. (B) Psychometric

→

←

functions for the brightness task. The figure is composed similarly to Figure 3. Psychometric data for the individual animals is given as the percentage of rightward choices as a function of the contrast between the central patch and its local background (symbols and error bars represent averages and 95% confidence intervals, respectively). Solid lines are fitted psychometric functions. The gray shaded areas correspond to the probabilistic choice model, whose parameters are given in the bottom-most of the small panels to the right. The four upper small panels to the right of each plot give distributions of parameters of the fitted psychometric functions. Averages and 95% confidence intervals are highlighted. Solid lines are fits with a hyperbolic ratio function.

After training, we conducted seven test sessions. Again test stimuli of lower contrast were interspersed with increasing rate into the set of training stimuli. Figure 5 shows the results of the psychometric analysis. Performance was not significantly different for the two stimulus sets (chi-squared test, $p > 0.06$ for all animals and contrasts), and the animals immedi-

ately performed at a stable level for each contrast (Figure S5C). As in the previous experiments, two of the animals showed arm preferences (Figure 5, lower panels). The psychometric data of all animals were consistent with the probabilistic choice model. The contrast parameter v was monotonously increasing with contrast c, and the general bias term b_0 was
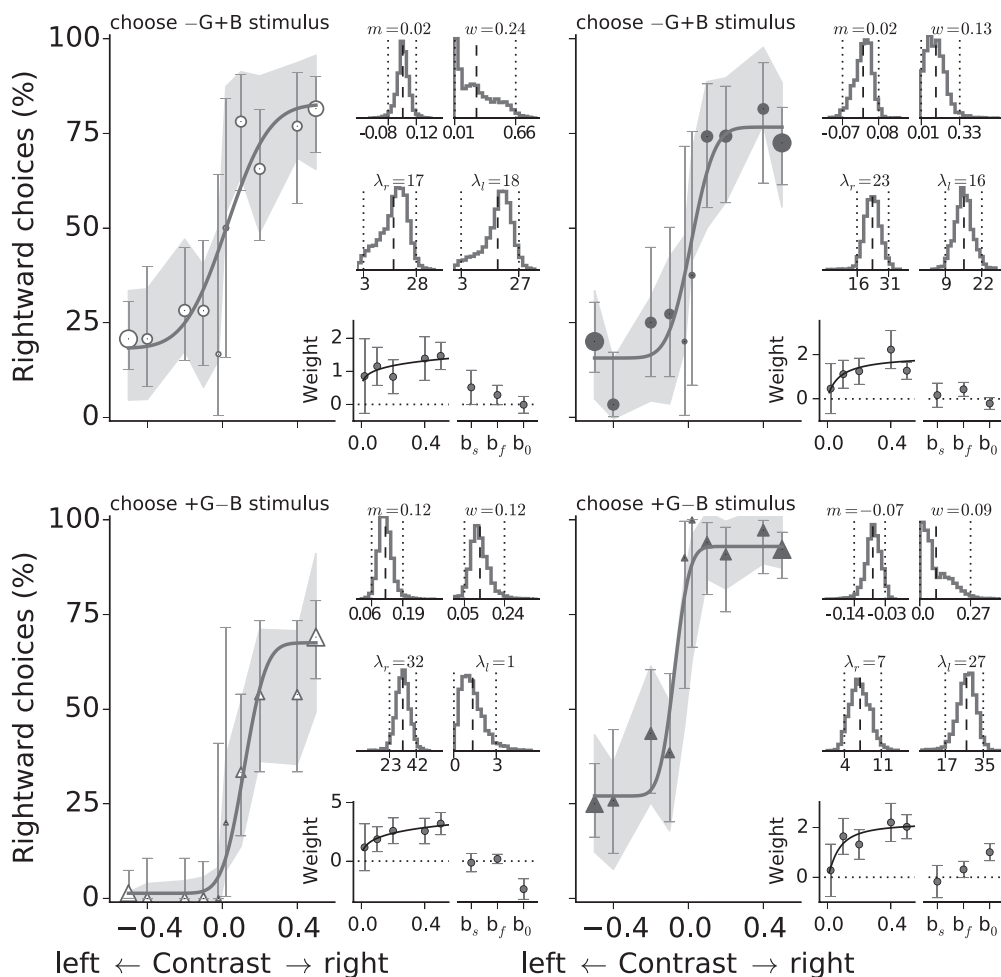
Figure 5. Psychometric results for color discrimination. The figure is composed similarly to Figure 3. The animals in the first row had to chose the −G+B patch, the animals in the second row the +G−B one. Psychometric data for the individual animals is given as the percentage of rightward choices as a function of the chromatic contrast (symbols and error bars represent averages and 95% confidence intervals, respectively). Solid lines are fitted psychometric functions. The gray shaded areas correspond to the probabilistic choice model, whose parameters are given in the bottom-most of the small panels to the right. The four upper small panels to the right of each plot give distributions of parameters of the fitted psychometric functions. Averages and 95% confidence intervals are highlighted. Solid lines are fits with a hyperbolic ratio function.

significant for the two animals that showed arm preferences. The history parameters b_s and b_f were again negligible. All animals could discriminate stimuli down to contrasts between about 0.1 and 0.2. These results demonstrate that gerbils are able to select visual stimuli based on relative color cues.

Discussion

In this study, we investigated the ability of Mongolian gerbils to perform brightness and color judgments. The behavioral tests were implemented using a VR setup for rodents (Thurley et al., 2014).

Intensity and contrast discrimination

To establish our psychophysical approach, we began with a simple intensity task. The results demonstrated the ability of gerbils to discriminate stimuli by intensity. However, for object vision under natural conditions, judging stimuli in relation to their visual context is more relevant (Foster & Nascimento, 1994). We therefore investigated whether gerbils are able to distinguish stimuli based on contrast to their background regardless of absolute intensity. To ensure that the animals' choices depended on brightness contrast, we used stimuli with varying intensities, such that the only indicator for reward in the stimuli was the achromatic contrast between stimulus patch and background. The animals successfully learned to choose the correct stimuli, indicating that gerbils can take context into account when using brightness cues for behavior. Finally, we tested whether gerbils are able to identify stimuli based on chromatic contrast regardless of intensity. As with achromatic contrasts, the animals learned to choose the correct stimuli, indicating that gerbils can use contextual color cues for behavior. Because brightness and color relationships between surfaces in a scene are strong cues to brightness and color constancy (Hurlbert & Wolf, 2004; Kraft & Brainard, 1999), the results presented here provide a first indication that gerbils are capable of such perceptual constancies.

With our paradigm, it is conceivable that animals would not choose the stimuli based on local brightness or color relationships but instead learn which of the two stimuli was rewarded for each stimulus pair separately. However, in the testing sessions, the animals' performance was above chance and at a stable level for each contrast from the very beginning. This corroborates the conclusion that the gerbils immediately generalized the task from the training stimuli to stimuli with contrasts and intensity levels they had never encountered before (Figures S3B, S4C, S5C).

Quantitatively, the thresholds measured psychophysically in our experiments were slightly lower than increment thresholds determined from electroretinogram measurements in gerbils as reported in previous studies (Jacobs & Deegan, 1994). Thresholds for achromatic and chromatic contrast discrimination tended to be lower than for intensity discrimination. This could be expected because, for intensity discrimination, intensities had to be compared across the arms of the maze whereas, in the contrast tasks, the primary comparison was between the stimulus patches and their immediate background.

Stimuli in our experiments were generated using a standard projector designed for human vision. Such a system achieves only marginal stimulation of gerbil S cones, whose sensitivity range lies at much shorter wavelengths than those of human S cones. Thus, although the relative differences, i.e., contrasts, were the same for S cones and M cones in the experiments, overall stimulation was estimated to be orders of magnitude lower for S cones than for M cones (Table S1). Nevertheless, the animals were able to make the spectral discriminations. It is conceivable that the gerbil S cones are actually more sensitive at their long-wavelength tails than indicated by the published spectral sensitivity curves (Jacobs & Deegan, 1994). Those curves, derived from templates (Dawis, 1981) going back to the Dartnall (1953) nomogram, provide accurate estimates of spectral sensitivity around the peak, but are notoriously unreliable for estimating the tails (Dawis, 1981). In particular, for spectral sensitivity curves peaking in the short-wavelength range, the width tends to be underestimated (Dawis, 1981). Moreover, the long-wavelength tail of the gerbil S cone log spectral sensitivity is just an extrapolation by a straight line (Jacobs & Deegan, 1994), which is a very coarse approximation. Even small changes in the slope of this line lead to substantial increases in the estimates of S cone stimulation. It is therefore not unlikely that S cone stimulation in our experiments was actually higher than estimated based on the published spectral sensitivity curves.

Alternatively, a contribution of rod signals, which is feasible in dichromat color vision (Kremers & Meierkord, 1999; Montag & Boynton, 1987; Reitner, Sharpe, & Zrenner, 1991), could underlie the discrimination performance of the animals. In any case, the performance exhibited by the gerbils in our experiments demonstrates the ability of these animals to make judgments based on relative spectral composition of the stimuli.

Given potential uncertainties in the cone spectral sensitivities, a concern could be that our estimates of cone excitations were imprecise such that the color

stimuli we used actually also contained brightness cues. We therefore calculated how far the M cone spectrum would have to be shifted toward longer wavelengths to make the bright −G+B stimuli darker than the dark +G−B stimuli, in which case it would have been possible to solve the task based on brightness cues. We found that such an intensity inversion would require a shift of the M cone sensitivity by more than 30 nm, which we consider unrealistic.

Further evidence that discrimination was based on spectral content and not brightness is provided by the initial behavior of the animals in the color task. In the preceding experiment, two of the animals had learned to choose the brighter stimulus; two had learned to choose the darker stimulus. If a brightness cue existed in the chromatic task, that is, either −G+B or +G−B were correlated with brightness, one would expect that two of the animals would have directly been able to solve the task. However, all animals had to relearn (Figure S4A), confirming that they could not rely on brightness to solve the task.

Behavioral analysis

Our approach allows for detailed analyses to determine psychophysical properties such as discriminability thresholds and lapse rates for the specific tasks. In trained animals, thresholds were comparable across individuals and tasks. Lapse rates did not differ strongly, indicating that the difficulty of the tasks was similar for all animals. We described the psychometric data using two different approaches: (a) psychometric function fitting (Kuss et al., 2005; Wichmann & Hill, 2001) and (b) choice modeling (Busse et al., 2011; Carandini & Churchland, 2013; Gold, Law, Connolly, & Bennur, 2008). Lapse rates depended on the arm on which the target stimulus was presented and could be attributed to biases due to preferences for choosing one of the arms in our maze. This was revealed because we tested over a rather wide range of contrasts that always included stimuli at which performance saturated. Therefore, arm preferences dominated the stimulus-independent contributions to choice behavior in our experiments and may thus explain why previous choices had negligible effects on the current choice, compared to what has been reported by others (Busse et al., 2011; Lau & Glimcher, 2005).

Analyzing the learning dynamics for the individual tasks, we were able to show how the initial preferences for one side of the Y maze across all animals disappeared with learning but reappeared when stimuli became harder to differentiate (i.e., at lower contrasts), indicating that the animals may have applied different strategies depending on their confidence about the stimulus. Such biases between influence from sensory

cues and internal preferences are well known for choice behavior (Busse et al., 2011; Gold et al., 2008).

VR with rodents

Since the first reports of successful application of VR for rodents (Dombeck, Khabbaz, Collman, Adelman, & Tank, 2007; Hölscher et al., 2005), VR setups became very popular. This popularity is due to the fact that VR setups allow for the use of advanced recording techniques in behaving animals, such as intracellular recordings (Domnisoru, Kinkhabwala, & Tank, 2013; Harvey et al., 2009) or optical imaging of populations of neurons (Harvey, Coen, & Tank, 2012; Keller, Bonhoeffer, & Hübener, 2012). The behavioral paradigms in use, however, are usually very limited compared to what is standard in psychophysics even with rodents (Carandini & Churchland, 2013). Nevertheless, 2AFC tasks were implemented before with rodents on a treadmill (Harvey et al., 2012; Thurley et al., 2014), but so far, no psychometric data were measured. The present study is the first that successfully determined discrimination thresholds in VR with rodents.

Conclusions

Brightness and color constancy and contextual influences on neural processing as potential underlying mechanisms have been investigated in primate (Locke, 1935; Wachtler, Sejnowski, & Albright, 2003) and nonprimate mammalian species (MacEvoy & Paradiso, 2001) but so far not in rodents. Our results show that Mongolian gerbils can perform visually guided behavior that requires judgments of stimuli in relation to their visual context and thus provide first evidence for the capability of brightness and color constancy in rodents.

Moreover, with the present study, we presented a psychophysical paradigm that can be used with rodents to investigate perceptual performance in behaviorally relevant tasks.

Keywords: virtual reality, gerbil vision, color vision, perceptual constancy

Acknowledgments

*CG and JH contributed equally to this article.
Commercial relationships: none.
Corresponding authors: Kay Thurley; Thomas Wachtler.
Email: thurley@bio.lmu.de; wachtler@bio.lmu.de.
Address: Department Biologie II, Ludwig-Maximilians-Universität, München, Germany.

References

Albrecht, D. G., & Hamilton, D. B. (1982). Striate cortex of monkey and cat: Contrast response function. *Journal of Neurophysiology, 48*(1), 217–237.

Busse, L., Ayaz, A., Dhruv, N. T., Katzner, S., Saleem, A. B., Schölvinck, M. L., . . . Carandini, M. (2011). The detection of visual contrast in the behaving mouse. *Journal of Neuroscience, 31*(31), 11351–11361.

Carandini, M., & Churchland, A. K. (2013). Probing perceptual decisions in rodents. *Nature Neuroscience, 16*(7), 824–831.

Dartnall, H. J. A. (1953). The interpretation of spectral sensitivity curves. *Br. Med. Bull, 9,* 24–30.

Dawis, S. M. (1981). Polynomial expressions of pigment nomograms. *Vision Research, 21,* 1427–1430.

Dombeck, D. A., Khabbaz, A. N., Collman, F., Adelman, T. L., & Tank, D. W. (2007). Imaging large-scale neural activity with cellular resolution in awake, mobile mice. *Neuron, 56*(1), 43–57.

Domnisoru, C., Kinkhabwala, A. A., & Tank, D. W. (2013). Membrane potential dynamics of grid cells. *Nature, 495*(7440), 199–204.

Dörr, S., & Neumeyer, C. (2000). Colour constancy in the goldfish: The limits. *Journal of Comparative Psychology A, 186,* 885–896.

Foster, D. H. (2011). Color constancy. *Vision Research, 51,* 674–700.

Foster, D. H., & Nascimento, S. M. C. (1994). Relational colour constancy from invariant cone-excitation ratios. *Proceedings of the Royal Society B, 257,* 115–121.

Fründ, I., Haenel, N. V., & Wichmann, F. A. (2011). Inference for psychometric functions in the presence of nonstationary behavior. *Journal of Vision, 11*(6):16, 1–19, http://www.journalofvision.org/content/11/6/16, doi:10.1167/11.6.16. [PubMed] [Article]

Gold, J. I., Law, C.-T., Connolly, P., & Bennur, S. (2008). The relative influences of priors and sensory evidence on an oculomotor decision variable during perceptual learning. *Journal of Neurophysiology, 100*(5), 2653–2668.

Govardovskii, V. I., Röhlich, P., Szél, A., & Khokhlova, T. V. (1992). Cones in the retina of the Mongolian gerbil, *Meriones unguiculatus*: An immunocytochemical and electrophysiological study. *Vision Research, 32*(1), 19–27.

Harvey, C. D., Coen, P., & Tank, D. W. (2012). Choice-specific sequences in parietal cortex during a virtual-navigation decision task. *Nature, 484*(7392), 62–68.

Harvey, C. D., Collman, F., Dombeck, D. A., & Tank, D. W. (2009). Intracellular dynamics of hippocampal place cells during virtual navigation. *Nature, 461*(7266), 941–946.

Hölscher, C., Schnee, A., Dahmen, H., Setia, L., & Mallot, H. A. (2005). Rats are able to navigate in virtual environments. *Journal of Experimental Biology, 208*(Pt. 3), 561–569.

Hunter, J. D. (2007). Matplotlib: A 2D graphics environment. *Computing In Science & Engineering, 9*(3), 90–95.

Hurlbert, A., & Wolf, K. (2004). Color contrast: A contributory mechanism to color constancy. *Progress in Brain Research, 144,* 147–160.

Jacobs, G. H., & Deegan, J. F., II. (1994). Sensitivity to ultraviolet light in the gerbil (*Meriones unguiculatus*): Characteristics and mechanisms. *Vision Research, 34*(11), 1433–1441.

Jacobs, G. H., & Neitz, J. (1989). Cone monochromacy and a reversed Purkinje shift in the gerbil. *Experientia, 45*(4), 317–319.

Keller, G. B., Bonhoeffer, T., & Hübener, M. (2012). Sensorimotor mismatch signals in primary visual cortex of the behaving mouse. *Neuron, 74*(5), 809–815.

Kraft, J. M., & Brainard, D. H. (1999). Mechanisms of color constancy under nearly natural viewing. *Proceedings of the National Academy of Sciences, USA, 96,* 307–312.

Kremers, J., & Meierkord, S. (1999). Rod-cone-interactions in deuteranopic observers: Models and dynamics. *Vision Research, 39,* 3372–3385.

Kuss, M., Jäkel, F., & Wichmann, F. A. (2005). Bayesian inference for psychometric functions. *Journal of Vision, 5*(5):8, 478–492, http://www.

journalofvision.org/content/5/5/8, doi:10.1167/5.5.8. [PubMed] [Article]

Lau, B., & Glimcher, P. W. (2005). Dynamic response-by-response models of matching behavior in rhesus monkeys. *Journal of the Experimental Analysis of Behavior, 84*(3), 555–579.

Locke, N. M. (1935). Color constancy in the rhesus monkey and in man. *Archives of Psychology 193*.

MacEvoy, S. P., & Paradiso, M. A. (2001). Lightness constancy in primary visual cortex. *Proceedings of the National Academy of Sciences, USA, 98*(15), 8827–8831.

Montag, E. D., & Boynton, R. M. (1987). Rod influence in dichromatic surface color perception. *Vision Research, 27,* 2153–2162.

Pietrewicz, A. T., Hoff, M. P., & Higgins, S. A. (1982). Activity rhythms in the Mongolian gerbil under natural light conditions. *Physiology & Behavior, 29*(2), 377–380.

Reitner, A., Sharpe, L. T., & Zrenner, E. (1991). Is colour vision possible with only rods and blue-sensitive cones? *Nature, 352,* 798–800.

Seabold, J., & Perktold, J. (2010). Statsmodels: Econometric and statistical modeling with Python. In S. van der Walt & S. Millman (Eds.), *Proceedings of the 9th Python in Science Conference* (pp. 57–61). June 28–July 3, 2010, Austin, Texas.

Thurley, K., Henke, J., Hermann, J., Ludwig, B., Tatarau, C., Wätzig, A., . . . Leibold, C. (2014). Mongolian gerbils learn to navigate in complex virtual spaces. *Behavioural Brain Research, 266,* 161–168.

Wachtler, T., Sejnowski, T. J., & Albright, T. D. (2003). Representation of color stimuli in awake macaque primary visual cortex. *Neuron, 37*(4), 681–691.

Wichmann, F. A., & Hill, N. J. (2001). The psychometric function: I. Fitting, sampling, and goodness of fit. *Perception & Psychophysics, 63*(8), 1293–1313.

4

Discussion

4.1 Rh1 is necessary to explain wavelength discrimination in Drosophila

In this work, I have explored the role of the rhodopsins in Drosophila color vision. I have predicted wild-type wavelength discrimination, by fitting models of opponent processing to published behavioral data. I have found that only models that incorporated the spectral information from rh1 fitted the data well. The major components of these better fits were a poor discrimination around 470 nm and an improvement in discrimination towards shorter and most importantly towards longer wavelength at around 500 nm. As rh1 is the only opsin that increased its absolute spectral slope between 470 nm and 500 nm, I concluded that this increase in discrimination - supported by two data-points - could only be explained by incorporation of rh1.

4.1.1 Contribution of the different opsins

To analyze the contributors to Drosophila wild type wavelength discrimination, I have fitted many potential rhodopsin combinations to existing data on Drosophila wavelength discrimination (Hernandez de Salomon and Spatz, 1983). From these, I determined the best fitting opponent models that either included or did not contain rh1. The well-fitting models all

made use of spectral information from rh1. Furthermore, the opsin that contributed most to these fits was rh6, directly followed by rh1. The rh1-rh6 opponency together with the rh6-rh4 opponency already explained most of the data and the inclusion of other mechanisms did not improve the fits but rather made them worse.

The reason for this can be found in the spectral profiles of the opponent mechanisms (see Paper 2 Figure 1). The only mechanism that had a maximum in the slope near 500 nm, where the data indicate good wavelength discrimination in the fly, was the rh1-rh6 opponency. For shorter wavelengths, around 470 nm, the behavioral data suggested a lower discrimination, requiring a lower slope, as exhibited by the rh1-rh6 mechanism.

Another increase in discrimination at even shorter wavelengths is also supported by the rh1-rh6 opponency. Above 500 nm, the data indicated a sharp decline in discriminability. This decrease is well explained by a reduction in the slope of the rh4-rh6 opponency. This mechanism also contributes to the increase in discriminability between 470 nm and 400 nm. Thus, a combination of the two opponent mechanisms, rh4-rh6 and rh1-rh6, already explains the data quite well.

4.1.2   Transformations of the behavioral data

Because there is some freedom in the derivation of a quantitative estimate of wavelength discriminability, the method of analysis of the behavioral data might have had an influence on the outcome. Therefore, I analyzed in detail whether changes in the assumptions underlying the derivation of behavioral wavelength discrimination data would affect the results.

I found that another data transformation resulted in a discrimination function that is less complex than the function obtained by the original transformation. Besides the reduction in the number of data points, the discrimination function indicates one region of good discrimination in the short wavelength range and one region of poor discrimination in the long wavelength range, with a rather steep transition. While, also for this transformed data, the best fitting model was a model with rh1, basically all fits

were poor. Thus, the other data transformation leads to $\delta\lambda$ estimates that can hardly be explained by a linear combination of the rhodopsin spectral sensitivity slopes. This clearly argues for using the original transformation to derive wavelength discrimination functions, at least in cases where the conditioning index functions are rather asymmetric concerning the reference wavelength.

4.1.3 Behavioral genetics supports a role of rh1

In cooperation, we have also tested the role of rh1 in behavioral experiments. In flies that had been genetically modified such that only a subset of photoreceptor cells would transduce signals, we found that fruit flies can discriminate stimuli based on chromatic differences even when only signals originating from rh1 and a single other opsin are present (Schnaitmann et al., 2013). This implied that rh1 must be used for color vision in the fruit fly.

In our experiments, the flies had been trained to associate either a blue or a green stimulus with a sugar reward. In a test condition the intensities of the green and blue stimulus were exchanged (see Figure. 2.6). As the flies still choose the stimulus with the conditioned color, we successfully demonstrated their ability to discriminate the stimuli based on color. The interpretation of his experiments critically depended on the inversion of the flies "brightness" perception of the stimuli. We, therefore, tested the relative signal strength of our stimuli in closed loop erg experiments, where we estimated the relative brightness of the stimuli by changing their intensity until they produced the same signals. This was performed for wild-type flies, flies with signals from individual rhodopsins only, and with dichromatic flies as used in the behavioral experiments. All recordings demonstrated that, at least from a retina perspective, our stimulation did indeed rule out brightness as a source of information for the flies and that they had discriminated the stimuli due to their spectral composition.

4.1.4 Statistic of natural reflectance spectra

I have established that the fruit fly does use signals from rh1 for color vision, yet, the usefulness of having five receptors for color vision can, as introduced above (see Chapter 2.6), be taken into question. Therefore, I analyzed a large set of natural reflectance spectra from an online database (Arnold et al., 2010).

I demonstrated that in the range around 500 nm, where I have found that rh1 is necessary to explain wild-type wavelength discrimination, information about spectra identity is available and that the receptor best suited to extract this information is rh1. In an additional theoretical analysis of the natural reflectance spectra in the frequency domain, I determined the number of receptor types that would suffice to approximate the data acceptably. I found that it would be sufficient to sample changes in reflectance that have a cycle length of 100 nm. Considering the sampling theorem (Kotel'nikov, 2006) and by assuming a visual range of 300 nm to 550 nm, I concluded that five receptors, evenly spaced 50 nm apart from each other (eg., with peaks at 325 nm, 375 nm, 425 nm, 475 nm, 525 nm) would perfectly sample the natural data variability.

Based on mutual information (Lewis and Zhaoping, 2006), I quantified the amount of information in the signals from rh1 and quantified the redundancy of this information with respect to the information from the other opsins. This analysis indicates that rh1 is the second most informative Drosophila opsin. In general, there is a trend that the more sensitive a receptor type is for long wavelengths, the higher is its mutual information. The differences of informational value in the four receptor systems are not very significant and the addition of rh1 to the traditional four-receptor system increases the information by only 7%. Compared to the information added when moving from three to four receptors, this seems not particularly significant. However, it is substantial considering that the fifth principle component accounts for only 3% of the variability in the data. The important aspect is that rh1 contributes information, even when considering that rh1 is highly correlated with both rh5 and rh6.

4.1.5 Comparison to established theories

My findings directly contradict the standard model of visual processing in dipteran (see above Chapter 2.4 Figure 2.8b). Interestingly, this standard model, which to some degree is implied by the anatomy, has little support regarding behavioral data. The study that is typically cited as experimental proof of the "two separate systems" theory is the study by Troje (1993), who as argued above, was rather careful when interpreting his findings (see Chapter 2.4). There are several prominent and also subtle differences between the data used in that study and the data I used. Like the data from Hernandez de Salomon and Spatz (1983), the results by Troje (1993) indicate good discrimination around 500 nm. Besides the difference that the model by Troje (1993) tries to predict the learning curves directly, whereas our models predict the wavelength discrimination function, given the similarities in the data, why do the results differ?

The critical difference lies in the spectral sensitivity functions used. In particular the rh6 spectral sensitivity function that we used, which was directly measured in Drosophila (Salcedo et al., 1999), is broader than the one used by Troje (1993, see Figure 1), which was measured in Musca (Hardie and Kirschfeld, 1983). This rh6 function has an absolute slope change in the region between 470 nm and 500 nm. It is likely that with the Drosophila rh6 spectral sensitivity the results by Troje (1993) would have been different.

A strong argument against using signals from the outer receptors has been that they are equipped with an accessory pigment which makes them sensitive in the UV range and practically gives them a two peaked sensitivity (Troje, 1993). Such an activity profile is not optimal for unambiguous spectral discrimination. In the yellow ommatidia of musca, however, this pigment is also present in the inner receptors. Whether this is the case for Drosophila is ambiguous, however, a functional coupling in yellow ommatidia has been reported in some studies (Salcedo et al., 2003, 1999).

My results suggest that rh1, rh4, and rh6 are needed to explain the wild-type wavelength discrimination, which interestingly are precisely the opsins

expressed in the yellow ommatidia where also the inner receptors might have an accessory pigment. Assuming an opponent processing, where the signals are subtracted from each other and by considering that the signals from the UV pigment would be the same in all receptors, this UV sensitivity could cancel out (see Figure 4.1c) and unambiguous color discrimination could be achieved.

4.1.6   Does color vision matter in Drosophila

It is a critical question whether color vision plays a role in Drosophila at all (Lunau, 2014). While the ability to discriminate stimuli based on spectral comparisons is well established within fruit flies (Menne and Spatz, 1977), they are nevertheless hard to train to such stimuli (Schnaitmann et al., 2013). Even if they can be trained to learn a color discrimination task, the success rate is not very high (Schnaitmann et al., 2013) and reported quantitative data on wavelength discrimination indicates performances which are poor (Hernandez de Salomon and Spatz, 1983) when compared to other animals (Helversen, 1972). Some studies have specifically argued that Drosophila is not optimal to study color vision, as there is no observed behavior where the animals do rely on the trait (Troje, 1993, 1994). These studies, which have often been cited as evidence against a role of rh1, have therefore analyzed color discrimination in goldflies, where indeed it is known that the females make use of spectral information during oviposition (Troje, 1993, 1994). From that perspective, it is imaginable that the findings presented here, are indeed limited to Drosophila and that they do not generalize whatsoever. To analyze the role of rh1 even further, it would certainly be interesting to do behavioral studies on other dipteran species, so far, however, such data is not available, and the author does not wish to claim anything concerning rh1 in any species other than Drosophila.

(a)
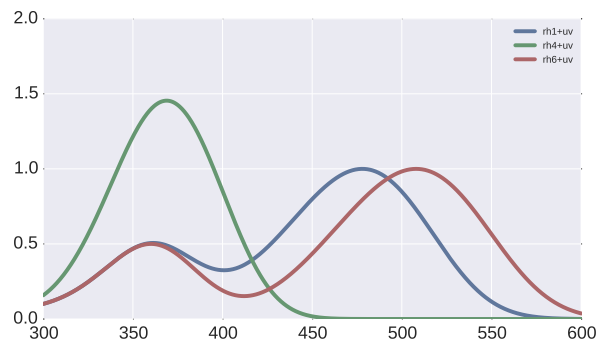
(b)
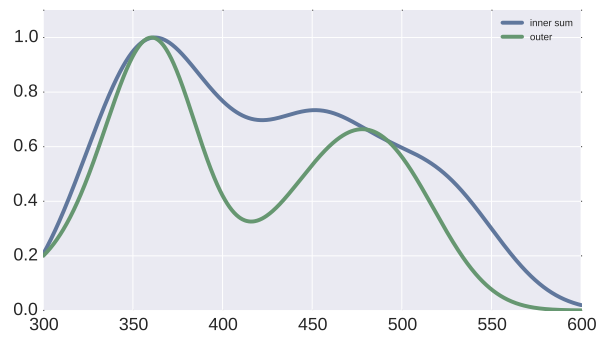
(c)
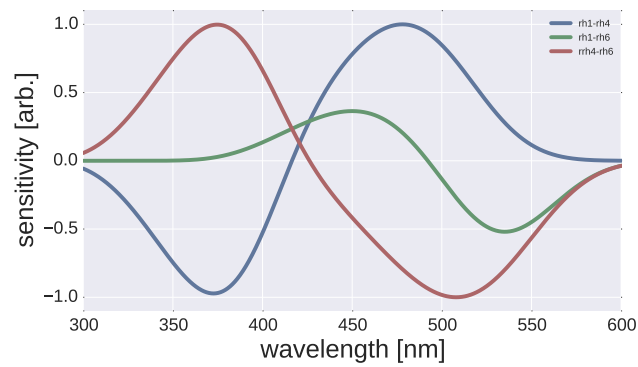
Figure 4.1: Hypothetical inclusion of he UV pigment: (a) shows idealized spectral profiles of the inner receptors in the yellow ommatidia (rh4, rh6) and in the outer receptors assuming the uv-pigment is present. (b) shows the spectral profile of the sum of inner receptors (rh3-rh6) and the spectral profile of the outer receptors. Due to the UV-pigment, the outer receptors roughly signal the envelope of the sum of the inner signals. (c) shows the idealized spectral profiles of an opponent comparisons between receptors from yellow ommatidia and outer receptors. In this configuration the UV pigment cancels out.

4.1.7 Mammalian rods and insect outer photoreceptors

The difference between outer and inner receptor types, as found in many invertebrates, is often directly compared to the human rods and cones difference respectively (Pichaud, Briscoe, and Desplan, 1999; Strausfeld and Lee, 1991) ((see Chapter 4.2.5) for details on rod and cone differences). As in both cases, a separation into different functional roles (motion vision vs. color vision) was anticipated, a comparison seemed to be suggestive. However, neither do the outer receptor types saturate in bright light as the rods do nor do the cones not contribute to motion vision. Furthermore, my results provide strong evidence for a role of outer receptors in color vision and other works (Wardill et al., 2012) have demonstrated a participation of inner photoreceptors in motion vision. Both findings argue strongly against a clear receptor-based separation.

In mammals signals from the retina feed into two prominent pathways. The first pathway, the so-called Magnocellular path (MC), combines signals from rods and cones (see Chapter 4.2.5 for more details on mammal photoreceptors) and is used for low acuity vision under low light or semi-dark conditions as well as for motion vision. As it just pools information from the photoreceptors, it is believed to be "color blind." The second pathway, the Parvocellular path (PC), which is mainly used to convey information from the cones, is used both for high acuity vision and, as it compares signals from different cone types, for color vision (Rodieck, 1998).

As sketched above, in mammals, the pathways are the critical determinants of function and not the receptors that feed into them. The same might be true in invertebrates or more specifically in Drosophila.

In Drosophila the outer photoreceptors, unlike the inner photoreceptors, terminate in the lamina neuropil. The three lamina monopolar cells (LMCs; L1, L2, and L3) convey the outputs of the outer photoreceptors directly to different layers of the medulla, where visual information of inner and outer photoreceptors converge (Fischbach and Dittrich, 1989; Meinertzhagen and O'Neil, 1991). This convergence is a possible location
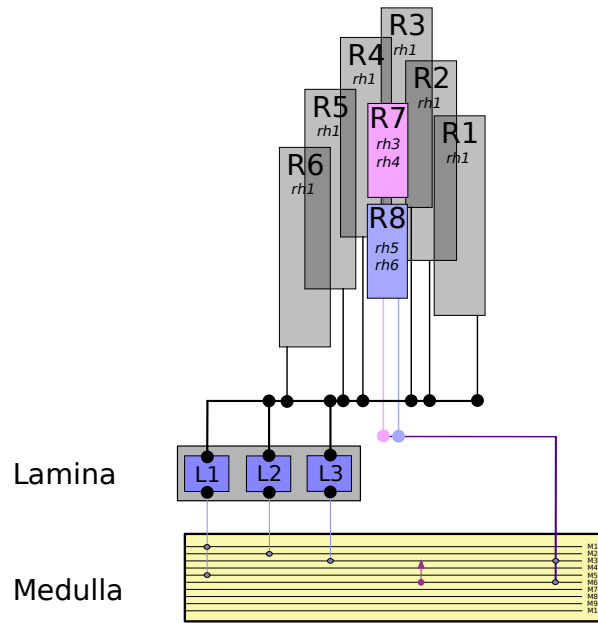
Figure 4.2: Convergence of signals from outer and inner receptors in the medulla: The outer receptors terminate in the Lamina Monopolar cells (L1-3), which in turn project to different parts (black lines M1-M10) of the medulla. The inner receptors do project directly to the medulla, where in turn a comparison of signals could be achieved.

where the signals of the inner and outer receptors might be combined for motion vision and compared for color vision (see Figure 4.2). A comparison between the two mammalian pathways (magno and parvocellular) and different potential paths through lamina and medulla might be a better comparison, than the analogy between rods vs. cones and outer vs. inner photoreceptors.

4.1.8 Conclusions

I have demonstrated that the behavioral data on wavelength discrimination in Drosophila can only be explained by incorporating rh1. This result is mainly due to an increase in discrimination around 470 nm and 500 nm which directly relates to the spectral sensitivity of the rh1 opsin. We corroborated a potential role for rh1 with tests in genetically modified dichromatic flies.

Furthermore, I showed that a model comparing signals from rh1, rh6,

and rh4 already provides a good explanation of the discrimination behavior of the wild type fly. Concerning the encoding of natural reflectance spectra, the spectral positioning of rh1 is not optimal for discrimination. The power spectral density of natural spectra indicates that five receptor spectral sensitivities would be optimal for the visual range of Drosophila. However, this argument is based on the assumption of an equidistant sampling of the spectrum with rather broad receptoral functions located roughly fifty nanometer apart, which is not the case in Drosophila. Furthermore, the double-peaked nature of the sensitivity of the rh1 containing receptors renders them sub-optimal for unambiguous spectral discrimination (Troje, 1993).

Whether color vision is important for Drosophila at all is an open question (Lunau, 2014), but the behavioral data indicate a role for rh1 when color discrimination is tested, and my theoretical analysis of natural reflectance data shows that there is information in the signals of a fifth opsin in general and rh1 in particular.

4.2 Visual constancy in Gerbils

Using a virtual reality paradigm, I have investigated the gerbils ability to select stimuli based on local contrast, i.e., relative to a local background both for achromatic and chromatic stimuli.

4.2.1 Lightness constancy

First, I tested whether gerbils were able to select stimuli based on their intensity relative to the immediate surround. In this experiment, the animals had to compare stimuli consisting of a central uniform stimulus patch on a background. To exclude that the animals used absolute intensity as a cue, two sets of stimulus pairs with different absolute intensity levels were used. Thus, to achieve above chance performance, the animals had to learn to either choose the side with the relatively "darker" or the relatively "lighter" stimulus.

Furthermore, to control for memorization artifacts (see below) and to estimate the discrimination threshold, unknown stimuli of lower contrast were interspersed into the stimulation once the animals seemed to have learned the task.

All animals successfully learned to discriminate the stimuli thus demonstrating their ability for lightness constancy.

4.2.2 Color constancy

In the second set of experiments, half of the animals had to choose stimuli where the stimulus patch color was shifted towards the green projector primary relative to the background. The other animals had to choose a side where the test patch color was shifted towards the blue primary. Sets of stimuli with different absolute intensity levels were used such that neither strategies based on achromatic contrast nor strategies based on absolute cone excitation would lead to above chance performance.

The animals successfully learned to identify the correct patches and their performance was significantly above chance. Thus, I have demonstrated that gerbils can identify a stimulus based on its local spectral contrast. As such contrasts are strong cues used to achieve color constancy I have furthermore shown that gerbils have all prerequisites needed for color constant object recognition.

4.2.3 Memorization does not explain the animals behavior

It is conceivable that the animals had just memorized all stimuli sets. However, to determine discrimination thresholds, I systematically altered the intensity and color settings during the experiments. This introduced variability to the stimuli sets used and gave me the ability to validate, whether such a confounding "memorization" strategies were used. It turned out that even for new stimuli the animals performed on a stable above chance level from beginning on. This provides substantial evidence that the ani-

mals did generalize a learned strategy and did not simply memorize stimuli.

4.2.4   Sub-optimal stimulation

Our experiments were done using a projector designed for human vision. As the gerbil s-cone sensitivity range lies at much shorter wavelengths than those of human s-cones, such a system does only provide very little s-cone stimulation for the gerbil. This does not affect relative differences, i.e., contrasts were the same for s-cones and m-cones in the experiments, however, the magnitude of estimated s-cone stimulation was by orders of magnitude lower for s-cones than for m-cones.

How did the animals do this discrimination nevertheless? It is possible that the gerbil s-cones are more sensitive at their long-wavelength tails than indicated by the published spectral sensitivity curves (Jacobs and Deegan II, 1994). Those curves, derived from templates (Dawis, 1981) going back to the Dartnall (1953) nomogram, provide accurate estimates of spectral sensitivity around the peak, but are notoriously unreliable for estimating the tails (Dawis, 1981). In particular, for spectral sensitivity curves peaking in the short-wavelength range, the width tends to be underestimated (Dawis, 1981). Moreover, the long-wavelength tail of the gerbil s-cone spectral sensitivity is just an extrapolation by a straight line in log space (Jacobs and Deegan II, 1994). I estimated that even small changes in the slope of this line lead to substantial increases in the estimates of s-cone stimulation. It is therefore not unlikely that s-cone stimulation in our experiments was higher than estimated based on the published spectral sensitivity curves. Furthermore, based on a rough assumption on the gerbil visual system and using photon catch, we quantified the theoretical stimulation and found that even this marginal stimulation was in a range typically thought to be detectable in humans.

4.2.5   Rod assisted color vision

In 1812, the Czech anatomist Jan Evangelista Purkyně discovered a fundamental principle of human visual perception. During one of his long walks

in the flower-rich fields of his Bohemian homeland, he had noticed that the red petals of some his favorite flowers (Geranium), while exposed to the bright sunlight of the afternoon, appeared brighter than the surrounding greenish foliage. However, at dawn, when the sun had faded (i.e., when all the proverbial cats become gray), the petals looked comparable darker than the green parts of the flowers. This effect, which is named Purkyně-shift in honor of its discoverer, happens because human vision (and for that matter the vision of all mammals) operates in different modes at different intensity levels. Both modes are maximally sensitive to light of different wavelength (Rodieck, 1998). The first operates under daylight conditions (photopic vision) and is maximally sensitive to long wavelength light. The other mode, optimized for low light vision (scotopic vision), is maximally sensitive to wavelengths at 500 nm. Therefore, Purkyněs perceived the reddish petals as brighter than the green foliage under photopic vision while this relationship reversed when he used scotopic vision.

The effect can be understood even better (as Purkyně had anticipated) by looking to the typical mammalian retina, which is equipped with two photoreceptor subtypes the so-called rods and cones. These two receptor subtypes are not only phylogenetically separated; there are strong morphological, physiological, and functional differences. Rods are smaller than cones and they are by far the more frequent receptor type (Rodieck, 1998). Their relative number increases the more nocturnal an animal species is, and they are typically differentially expressed in different parts of the retina (Heldmaier, Neuweiler, and Rössler, 2012). For example, in humans (which have a rather diurnal lifestyle), rods are 20 times more frequent than cones, but in the fovea, which is the retinal spot of highest visual acuity, is practically rod free (Basbaum, 2007). Most importantly, at least in this context, rods are very sensitive under scotopic light conditions and saturate as soon as the illumination becomes photopic. Cones, on the other side, are not sensitive enough to reliably signal under low light conditions but are still operational when the rods have saturated under photopic conditions (Rodieck, 1998). This difference explains the Purkyně-shift. Under scotopic conditions, vision is mainly driven by the rods and therefore green

foliage appears brighter than red petals. Under photopic conditions, the cones take over, and as their spectral sensitivity is shifted towards longer wavelength, petals now look brighter than the foliage.

As the rods are mainly operational under such rather scotopic conditions and because they have been shown to stop signaling under bright light in laboratory experiments (Schneeweis and Schnapf, 1995), they are typically assumed to play no role in mammalian color vision. There is however evidence that would support a role of rods in color vision as exemplified in human and other primate dichromats (Montag and Boynton, 1987; Reitner, Sharpe, and Zrenner, 1991; Kremers and Meierkord, 1999). Strong arguments for a rod input to color channels come from neuroanatomy and electrophysiology.

Connections from rods to the cones via electric junctions and/or amacrine cells have been documented in the trichromatic macaque retina, where rods and cones share visual pathways to the brain (Dacheux and Raviola, 1986; Daw, Jensen, and Brunken, 1990; Wässle, H et al., 1991; Schneeweis and Schnapf, 1995) and neuronal connections from rods to both magnocellular and parvocellular pathways (see above Chapter 4.1.7) do exist (Gouras and Link, 1966; Grünert, 1997). However, electrophysiological studies in trichromatic animals (*Macaca fascicularis*) have only found significant rod input to the MC pathway (Gouras and Link, 1966; Wiesel and Hubel, 1966; Lee et al., 1990; Purpura et al., 1990). On the other hand, in the dichromatic marmosets (*Callithrix jacchus*), rod influence in parvocellular cells was found to be strong, up to high levels of retinal illuminance (Weiss, Kremers, and Maurer, 1998).

Furthermore, the ability for color vision has been observed in cone monochromatic aquatic mammals (Griebel and Schmid, 1992; Griebel and Peichl, 2003; Oppermann, Schramme, and Neumeyer, 2016). As these animals have only one cone type, a situation comparable to the situation with our genetically engineered flies, such abilities practically must rely on a comparison between rod and cone signals.

If differential rod information could be extracted, maybe in a scheme involving differential coding in on and off cell types (Garbers, Wachtler,

and Hertel, 2011), a rod assisted color vision would be feasible also in gerbils. Such a use of rod signaling could also explain my findings, but the contrast between rod cells and gerbil m-cones, for the stimuli used, would be rather small. Color vision using rods, even with small rod-cone contrasts, however, has been reported recently (Oppermann, Schramme, and Neumeyer, 2016).

4.2.6 Context and behavior

Constancy effects are not limited to vision. Certainly color (Garbers et al., 2015; Balkenius and Kelber, 2004; Neumeyer et al., 2002; Dörr and Neumeyer, 2000; Kinoshita and Arikawa, 2000; Walsh et al., 1993; Braaten and Hulse, 1991; Wild et al., 1985; Locke, 1935), size (Gunter, 1951; Heller, 1968; Humphrey and Weiskrantz, 1969; Douglas, Eva, and Guttridge, 1988) and lightness (Wallach, 1948; Campenhausen, 1986; MacEvoy and Paradiso, 2001; Garbers et al., 2015) constancy have earned most attention in animal experiments, however constancy phenomena have also been demonstrated with particular auditory stimuli (Braaten and Hulse, 1991).

In humans, numerous constancy effects are known and exploits build on them are encountered by us on a daily basis. For example in supermarkets, expensive products are placed such that mid-priced products seem to be more desirable in context of their expensive counterparts. In cognitive psychology, such context effects are a focus of research and Bayesian inference is typically used to explain how they do emerge (Goldreich and Peterson, 2012; Lloyd and Leslie, 2013). In general, the usage of both, sensory data and prior knowledge to reach an optimal behavior, is the central idea in optimal probabilistic reasoning (Goldreich and Peterson, 2012; Lloyd and Leslie, 2013; Petzschner and Glasauer, 2011), and it is not surprising that such reasoning has also been used in conjunction with color vision (Brainard and Freeman, 1997).

Indeed it has turned out that the information the brain receives, about a visual scene, is not abundant enough to determine the illumination unambiguously, and therefore unambiguous color constancy is also impossible

to achieve with the information the brain gets from just one scene. In such cases, Bayesian reasoning has been demonstrated as a possible candidate to achieve color constancy in humans (Brainard and Freeman, 1997; Brainard and Maloney, 2004; Brainard et al., 2006). However, if this would also be possible with more complex, and maybe, even more, demanding more simple, visual systems is unknown. Such modeling, together with more behavioral experiments maybe in conjunction with clever genetic modifications and electrophysiological recordings, might help us to gain a better understanding of the mechanisms behind color constancy and even more important the machinery behind contextual effects in general.

4.2.7 Conclusions

In conclusion, brightness and color constancy, as well as contextual influences on neural processing as potential underlying mechanisms, have been investigated in primate (Wachtler, Sejnowski, and Albright, 2003) and non-primate mammalian species (MacEvoy and Paradiso, 2001), but so far not in rodents. My results show that Mongolian gerbils can perform a visually guided behavior that requires judgments of stimuli in relation to their visual context, and thus, provide first evidence for the capability of brightness and color constancy in rodents. They also demonstrate and showcase a paradigm where such abilities can be tested for using virtual environments.

References

Arnold, S. E. J., Faruq, S., Savolainen, V., McOwan, P. W., and Chittka, L. FReD: The Floral Reflectance Database — A Web Portal for Analyses of Flower Colour. *Plos One*, 5:e14287, 2010.

Autrum, H. Carl v. Hess und der Aufbruch der vergleichenden Physiologie: Farbensinn und Farbensehen. *Albrecht von Graefes Archiv für Ophthalmologie*, 166:3, 1963.

Autrum, H. Das Farbensehen der Tiere Von Carl von Hess bis heute. *Klinische Monatsblätter für Augenheilkunde*, 197:191, 2008.

Autrum, H. and Zwehl, V. v. Die spektrale Empfindlichkeit einzelner Sehzellen des Bienenauges. *Zeitschrift für vergleichende Physiologie*, 48:357, 1964.

Balkenius, A. and Kelber, A. Colour constancy in diurnal and nocturnal hawkmoths. *Journal of Experimental Biology*, 207:3307, 2004.

Basbaum, A. I. *The Senses: A Comprehensive Reference, Six-Volume Set*. Academic Press, 1 edition, 2007.

Bauer, V. Über das Farbenunterscheidungsvermögen der Fische. *Pflüger's Archiv für die gesamte Physiologie des Menschen und der Tiere*, 133:7, 1910.

Bauer, V. Zu meinen Versuchen über das Farbenunterscheidungsvermögen der Fische. *Pflüger's Archiv für die gesamte Physiologie des Menschen und der Tiere*, 137:622, 1911.

Benshoff, H. M., Brainard, G. C., Rollag, M. D., and Lynch, G. R. Suppression of pineal melatonin in Peromyscus leucopus by different monochromatic wavelengths of visible and near-ultraviolet light (UV-A). *Brain research*, 420:397, 1987.

Braaten, R. F. and Hulse, S. H. A songbird, the European starling (Sturnus vulgaris), shows perceptual constancy for acoustic spectral structure. *Journal of Comparative Psychology*, 105:222, 1991.

Brainard, D. H. and Freeman, W. T. Bayesian color constancy. *Journal of the Optical Society of America A*, 14:1393, 1997.

Brainard, D. H., Longère, P., Delahunt, P. B., Freeman, W. T., Kraft, J. M., and Xiao, B. Bayesian model of human color constancy. *Journal of Vision*, 6, 2006.

Brainard, D. H. and Maloney, L. T. Perception of color and material properties in complex scenes. *Journal of Vision*, 4, 2004.

Braitenberg, V. v. Patterns of projection in the visual system of the fly. I. Retina-lamina projections. *Experimental Brain Research*, 3:271, 1967.

Breuninger, T., Puller, C., Haverkamp, S., and Euler, T. Chromatic Bipolar Cell Pathways in the Mouse Retina. *The Journal of Neuroscience*, 31:6504 , 2011.

Brown, P. and Wald, G. Visual pigments in human and monkey retinas. *Nature*, 200:37, 1963.

Cahan, D. *Hermann Von Helmholtz and the Foundations of Nineteenth-century Science*. University of California Press, Berkeley/Los Angeles/London, 1993.

Campenhausen, C. v. Photoreceptors, lightness constancy and color vision. *Naturwissenschaften*, 73:674, 1986.

Carrière, J. Memoirs: On the Eyes of Some Invertebrata. *Quarterly Journal of Microscopical Science*, 2:673, 1884.

Chang, L., Breuninger, T., and Euler, T. Chromatic Coding from Cone-type Unselective Circuits in the Mouse Retina. *Neuron*, 77:559, 2013.

Cole, G. R., Hine, T., and McIlhagga, W. Detection mechanisms in L-, M-, and S-cone contrast space. *Journal of the Optical Society of America A*, 10:38, 1993.

Dacheux, R. F. and Raviola, E. The rod pathway in the rabbit retina: a depolarizing bipolar and amacrine cell. *Journal of Neuroscience*, 6:331, 1986.

Dartnall, H. J. A. The Interpretation of Spectral Sensitivity Curves. *British Medical Bulletin*, 9:24, 1953.

Darwin, C. *On the various contrivances by which British and foreign orchids are fertilised by insects.* John Murray, London, 1862.

Darwin, C. *The effects of cross and self fertilisation in the vegetable kingdom.* John Murray, London, 1876.

Daumer, K. Reizmetrische Untersuchung des Farbensehens der Bienen. *Zeitschrift für vergleichende Physiologie*, 38:413, 1956.

Daw, N. W., Jensen, R. J., and Brunken, W. J. Rod pathways in mammalian retinae. *Trends in Neurosciences*, 13:110, 1990.

Dawis, S. M. Polynomial expressions of pigment nomograms. *Vision Research*, 21:1427, 1981.

De Valois, R. L. and De Valois, K. K. A multi-stage color model. *Vision Research*, 33:1053, 1993.

Douglas, R. H., Eva, J., and Guttridge, N. Size constancy in goldfish (Carassius auratus). *Behavioural Brain Research*, 30:37, 1988.

Dörr, S. and Neumeyer, C. Color constancy in goldfish: the limits. *Journal of Comparative Physiology A*, 186:885, 2000.

Fischbach, P. K.-F. and Dittrich, A. P. M. The optic lobe of Drosophila melanogaster. I. A Golgi analysis of wild-type structure. *Cell and Tissue Research*, 258:441, 1989.

Fischer, H. *Die Geschichte der Augenklinik zu Würzburg.* Universitäts-druckerei H. Stürtz, Würzburg, 1971.

Forel, A. *Das Sinnesleben der Insekten: eine Sammlung von experimentellen und kritischen Studien über Insektenpsychologie.* E. Reinhardt, München, 1910.

Foster, D. H., Amano, K., Nascimento, S. M. C., and Foster, M. J. Frequency of metamerism in natural scenes. *Journal of the Optical Society of America A*, 23:2359, 2006.

Frisch, K. v. Sind die Fische farbenblind. *Zoologische Jahrbucher Abteilung fuer Allgemeine Zoologie und Physiologie der Tiere*, 33:107, 1912.

Frisch, K. v. Weitere Untersuchungen über den Farbensinn der Fische. *Zoologische Jahrbucher Abteilung fuer Allgemeine Zoologie und Physiologie der Tiere*, 34:43, 1913a.

Frisch, K. v. Über den Farbensinn der Bienen und die Blumenfarben. *Münchener Medizinischen Wochenschrift*, pages 1–10, 1913b.

Frisch, K. v. Demonstration von Versuchen zum Nachweis des Farbensehens bei angeblich total farbenblinden Tieren. *Verhandlungen der deutschen Zoologischen Gesellschaft*, pages 50–58, 1914.

Frisch, K. v. *Erinnerungen eines Biologen.* Springer, Berlin, Heidelberg, New York, 3 edition, 1973.

Garbers, C., Henke, J., Leibold, C., Wachtler, T., and Thurley, K. Contextual processing of brightness and color in Mongolian gerbils. *Journal of Vision*, 15:13, 2015.

Garbers, C., Wachtler, T., and Hertel, R. A Model of human dichromat color vision that may help to explain the evolution of trichromacy. *Front. Comput. Neurosci. Conference Abstract: BC11 : Computational Neuroscience & Neurotechnology Bernstein Conference & Neurex Annual Meeting 2011.*, 2011.

Goethe, J. W. v. Zur Farbenlehre. 1810.

Goldreich, D. and Peterson, M. A. A Bayesian Observer Replicates Convexity Context Effects in Figure–Ground Perception. *Seeing and Perceiving*, 25:365, 2012.

Gouras, P. and Link, K. Rod and cone interaction in dark-adapted monkey ganglion cells. *The Journal of Physiology*, 184:499, 1966.

Govardovskii, V., Röhlich, P., Szel, A., and Khokhlova, T. Cones in the retina of the Mongolian gerbil,Meriones unguiculatus: an immunocytochemical and electrophysiological study. *Vision Research*, 32:19, 1992.

Griebel, U. and Peichl, L. Colour vision in aquatic mammals-facts and open questions. *Aquatic Mammals*, 29:18, 2003.

Griebel, U. and Schmid, A. Color vision in the California sea lion (*Zalophus californianus*). *Vision Research*, 32:477, 1992.

Grünert, U. Anatomical evidence for rod input to the parvocellular pathway in the visual system of the primate. *The European Journal of Neuroscience*, 9:617, 1997.

Guild, J. The colorimetric properties of the spectrum. *Philosophical Transactions of the Royal Society of London. Series A*, pages 149–187, 1932.

Gunter, R. Visual size constancy in the cat. *British Journal of Psychology. General Section*, 42:288, 1951.

Guth, S. L., Donley, N. J., and Marrocco, R. T. On luminance additivity and related topics. *Vision Research*, 9:537, 1969.

Guth, S. L., Massof, R. W., and Benzschawel, T. Vector model for normal and dichromatic color vision. *Journal of the Optical Society of America*, 70:197, 1980.

Göthlin, G. F. *Interaction of excitatory and inhibitory processes in the synthesis of the sensation of colour and of white.* Upsala Lek refurenings Furhandlingar, 1944.

Hardie, R. C. and Kirschfeld, K. Ultraviolet sensitivity of fly photoreceptors R7 and R8: Evidence for a sensitising function. *Biophysics of Structure and Mechanism*, 9:171, 1983.

Hassenstein, B. Modellrechnung zur Datenverarbeitung beim Farbensehen des Menschen. *Kybernetik*, 4:209, 1968.

Heldmaier, G., Neuweiler, G., and Rössler, W. *Vergleichende Tierphysiologie.* Springer Spektrum, 2 edition, 2012.

Heller, D. P. Absence of size constancy in visually deprived rats. *Journal of comparative and physiological Psychology*, 65:336, 1968.

Helmholtz, V. H. v. *Handbuch der physiologischen Optik.* 1860.

Helson, H. Some Factors and Implications of Color Constancy. *Journal of the Optical Society of America*, 33:555, 1943.

Helversen, O. v. Zur spektralen Unterschiedsempfindlichkeit der Honigbiene. *Journal of Comparative Physiology*, 80:439, 1972.

Hering, E. Zur Lehre von Lichtsinne-Grundzuege einer Theorie des Farbsinnes. *Sitzungsberichte der Kaiserliche Akademie der Wissenschaften in Wien*, 70, 1875.

Hernandez de Salomon, C. and Spatz, H. C. Colour vision inDrosophila melanogaster: Wavelength discrimination. *Journal of Comparative Physiology A*, 150:31, 1983.

Hess, C. Über den angeblichen Nachweis von Farbensinn bei Fischen. *Pflüger's Archiv für die gesamte Physiologie des Menschen und der Tiere*, 134:1, 1910.

Hess, C. *Vergleichende physiologie des Gesichtssinnes*. G. Fischer, Jena, 1912.

Hess, C. Beiträge zur Frage nach einem Farbensinne bei Bienen. *Pflüger's Archiv für die gesamte Physiologie des Menschen und der Tiere*, 170:337, 1918.

Hess, G. Experimentelle Untersuchungen uber den angeblichen Farbensinn der Bienen. *Zoologische Jahrbücher. Abteilung für allgemeine Zoologie und Physiologie der Tiere*, pages 81–108, 1913.

Humphrey, N. K. and Weiskrantz, L. Size constancy in monkeys with inferotemporal lesions. *The Quarterly journal of experimental psychology*, 21:225, 1969.

Hurlbert, A. and Wolf, K. Color contrast: a contributory mechanism to color constancy. *Progress in Brain Research*, 144:145, 2004.

Hurvich, L. M. and Jameson, D. An opponent-process theory of color vision. *Psychological Review*, 64:384 , 1957.

Ingling, C. R., Barley, J. P., and Ghani, N. Chromatic Content of Spectral Lights. *Vision Research*, 36:2537, 1996.

Ingling, C. R. and Huong Peng Tsou, B. Orthogonal combination of the three visual channels. *Vision Research*, 17:1075, 1977.

Jacobs, G. H. and Deegan II, J. F. Sensitivity to ultraviolet light in the gerbil (Meriones unguiculatus): Characteristics and mechanisms. *Vision Research*, 34:1433, 1994.

Jacobs, G. H., Neitz, J., and Deegan, J. F. Retinal receptors in rodents maximally sensitive to ultraviolet light. *Nature*, 353:655, 1991.

Kelber, A. and Osorio, D. From spectral information to animal colour vision: experiments and concepts. *Proceedings of the Royal Society B*, 277:1617, 2010.

Kinoshita, M. and Arikawa, K. Colour constancy in the swallowtail butterfly Papilio xuthus. *Journal of Experimental Biology*, 203:3521, 2000.

Kirschfeld, D. K. and Franceschini, N. Optische Eigenschaften der Ommatidien im Komplexauge von Musca. *Kybernetik*, 5:47, 1968.

Koshitaka, H., Kinoshita, M., Vorobyev, M., and Arikawa, K. Tetrachromacy in a butterfly that has eight varieties of spectral receptors. *Proceedings of the Royal Society B*, 275:947, 2008.

Kotel'nikov, V. A. On the transmission capacity of 'ether' and wire in electric communications. *Physics-Uspekhi*, 49:736, 2006.

Kraft, J. M. and Brainard, D. H. Mechanisms of color constancy under nearly natural viewing. *Proceedings of the National Academy of Sciences*, 96:307, 1999.

Kremers, J. and Meierkord, S. Rod-cone-interactions in deuteranopic observers: models and dynamics. *Vision Research*, 39:3372, 1999.

Kretz, R. A behavioural analysis of colour vision in the ant Cataglyphis bicolor (Formicidae, Hymenoptera). *Journal of Comparative Physiology*, 131:217, 1979.

Kries, J. v. Theoretische Studien über die umstimmung des Sehorgans. *Festschrift der Albrecht-Ludwigs-Universität in Freiburg Zum Fünfzigjährigen Regierungs-Jubiläum seiner Königlichen Hoheit Des Grossherzogs Friedrich*, pages 145–148, 1902.

Kuehni, R. G. Memoir concerning certain phenomena of vision by M. Monge "Memoire sur quelques phénomènes de la vision" Annales de Chimie 3 131–147 (1789). *Color Research & Application*, 22:199, 1997.

Kölreuter, J. G. *Vorläufige Nachricht von einigen das Geschlecht der Pflanzen betreffenden Versuchen und Beobachtungen, nebst Fortsetzungen 1,2 und 3. (1761-1766)*. W. Engelmann, Leipzig, 1761.

Kühn, A. Über den Farbensinn der Bienen. *Zeitschrift für vergleichende Physiologie*, 5:762, 1927.

Land, E. H. Color Visin and the natural Image Part I*. *Proceedings of the National Academy of Sciences*, 45:115, 1959.

Land, E. H. and Mc Cann, J. J. Lightness and Retinex Theory. *Journal of the Optical Society of America*, 61:1, 1971.

Lee, B. B., Pokorny, J., Smith, V. C., Martin, P. R., and Valberg, A. Luminance and chromatic modulation sensitivity of macaque ganglion cells and human observers. *Journal of the Optical Society of America A*, 7:2223 , 1990.

Lewis, A. and Zhaoping, L. Are cone sensitivities determined by natural color statistics? *Journal of Vision*, 6, 2006.

Lloyd, K. and Leslie, D. S. Context-dependent decision-making: a simple Bayesian model. *Journal of The Royal Society Interface*, 10:20130069, 2013.

Locke, N. M. Color constancy in the rhesus monkey and in man. *Archiv für Psychologie*, 193, 1935.

Lubbock, J. *Ameisen, Bienen und Wespen: Beobachtungen über die Lebensweise der geselligen hymenopteren*, volume 57. FA Brockhaus, Leipzig, 1883.

Lubbock, J. *Die Sinne und das geistige Leben der Thiere, insbesondere der Insekten*, volume 67. FA Brockhaus, Dresden, 1889.

Lunau, K. Visual ecology of flies with particular reference to colour vision and colour preferences. *Journal of Comparative Physiology A*, 200:497, 2014.

MacEvoy, S. P. and Paradiso, M. A. Lightness constancy in primary visual cortex. *Proceedings of the National Academy of Sciences*, 98:8827, 2001.

Maloney, L. T. Evaluation of linear models of surface spectral reflectance with small numbers of parameters. *Journal of the Optical Society of America A*, 3:1673, 1986.

Mausfeld, R. Colour'as part of the format of different perceptual primitives: the dual coding of colour. *Colour perception: Mind and the physical world*, pages 381–430, 2003.

Meinertzhagen, I. A. and O'Neil, S. D. Synaptic organization of columnar elements in the lamina of the wild type in Drosophila melanogaster. *Journal of comparative Neurology*, 305:232, 1991.

Menne, D. and Spatz, H. C. Colour vision in Drosophila melanogaster. *Journal of Comparative Physiology A*, 114:301, 1977.

Menzel, R. Untersuchungen zum Erlernen von Spektralfarben durch die Honigbiene (Apis mellifica). *Zeitschrift für vergleichende Physiologie*, 56:22, 1967.

Meyer, D. E. Goethes botanische Arbeit in Beziehung zu Christian Konrad Sprengel (1750-1816) und Kurt Sprengel (1766-1833) auf Grund neuer Nachforschungen in Briefen und Tagebuechern. *Berichte der Deutschen Botanischen Gesellschaft*, 80:209, 1967.

Monge, M. Memoire Sur Quelques Phénomène de la Vision. *Annales de Chimie*, 3:131, 1789.

Montag, E. D. and Boynton, R. M. Rod influence in dichromatic surface color perception. *Vision Research*, 27:2153, 1987.

Morante, J. and Desplan, C. Building a projection map for photoreceptor neurons in the Drosophila optic lobes. *Seminars in Cell & Developmental Biology*, 15:137, 2004.

Müller, H. Versuche über die Farbenliebhaberei der Honigbiene. *Kosmos: Zeitschrift für Entwicklungslehre und einheitliche Weltanschauung*, 12:273, 1882.

Nagel, W. A. *Der Farbensinn der Tiere.* J. F. Bergmann, Wiesbaden, 1902.

Neumeyer, C., Dörr, S., Fritsch, J., and Kardelky, C. Colour constancy in goldfish and man: influence of surround size and lightness. *Perception*, 31:171, 2002.

Oppermann, D., Schramme, J., and Neumeyer, C. Rod-cone based color vision in seals under photopic conditions. *Vision Research*, 125:30, 2016.

Osorio, D., Smith, A. C., Vorobyev, M., and Buchanan-Smith, H. M. Detection of Fruit and the Selection of Primate Visual Pigments for Color Vision. *The American Naturalist*, 164:696, 2004.

Osorio, D. and Vorobyev, M. Colour vision as an adaptation to frugivory in primates. *Proceedings of the Royal Society of London. B*, pages 593 – 599, 1996.

Osorio, D. and Vorobyev, M. A review of the evolution of animal colour vision and visual communication signals. *Vision Research*, 48:2042, 2008.

Palmer, G. *Theory of colours and vision.* S. Leacroft, 1777.

Petzschner, F. H. and Glasauer, S. Iterative Bayesian estimation as an explanation for range and regression effects: a study on human path integration. *The Journal of Neuroscience*, 31:17220, 2011.

Pichaud, F., Briscoe, A., and Desplan, C. Evolution of color vision. *Current Opinion in Neurobiology*, 9:622, 1999.

Pokorny, J. and Smith, V. C. Wavelength discrimination in the presence of added chromatic fields. *Journal of the Optical Society of America A*, 60:562, 1970.

Purpura, K., Tranchina, D., Kaplan, E., and Shapley, R. M. Light adaptation in the primate retina: analysis of changes in gain and dynamics of monkey retinal ganglion cells. *Visual Neuroscience*, 4:75, 1990.

Reitner, A., Sharpe, L. T., and Zrenner, E. Is colour vision possible with only rods and blue-sensitive cones? *Nature*, 352:798, 1991.

Rodieck, R. W. *The First Steps in Seeing.* Sinauer Associates: Sunderland (MA), 1st edition, 1998.

Salcedo, E., Huber, A., Henrich, S., Chadwell, L. V., Chou, W.-H., Paulsen, R., and Britt, S. G. Blue- and Green-Absorbing Visual Pigments of Drosophila: Ectopic Expression and Physiological Characterization of the R8 Photoreceptor Cell-Specific Rh5 and Rh6 Rhodopsins. *The Journal of Neuroscience,*, 19:10716, 1999.

Salcedo, E., Zheng, L., Phistry, M., Bagg, E. E., and Britt, S. G. Molecular Basis for Ultraviolet Vision in Invertebrates. *The Journal of Neuroscience*, 23:10873 , 2003.

Sankeralli, M. J. and Mullen, K. T. Estimation of the L-, M-, and S-cone weights of the postreceptoral detection mechanisms. *Journal of the Optical Society of America A.*, 13:906, 1996.

Schnaitmann, C., Garbers, C., Wachtler, T., and Tanimoto, H. Color Discrimination with Broadband Photoreceptors. *Current Biology*, 23:2375, 2013.

Schneeweis, D. M. and Schnapf, J. L. Photovoltage of rods and cones in the macaque retina. *Science*, 268:1053, 1995.

Sperling, H. G. and Harwerth, R. S. Red-green cone interactions in the increment-threshold spectral sensitivity of primates. *Science*, 172:180, 1971.

Sprengel, C. K. *Das entdeckte Geheimnis der Natur im Bau und in der Befruchtung der Pflanzen.* Friedrich Vieweg dem Aeltern, Berlin, 1793.

Stiles, W. S. Color Vison: The approach through Increment-Threshold Sensitivity. *Proceedings of the National Academy of Sciences*, 45:100, 1959.

Stockman, A. and Sharpe, L. T. The spectral sensitivities of the middle- and long-wavelength-sensitive cones derived from measurements in observers of known genotype. *Vision Research*, 40:1711, 2000.

Stockman, A., Sharpe, L. T., and Fach, C. The spectral sensitivity of the human short-wavelength sensitive cones derived from thresholds and color matches. *Vision Research*, 39:2901, 1999.

Strausfeld, N. J. and Lee, J.-K. Neuronal basis for parallel visual processing in the fly. *Visual Neuroscience*, 7:13, 1991.

Thoen, H. H., How, M. J., Chiou, T.-H., and Marshall, J. A Different Form of Color Vision in Mantis Shrimp. *Science*, 343:411, 2014.

Trincker, D. Hess, Carl von. In *Neue Deutsche Biographie*, 9. Duncker & Humblot, Berlin, 1972.

Troje, N. Spectral categories in the learning behaviour of blowflies. *Zeitschrift für Naturforschung C*, 48:96, 1993.

Troje, N. F. *Wellenlängenunterscheidung bei der Goldfliege Lucilla spec.* Inaugural dissertation, Albert-Ludiwgs Universitaet Freiburg, 1994.

Trujillo-Cenóz, O. The structural organization of the compound eye in insects. In *Physiology of Photoreceptor Organs*, pages 5–62. Springer, 1972.

Vogt, K. The Chromophore of the Visual Pigment in Some Insect Orders. *Zeitschrift für Naturforschung C*, 39:196, 1984.

Vorobyev, M. Costs and benefits of increasing the dimensionality of colour vision system. *Biophysics of photoreception: molecular and phototransductive events*, pages 280–289, 1997.

Vorobyev, M., Brandt, R., Peitsch, D., Laughlin, S. B., and Menzel, R. Colour thresholds and receptor noise: behaviour and physiology compared. *Vision Research*, 41:639, 2001.

Vorobyev, M. and Ibarra, N. H. Honey Bee Vision in Relation to Flower Patterns. In C. G. Galizia, D. Eisenhardt, and M. Giurfa, editors, *Honeybee Neurobiology and Behavior*, pages 285–301. Springer Netherlands, Dordrecht, 2012.

Vorobyev, M. and Osorio, D. Receptor noise as a determinant of colour thresholds. *Proceedings of the Royal Society of London. Series B*, 265:351, 1998.

Vorobyev, M., Osorio, D., Bennett, A. T., Marshall, N. J., and Cuthill, I. C. Tetrachromacy, oil droplets and bird plumage colours. *Journal of comparative physiology. A*, 183:621, 1998.

Wachtler, T., Sejnowski, T. J., and Albright, T. D. Representation of Color Stimuli in Awake Macaque Primary Visual Cortex. *Neuron*, 37:681, 2003.

Wallach, H. Brightness constancy and the nature of achromatic colors. *Journal of Experimental Psychology*, 38:310, 1948.

Walls, G. L. "Land! Land!". *Psychological Bulletin*, 57:29, 1960.

Walsh, V., Carden, D., Butler, S., and Kulikowski, J. The effects of V4 lesions on the visual abilities of macaques: hue discrimination and colour constancy. *Behavioural Brain Research*, 53:51, 1993.

Wardill, T. J., List, O., Li, X., Dongre, S., McCulloch, M., Ting, C.-Y., O'Kane, C. J., Tang, S., Lee, C.-H., Hardie, R. C., and Juusola, M. Multiple Spectral Inputs Improve Motion Discrimination in the Drosophila Visual System. *Science*, 336:925, 2012.

Washburn, M. F. and Bentley, I. The establishment of an association involving color-discrimination in the creek chub, semotilus atromaculatus. *Journal of Comparative Neurology and Psychology*, 16:113, 1906.

Weiss, S., Kremers, J., and Maurer, J. Interaction between rod and cone signals in responses of lateral geniculate neurons in dichromatic marmosets (*Callithrix jacchus*). *Visual Neuroscience*, 15:931, 1998.

Wiesel, T. N. and Hubel, D. H. Spatial and chromatic interactions in the lateral geniculate body of the rhesus monkey. *Journal of Neurophysiology*, 29:1115, 1966.

Wild, H. M., Butler, S. R., Carden, D., and Kulikowski, J. J. Primate cortical area V4 important for colour constancy but not wavelength discrimination. *Nature*, 313:133, 1985.

Wright, W. D. A re-determination of the trichromatic coefficients of the spectral colours. *Transactions of the Optical Society*, 30:141, 1929.

Wright, W. D. The sensitivity of the eye to small colour differences. *Proceedings of the Physical Society*, 53:93, 1941.

Wright, W. D. The Characteristics of Tritanopia. *Journal of the Optical Society of America*, 42:509, 1952.

Wyszecki, G. and Stiles, W. S. *Color Science*, volume 8. Wiley New York, 1982.

Wässle, H, Yamashita, M., Greferath, U., Grünert, U., and Müller, F. The rod bipolar cell of the mammalian retina. *Visual Neuroscience*, 7:99, 1991.

Young, T. An account of some cases of the production of colours, not hitherto described. *Philosophical Transactions of the Royal Society of London*, 92:387, 1802.

Zolotnitsky, N. Les poissons distinguent-t-ils les couleurs. *Archives de zoologie expérimentale et générale.*, 9:721, 1901.

Acknowledgments

Publications/Contributions:

Garbers, Christian, und Thomas Wachtler. „Wavelength Discrimination in Drosophila Suggests a Role of Rhodopsin 1 in Color Vision". *PLOS ONE* 11, Nr. 6 (3. Juni 2016)
Conceived and designed the experiments: C.G. T.W.
Analyzed the data: C.G.
Wrote the paper: C.G T.W.

Schnaitmann, Christopher, Christian Garbers, Thomas Wachtler, und Hiromu Tanimoto. „Color Discrimination with Broadband Photoreceptors". *Current Biology* 23, Nr. 23 (2. Dezember 2013): 2375–82.
H.T. and C.S. conceived the project.
All authors designed and C.S. conducted all behavioural experiments with the help of C.G.
Instrumentation for the modified visual learning apparatus was desiged by H.T. and C.S.
The modified light-clamp method for electrophysiological measurements was devised by C.G. with the help of C.S.
T.W. and C.G. designed and C.G. performed the modelling experiments. C.S. and H.T. wrote the paper with the help of the other authors.

Garbers, Christian, Josephine Henke, Christian Leibold, Thomas Wachtler, und Kay Thurley. „Contextual Processing of Brightness and Color in Mongolian Gerbils". *Journal of Vision* 15, Nr. 1 (14. Januar 2015): 13.
Conceived and designed the experiments: C.G. K.T. T.W. C.L.
Performed the experiments: J.H. K.T.
Analyzed the data: C.G. K.T.
Wrote the paper:C.G. C.L. J.H. K.T. T.W.

_____   _____

Christian Garbers   Thomas Wachtler